1-1-2007

Physicochemical properties of individual and mixed oxides of SiO2, Al203, TiO2, and photocatalytic behaviour of organosilane modified ST samples

Kalyani Gude

Eastern Illinois University

This research is a product of the graduate program in Chemistry at Eastern Illinois University. Find out more about the program.

THESIS REPRODUCTION CERTIFICATE

TO: Graduate Degree Candidates (who have written formal theses)

SUBJECT: Permission to Reproduce Theses

The University Library is receiving a number of request from other institutions asking permission to reproduce dissertations for inclusion in their library holdings. Although no copyright laws are involved, we feel that professional courtesy demands that permission be obtained from the author before we allow these to be copied.

PLEASE SIGN ONE OF THE FOLLOWING STATEMENTS:

Booth Library of Eastern Illinois University has my permission to lend my thesis to a reputable college or university for the purpose of copying it for inclusion in that institution's library or research holdings.

Kalyani. _____   _11|16|07_ _____

Author's Signature   Date

I respectfully request Booth Library of Eastern Illinois University **NOT** allow my thesis to be reproduced because:

_____

_____

_____

_____   _____

Author's Signature   Date

This form must be submitted in duplicate.

Physicochemical properties of individual and mixed oxides of SiO2, Al2O3, TiO2

and Photocatalytic behaviour of organosilane modified ST samples

(TITLE)

BY

Kalyani Gude

THESIS

SUBMITTED IN PARTIAL FULFILLMENT OF THE REQUIREMENTS
FOR THE DEGREE OF

Master of Science in Chemistry

IN THE GRADUATE SCHOOL, EASTERN ILLINOIS UNIVERSITY
CHARLESTON, ILLINOIS

2007

YEAR

I HEREBY RECOMMEND THAT THIS THESIS BE ACCEPTED AS FULFILLING
THIS PART OF THE GRADUATE DEGREE CITED ABOVE

11/17/07		
DATE		THESIS DIRECTOR

11/16/07		
DATE		DEPARTMENT/SCHOOL HEAD

Physicochemical properties of individual and mixed oxides of SiO_2, Al_2O_3, TiO_2
&
Photocatalytic behaviour of organosilane modified ST samples

Kalyani Gude

This thesis has been read and approved by each member of the following supervisory committee:

_____   11/17/07

Dr. Jonathan P. Blitz   Date

_____   11/16/07

Dr. Douglas G. Klarup   Date

_____   11/16/07

Dr. Daniel J. Sheeran   Date
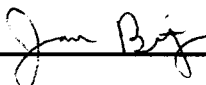

_____   11/16/07

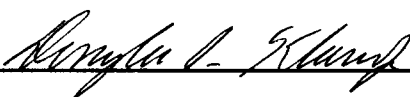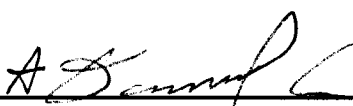Dr. Scott M. Tremain   Date

Physicochemical properties of individual and mixed oxides of SiO_2, Al_2O_3, TiO_2

&

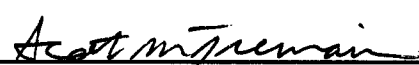# Photocatalytic behaviour of organosilane modified ST samples

By

Kalyani Gude

ABSTRACT

A variety of oxides such as silica, alumina, titania and mixed oxides such as silica/alumina (SA), silica/titania (ST) and alumina/silica/titania (AST) are investigated by TGA and FTIR. These mixed oxides are analyzed because of their applications as catalysts. Thermogravimetric analysis is done on all the samples to determine the temperature at which the weakly adsorbed water is lost and the surface is left with only surface hydroxyls. TGA data showed the loss of most of the adsorbed water at around 100°C.

From the diffuse reflectance FTIR spectra taken at 200 and 300°C the silanol content is estimated from the 3740 cm^{-1} band intensity. Silanol content is estimated for SA and ST samples in order to determine the loss of silanol content with increase in titania or alumina phase. The decrease in silanol content with an increase in alumina and titania contents is observed, though the trend is not smooth at low alumina and titania contents. Among ST samples ST 20 did not show much loss in silanol content.

ST samples are extensively studied as these represent a novel class of catalyst. Catalytic active sites are generated on the surface of ST samples as a result of formation of Si-O-Ti bonds. Quantitative characterization of Si-O-Ti linkages by FTIR transmission spectroscopy shows maximum Si-O-Ti bond formation for ST 20 (80% of silica and 20% of titania). The formation of a maximum number of Si-O-Ti bonds for ST 20 is an indication of greater degree of dispersion of titania in the silica matrix.

Adsorption studies are done on the silica surface modified with various organofunctional silanes for the purpose of enhancing adsorption for photocatalytic decomposition on silica-titanias. Methylene blue is chosen as a dye for studying the

adsorption behaviour of silica and various modified silicas. Adsorption isotherms of thiocyano and thiol groups modified on silica showed a greater adsorption for methylene blue and hence these groups were chosen for surface modification on to ST samples.

Since ST 20 did not exhibit significant loss in silanol content while retaining considerable titania content, this material was chosen for photocatalytic experiments. The relatively large silanol content provides the capability for significant surface functionalization to control adsorption properties, while retaining the photocatalytic titania active sites.

After modification of ST 20 with thiol and thiocyano groups, adsorption and photocatalytic decomposition behavior of methylene blue with ST 20, thiol modified ST 20 and thiocyano modified ST 20 were studied. From these studies, photocatalytic activity of SCN modified ST 20 is found to be greater than that of ST 20.

ACKNOWLEDGEMENTS

First and foremost, I offer my sincere gratitude to my advisor, Dr. Jonathan P. Blitz, who has supported and encouraged me throughout my thesis with his knowledge and patience. I thank the faculty and staff at Department of chemistry for making this project successful. Specially, I would like to thank Dr. Barbara Lawrence for her invaluable support and advice during the initial days of my studies at Eastern Illinois University. I thank International Programs and Department of Chemistry at EIU for the financial support. I thank my committee members, Dr. Douglas G. Klarup, Dr. Daniel J. Sheeran and Dr. Scott M. Tremain for their suggestions during the research work.

I thank my parents, family members and friends. Without their love, encouragement and support, none of this would have been possible. I thank my husband, Dinesh, who has encouraged me throughout the completion of coursework and thesis.

Table of Contents

List of Figures

List of Tables

CHAPTER I

INTRODUCTION

SILICA

Silicon dioxide, also known as silica, is the oxide of silicon formed when silicon is exposed to oxygen (air). Silicon is a tetravalent chemical element with the symbol Si. It is the second most abundant element of the earth's crust that makes up 25.7% by weight. Silica is available in crystalline and non-crystalline forms. The amorphous form of silica has a low temperature of linear expansion coefficient, high internal surface area, high chemical stability, high resistance on exposure to radiation, and optical transparency from infrared to ultraviolet radiation.[1] Its ability to adsorb liquids makes it applicable as catalysts, anti-caking agents in food and pharmaceutical products, desiccants, cosmetics, adhesives and extracting oils.[1]

Three different types of silanol groups are present on silica surfaces as shown in scheme I below.
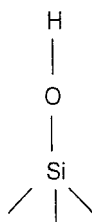
Isolated silanol or non-hydrogen bonded silanol
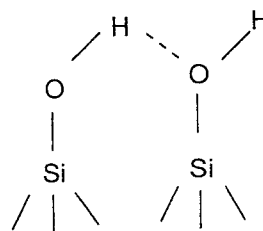
Vicinal silanol or hydrogen bonded silanol
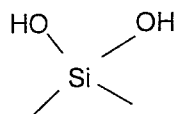
Geminal silanol

These different types of silanol groups have been identified by Fourier transform infrared spectroscopy and solid state ^{29}Si CP (cross polarization)-MAS (magic angle spinning) NMR spectroscopy. The sharp peak at 3745 cm^{-1} detected by infrared spectroscopy corresponds to isolated or non-hydrogen bonded silanols, and a broader peak at lower wave number corresponds to vicinal or hydrogen bonded silanols. Hydrogen bonded silanols undergo dehydration or dehydroxylation at higher temperatures. The silica surface undergoes dehydration at higher temperature due to loss of adsorbed water and a thermal dehydration reaction. The loss of water from the surface of silica occurs at higher temperatures due to condensation of hydroxyl groups whereby the two neighbouring silanols get condensed into a siloxane bridge as shown in scheme II.
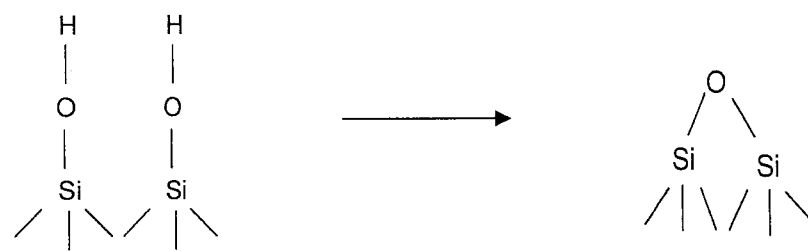
Two neighbouring silanols   Condensed siloxane bridge

Dehydration or dehydroxylation at higher temperatures causes a decrease in IR band at 3600 cm^{-1}. **Figure 1** shows the IR spectra of fumed silica in the Si-OH vibration range after thermal treatment. It shows a decrease in IR band at 3600 cm^{-1} with an increase in

temperature from 325°C to 1000°C. Non-hydrogen bonded silanol groups are more

reactive to surface modifying reagents than hydrogen bonded silanols. It is important to

characterize these peaks because they act as reactive sites for catalytic activity.[2]
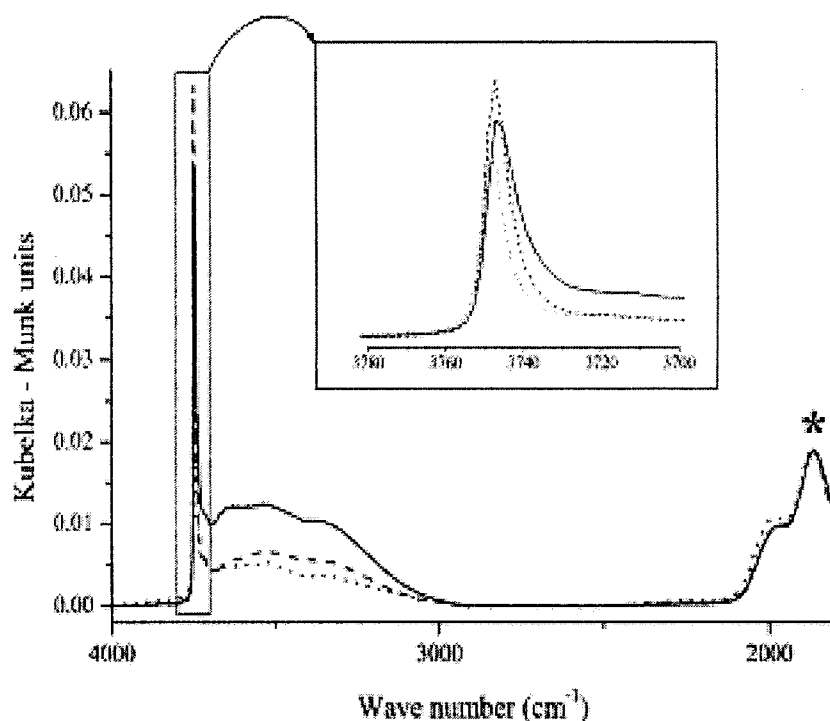
Figure 1: IR spectra of fumed silica. — spectra at 325°C, --- spectra at 700°C, ... spectra

at 1000°C [2]

ALUMINA

Aluminum oxide (Al_2O_3), also known as alumina, is an oxide of aluminum. It is

the main component of bauxite, the principal ore of aluminum. It is mainly used in the

manufacturing of ceramics because of its high hardness, wear and chemical resistance. It

is also used as a catalytic support, abrasive material, polishing material and as a medium

for chromatography. It has good thermal and insulating characteristics.

SILICA/ALUMINA

Amorphous silica/alumina (SA) mixed oxides catalyze many reactions like polymerization, isomerization, alkylation and cracking reactions.[4] Silica/alumina catalysts are active for these purposes because of the acidic nature of the mixed oxide, where a tetravalent silicon atom is replaced by the tri-valent aluminum atom in the silica lattice.[4] Silica/alumina mixed oxides are synthesized by many methods like sol-gel, high temperature hydrolysis, chemical vapor deposition, etc. Characteristics of these mixed oxides which determine the interaction with the surroundings is associated with the nature of the surface and reactive sites on the surface. The composition of these mixed oxides and different hydroxyls such as bridging and terminal determine the physicochemical properties of materials like catalytic activity and adsorbent capacity.[3, 4]

Water molecules adsorb dissociatively on oxides and form active sites such as ≡MOH, ≡M-O(H)-M, etc., which influence physicochemical properties of the surface.[3] Characteristics of the active surface sites and adsorbed water on the surface of the mixed oxides depend on the availability of impurities, other phases in the matrix, point defects or dislocations, pretreatment temperature, etc.[3] Coordination number of the metal and oxygen atoms also influences surface characteristics. The interpretation of experimental data becomes difficult because of the variety of factors having influence on the surface states.[3]

The acid sites on the oxide surfaces are of two types: Lewis and Bronsted.[4] Bronsted acid sites are capable of donating a proton to the adsorbate molecule, and Lewis acid sites are capable of accepting electrons from the adsorbate molecule. Bronsted and Lewis sites are considered to be independent. The major contribution to acidity is from

Lewis sites on a dehydrated surface. Addition of small amount of water to a surface possessing Lewis sites convert them to Bronsted sites which donate protons to the adsorbate molecules.[4]

Silica/alumina have Bronsted acid sites ≡Al-O(H)-Si≡ and terminal hydroxyls ≡MOH (M = Si or Al) which are considered as dissociatively adsorbed water molecules. Water is easily adsorbed dissociatively on a pure oxide surface. Thus, the oxide surface is always hydrated under standard conditions, but the amounts of different hydroxyls associated with it are varied.[3]

Several distinctions were observed between the mixed oxides obtained by chemical vapor deposition (CVD) of the second phase and pyrogenic mixed oxides, due to differences in the nature of the interface and distribution of the second phase. The ≡$M_{(1)}$-O-$M_{(2)}$≡ bonds are more easily hydrolysable for CVD mixed oxides and hence the interface acts as a boundary between hydrated and hydrogen-bonded surface of the particles with different phases resulting in the absence of IR bands. However, the IR band for ≡$M_{(1)}$-O-$M_{(2)}$≡ bond appears in the case of pyrogenic mixed oxides. Heating the CVD mixed oxides may also result in the appearance of the IR band due to dehydration.[3] The oxide surface properties depend largely on the availability of adsorbed water on it. Though there are many studies relating to the adsorbed water on the surface, investigations are still being made on the interfacial water on mixed oxides, influence of oxide synthesis method and on the nature of the interfaces.[3]

The study of influence of alumina content on pyrogenic silica/alumina sample (AS_{23} with 23 wt% alumina) have not shown any individual bands in the IR which can be connected to ≡AlOH, ≡Al-O-Si≡ or ≡Al-O(H)-Si≡ bonds, but the spectra

appeared similar to that of silica. The presence of alumina had shown a difference in the shape of the curves in the 3400-3650 cm^{-1} as well as at 900 cm^{-1} which can be attributed to the influence of alumina phase, or removal of water from SA by means of an associative desorption mechanism. The reason for not observing the $\equiv$AlOH, $\equiv$Al-O(H)-Si$\equiv$ bonds for the hydrated SA samples can be attributed to the formation of hydrogen bonds with the adsorbed water and the high heterogeneity of amorphous pyrogenic SA samples. This leads to the broadening of bands in the 3400-3700 cm^{-1} region. The participation of OH groups from $\equiv$AlOH, $\equiv$Al-O(H)-Si$\equiv$ in the dehydration of the surface by means of loss of water molecules by an associative desorption mechanism was also the reason for difficulty in the observation of the respective bands. Also, some part of the alumina phase was covered by the mosaic silica shell surface during the synthesis. Thus the amorphous nature of AS, high heterogeneity obtained by pyrogenic methods and easy removal of adsorbed water result in the absence of IR separated bands for $\equiv$AlOH, $\equiv$Al-O(H)-Si$\equiv$ groups.[3]

TITANIA

Titanium dioxide, also known as titania is an oxide of titanium. It is found along with contaminant metals such as iron. It is used mostly as a white pigment because of its brightness. TiO_2 in powder form acts as an opacifier and hence it is used to provide opacity to paints, coatings, paper and plastics, etc. TiO_2 powders are inexpensive, chemically inert and do not show absorption in the visible region.[7] But it is active under ultra-violet light irradiation and induces some chemical reactions, which was known from flaking of paints and decomposition of fabrics containing TiO_2 under sunlight.[7]

TiO_2 exists mainly in two crystallographic forms, anatase and rutile.[5] The anatase form has a band gap of 3.23 eV or 384 nm and rutile has a band gap of 3.02 eV or 411 nm in the near ultraviolet region of the spectrum. The energy band gaps combine with the valence band positions and results in the generation of highly energetic holes at the interface, which give rise to easy oxidation reactions. Anatase is more reactive photocatalytically than rutile, and is formed at lower temperatures (less than 600°C). It has a high specific surface area and high surface density of active sites for adsorption and photocatalytic purposes.[6] The most popular form of TiO_2 is produced by the German company Degussa with the name P-25, containing 80% anatase and 20% rutile. Since it has a high percentage of anatase, it is considered to be most reactive.[5]

The properties of fumed titania depend on the phase composition of the particles, such as anatase and rutile phases. The difference in their surface characteristics are due to the nature and concentration of active sites such as TiOH, TiO(H)Ti, Ti^{3+}, etc. on different faces of anatase or rutile. The study of surface characteristics of fumed titania is important because of the wide variety of industrial applications. Fumed titania prepared via hydrolysis of $TiCl_4$ in an oxygen-hydrogen flame at a temperature above 1300 K showed the presence of both rutile and anatase phases.[6] Water molecules can dissociatively adsorb on the surface of dry titania surface at a temperature above 200 K. The IR study of titania showed the availability of terminal hydroxyl (TiOH) and bridging hydroxyl groups (Ti-O(H)-Ti).[6]

The relationship between hydrophilicity and the amount of OH groups on TiO_2 were studied by using FTIR spectroscopy. IR bands at 3695 cm^{-1} observed on TiO_2 surface were assigned to the stretching of OH groups chemisorbed on the surface. An IR

band at 3300 cm^{-1} was assigned to hydroxyls of both dissociated and molecular adsorbed water. A band at 1623 cm^{-1} was assigned to H-O-H bending of molecular water. This observation showed the co-existence of molecular and dissociated water on the TiO$_2$ surface.[7, 25]

TiO$_2$ when stored in the dark for one week resulted in the decrease of all bands which showed loss of molecular and dissociated water. (i.e., molecular and dissociated water desorption had taken place). When a TiO$_2$ surface is irradiated with UV light, the intensity of 1623 cm^{-1} band decreased while the intensity of the band at 3695 cm^{-1} increased, which showed an increase in the amount of adsorbed dissociated water and a decrease in the amount of molecular adsorbed water. Nakumara *et al.* reported an increase in the amount of chemisorbed water on the TiO$_2$ surface (band at 3270 cm^{-1}) after irradiation with UV light using surface enhanced IR absorption spectroscopy.[7, 29] Uosaki *et.al* had shown an increase in the amount of adsorbed water on a TiO$_2$ surface after UV irradiation[30]. This was shown as a broad band with a peak at 3400 cm^{-1} and a shoulder at 3200 cm^{-1}, which was assigned to an increase in the hydrophilicity of the surface.[7,30]

SILICA/TITANIA

Silica/Titania represents a novel class of catalytic materials that have been in use in recent years.[8] These materials are extensively used as catalysts, pigments, supports, etc. The structural characteristics and physico-chemical properties of ST are important because of their applications in a wide variety of industries. These materials have the advantages of TiO$_2$, as a semi-conductor and active catalytic support and SiO$_2$, possessing

high thermal stability and excellent mechanical strength. New catalytic active sites are generated on the surface of ST samples due to interaction of TiO_2 with SiO_2.[8]

The applications of silica/titania can be categorized into three different ways based on their unique physico-chemical properties: the photocatalytic activity that is associated with the quantum size effect and support effect, acid catalytic activity that is associated with the generation of new-acid sites, and excellent mechanical activity that is associated with excellent mechanical and thermal stability.[8]

Two types of interactions that are possible for the ST samples are the physically mixed interactions where the interaction forces are nothing more than the weak van der Waals forces, and chemically bonded interactions which are very strong and different from that of simple combination of individual phases (mechanical mixtures).[8] The extent of interactions and dispersion methods are widely dependent on the preparation methods and synthetic conditions. The most widely used methods for the preparation of ST samples are sol-gel hydrolysis, impregnation and co-precipitation methods. Sol-gel is the most widely used method because ST mixed oxides prepared by this method have the capability of controlling textural and surface properties of mixed oxides. The chemical interactions of these mixed oxides result in the formation of Si-O-Ti linkages.[8]

Titania in the fumed ST mixed oxides also has a biphasic structure as of original titania i.e., anatase and rutile phases. X-ray studies of the ST samples prepared by the sol-gel method have shown an increase anatase phase with an increase in titania wt %.[6]

Two types of Ti species are present on the surface of Silica/Titania mixed oxides. One is the isolated Ti species and the other is segregated TiO_2 microdomains with relative ratio depending on the chemical composition, preparation methods and synthesis

conditions like the hydrolysis route, drying method, calcination temperature, Ti content etc.[8] The degree of homogeneity is associated with the relative amount of Si-O-Ti linkages in the ST mixed oxides. The Si-O-Ti bonds are more effectively formed with an increase in homogeneity.[8]

The experimental evidence of Si-O-Ti linkages in the Silica/Titania has been detected by IR spectroscopy. The characteristic vibration observed at 910-960 cm^{-1} is widely accepted to be due to Ti-O-Si bonds. The exact band position depends on both chemical composition of the sample as well as calibration and resolution of the instrument.[8] The intensity of the IR band was used to evaluate the absolute amount of Si-O-Ti linkages. It has been shown that the amount of Si-O-Ti linkages increase up to a titania content of 20 wt% titania.[6, 8] The degree of homogeneity or the dispersion of Ti in the SiO_2 matrix has been associated with the ratio of IR vibration due to Ti-O-Si bond at 930-960 cm^{-1} to that due to IR band at 1210 cm^{-1}. An IR band observed at ~665 cm^{-1} was also assigned to an Si-O-Ti vibration.[8]

FTIR SPECTROSCOPY

FTIR spectroscopy deals with the absorption and emission by molecules and materials of all wavelengths in the infrared region of the electromagnetic spectrum. It is mainly used for the identification of functional groups and molecular structures. In this work FTIR spectroscopy is being used for obtaining transmission or reflectance spectra to determine the surface groups. Transmission FTIR studies involve passing infrared radiation completely through the sample and measuring the extent of absorption. The spectral intensity obtained depends on the path length through which the light travels, the thickness of the sample, absorption coefficient and reflectivity of the sample. DRIFT

(Diffuse Reflectance Infrared Fourier Transform Spectroscopy) involves numerous light sample interactions. It is done by illuminating the sample and collecting the radiation scattered at a wide range of angles with the help of ellipsoidal mirrors. Spectra obtained by this technique display the features of transmission spectra. Samples which are highly absorbing or possessing high refractive index are diluted with a diffusively scattering matrix, like KBr.[23]

THERMOGRAVIMETRIC ANALYSIS

Thermogravimetric analysis is a technique that is used to determine the amount and rate of weight change of a material as a function of increasing temperature, or as a function of time under controlled atmospheric conditions. It can be used to characterize any material that shows weight changes. It can also be used to detect phase changes that occur due to decomposition, oxidation or dehydration. Many of the weight loss curves look similar and hence these are transformed to derivative weight loss curves to know the point where the rate of weight loss is at a maximum. A thermogravimetric analyzer consists of a sample loaded on a high-precision pan. The sample along with the pan is positioned in an electrically heated furnace containing a thermocouple, which accurately measures the temperature. The atmosphere is purged with an inert gas to stop undesirable reactions like oxidation etc.

PHOTOCATALYSIS

Wastes, which come from various sources such as chemical fertilizers, pesticides, herbicides, chemical wastes, underground storage tanks, dump sites, etc. is a serious and ever growing problem. Because of these conditions, surrounding soil and underground water aquifiers are contaminated with hazardous toxic chemicals. Nutrients which are

essential for mankind are extracted from the earth's crust and wastes are released into receiving water in rivers, lakes and ocean. Industries also produce large amounts of waste while processing raw materials and discharge them into the surrounding environment. The commercial and defense sectors of most industrialized nations are faced with serious environmental problems related to contaminated ground waters, toxic air contaminants and hazardous waste. So, the problem relating to hazardous waste remediation has become a concern in the national and international community in recent years. In order to address these problems, i.e., for the characterization and elimination of hazardous waste from soil, water and air, extensive research has been done and is going on in analytical, biochemical and physicochemical fields.[9]

A catalyst is a substance which increases the rate of a chemical reaction without modifying itself by the overall reaction. Photocatalysis is a process of acceleration of a chemical reaction in the presence of light. This is a technique that is in use for the removal of hazardous waste from water. Photocatalytic technology used for air and water purification, form a group of processes known as Advanced Oxidation Processes (AOP). This method offers the advantage of destroying pollutants, in contrast to conventional techniques such as activated carbon or air stripping that only transfer contaminants from one phase to the other. These AOP's generate very reactive free radicals ($^{\cdot}OH$) and mineralize organic compounds to carbon dioxide, water and mineral acids. AOP's include reactions such as direct homogeneous photolysis (vacuum UV included) and heterogeneous photolysis. Hydrogen peroxide, ozone and ultraviolet lights have been utilized for homogeneous photocatalysis where as semiconductors like TiO_2 have been utilized for heterogeneous photocatalysis.[5]

Heterogeneous photocatalytic processes have several advantages over homogeneous photocatalytic processes. Heterogeneous reactions can mineralize a wide variety of organic chemical components, can utilize solar light for exciting the catalysts, and can reuse the catalyst. Organic and inorganic pollutants can be treated at the same time as oxidation and reduction reactions occur simultaneously. This heterogeneous process can be used for both gases and liquids.[5]

SEMICONDUCTOR PHOTOCATALYSIS

Advanced physicochemical processes such as semiconductor photocatalytic methods are supposed to be complementary and supplementary to the more conventional approaches such as high temperature incineration and conventional physicochemical treatments for the destruction of hazardous chemical wastes. Semiconductor photocatalysis is a technique that is widely used for the treatment of water and air. TiO_2, a semiconductor photocatalyst, has been used for a variety of environmental problems. Apart from air and water purification, it has also been shown to be useful for the destruction of microorganisms like bacteria and viruses, for the inactivation of cancer cells, for the control of odor, for the photo-splitting of water to produce hydrogen gas, and for nitrogen fixation.[9]

HETEROGENEOUS PHOTOCATALYTIC PROCESS

Heterogeneous photocatalytic processes can be understood from Figure 2. The picture shows heterogeneous photocatalytic process occurring on an illuminated semiconductor particle. Semiconductors such as TiO_2, ZnO, Fe_2O_3, CdS act as sensitizers for light induced processes because of their electronic structure. They are characterized

by a highest occupied energy band called the valence band, and lowest unoccupied energy band called the conduction band separated by a band gap, E_g.
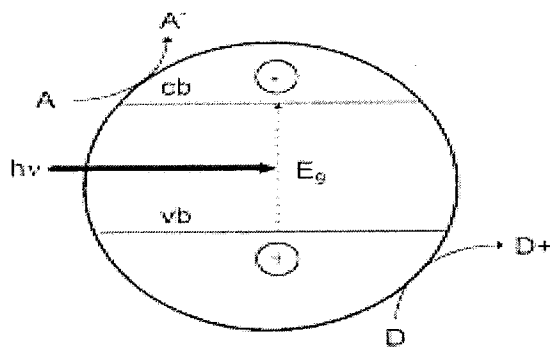
Figure 2: Heterogeneous photocatalytic process occurring on an illuminated semiconductor particle[5]

When a photon with an energy hv matches or exceeds the band gap energy, E_g of the semiconductor particle, an electron from the valence band is promoted to the conduction band, leaving a hole $h_{vb}{}^+$ in the valence band. Excited state conduction band electrons and valence band holes can recombine on the surface or in the bulk of the particle in a few nanoseconds, or get trapped on the surface and react with donor or acceptor species adsorbed on the surface or near to the surface of the particle. The stored energy is dissipated in the form of heat in a few nanoseconds by recombination in the absence of suitable electron or hole scavengers. If suitable scavengers are available to trap the electron or hole, recombination is prevented and subsequent redox reactions may occur.[5,10]

ROLE OF ADSORPTION IN HETEROGENEOUS PHOTOCATALYTIC PROCESS

The basic concept of heterogeneous photocatalysis can be explained by scheme III as below

Reactant + Surface $\longleftrightarrow$ Reactant....Surface complex

(Adsorption)

Reactant....Surface $\longrightarrow$ Product.....Surface complex

(Reaction)

Product....Surface $\longrightarrow$ Product + Surface

(Desorption)
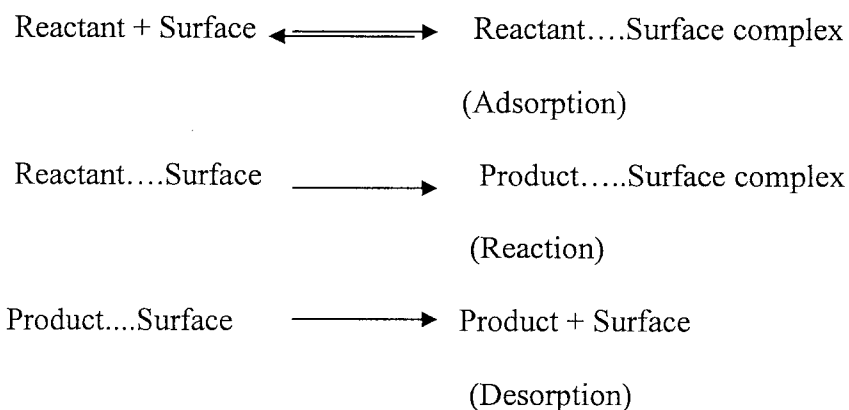
In a heterogeneous photocatalytic process, the reactants transfer to the surface of the catalyst, adsorb onto the surface, result in the formation of reactant....surface complex. Reaction in the adsorbed phase result in the formation of product...surface complex. The product gets removed from the surface by means of desorption and finally the product is removed from the interfacial region. In this whole process, adsorption of reactant on the surface is often the rate-limiting step. Therefore, for the photocatalytic process to occur, adsorption is an important step that needs to be considered.

TiO_2 AS PHOTOCATALYST

TiO_2 is a semiconductor widely used for photocatalytic degradation process because of its unique photocatalytic efficiency and inertness. It is widely useful for photocatalysis because it possesses exceptional optical and electronic properties. TiO_2 is chemically and biologically stable with respect to photo-corrosion and chemical corrosion and is non-toxic and inexpensive.[9] Photo degradation in the presence of TiO_2 is

a typical interfacial reaction that occurs only at the surface of a TiO_2 particle and not in the bulk solution. When a photon having energy equal to or greater than the band gap energy of TiO_2 strikes the surface of TiO_2, the electrons in the valence band are promoted to the conductance band and result in the formation of hydroxyl radicals which degrades the adsorbed chemical species on its surface.[17]

SILYLATION

Silica surfaces modified by organofunctional silanes have a wide variety of applications in the field of analytical chemistry for the purpose of ion-exchange chromatography and size exclusion chromatography, in the field of synthetic chemistry for the purpose of heterogeneous catalysis and phase transfer catalysis, in the field of biochemistry for the purpose of enzyme immobilization and affinity chromatography and in industries as semiconductor devices.[11]

Silica surfaces consist of silanol and siloxane groups. Surface silanols play an important role in surface modification reactions. Surface silanols are relatively inert but can be modified under certain conditions to impart the desirable properties for which unmodified silica surfaces are poorly suited. For example, in the case of stationary phases for reversed phase chromatography, silica surfaces possessing silanol groups cannot be used but the silylated surface having silanols modified by organofunctional silanes can be used as a stationary phase. Chemical modification of surface silanol or siloxane groups changes the physical and chemical properties of silica.[12] Transmission IR spectroscopy has been used for the study of silica and surface modified silicas, but these studies have shown the hydrolysis of adsorbed silane in dry toluene medium on Cab-O-Sil® modified

with trimethoxy methyl silane. Diffuse reflectance FTIR proved to be an ideal sampling technique for getting quantitative information regarding surface silane loading.[13]

Surface modification of all silanols cannot be attained in an aqueous medium and hence benzene or toluene was used as a medium for the silylation reaction. Pyridine was used as a catalyst for the modification of silica with alkylchloro silanes and alkoxy methyl silanes. Later amine catalysts having an exchangeable proton were used for the reaction of alkylmethoxy silanes with silica at room temperature. It was shown that the reactivity of surface silanols noticeably increased in the presence of basic amines at room temperature and their catalytic activity diminished at higher temperature as the lifetime of the adsorbed complexes is too short for the reaction to occur effectively. Amine catalysts having an exchangeable proton permitted the reaction to proceed through a lower energy pathway. Amine catalysts in non-aqueous media gave products of higher strength and better wet strength retention.[13]

The chemical steps involved in the modification of silica with alkylmethoxy silanes in the presence of amine catalyst followed by hydrolysis can be outlined as follows where X is CN, NH_2, SCN and SH.[14]

$$\text{H}_2\text{O}$$

$$\downarrow$$

OH

O—Si———(CH$_2$)$_3$X

OH
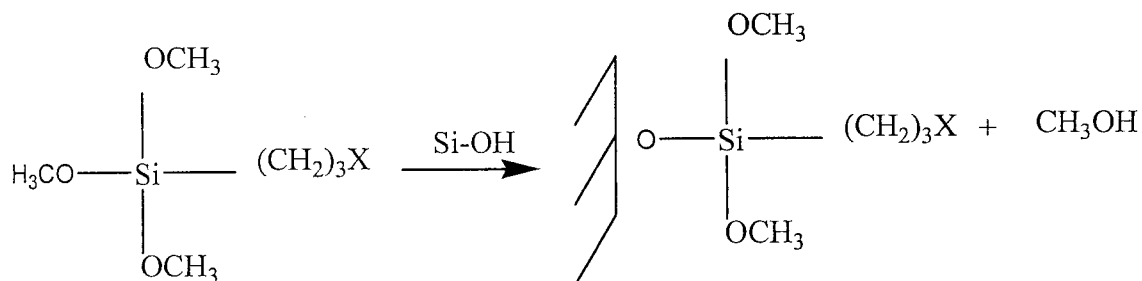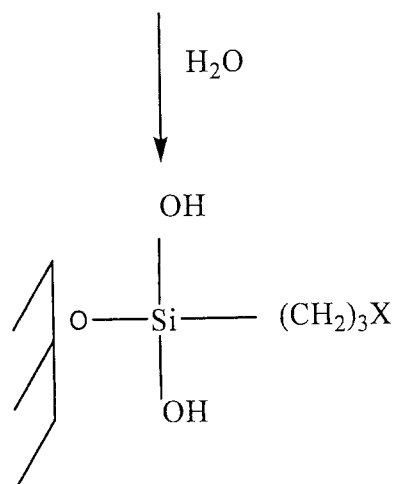
ADSORPTION

Adsorption is defined as a process of accumulation of gas or liquid solute on the surface of a solid. This process can be categorized into two forms, physical and chemical depending on the nature of forces involved. The process which occurs without any chemical reaction is termed physical adsorption or physisorption. It occurs because of the weak van der Waals forces that are electrostatic in origin and are termed dispersion forces. Dispersion forces often account for the major part of adsorbate-adsorbent potential, as they exist in all types of matter despite the nature of other interactions. Physical adsorption is affected by many parameters including the properties of the adsorbate material like molecular size, molecular mass, boiling point, polarity and properties of the adsorbent material like polarity, pore size, etc. The process which occurs because of the chemical interaction between adsorbate and adsorbent is termed chemical adsorption or chemisorption. This process occurs because of the sharing of electrons between adsorbate molecules and the surface of the adsorbent. Chemisorption is confined to a single layer of molecules on the surface and may be followed by additional layers of

physically adsorbed molecules. Both physisorption and chemisorption can occur simultaneously or alternatively under favorable conditions.[15,16]

Adsorption is widely used in industrial processes like separation and purification. This technique is widely employed for the removal of low concentrations of organic pollutants from large volumes of potable water, waste water and process effluents. Textile industries use a wide variety of dyes like reactive, acidic and basic dyes which are considered toxic and carcinogenic. The main source of dyes in waste water is from textile industries and extensive research is under investigation to remove these dyes effectively. For the removal of these dyes, adsorbents having high functionality and possessing high surface area are widely used.

Basic dyes also known as synthetic dyes are present in waste water effluents. These are in general, cationic dyes possessing cationic properties, consisting of positively charged nitrogen or sulfur atoms. The positive charge is more localized on the nitrogen atom. Basic dyes are named because of their affinity to basic textile materials with net negative charge. Basic dyes exist in shiny crystalline forms.[15]

Methylene blue is the most important basic dye discovered by Caro in 1878. It is an aromatic chemical compound with the structure as below.
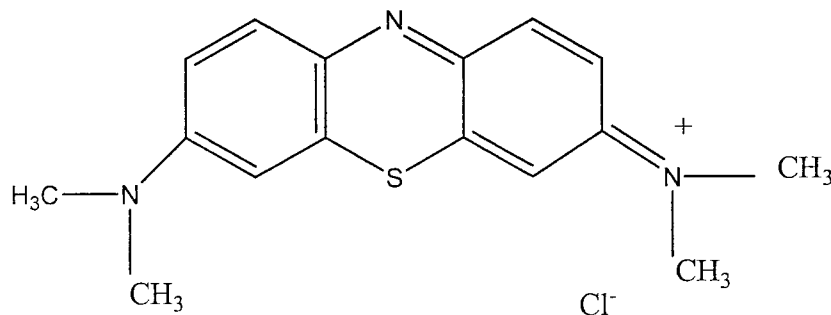
It appears as a dark green powder and crystalline solid at room temperature and yields blue colored solutions when dissolved in water. It is used as a redox indicator in

chemistry and as a stain in biology. It dissociates like electrolytes into methylene blue cation and chloride anion in aqueous solution. It has some harmful effects on human beings and hence it is desirable to be removed from waste water. To understand the adsorption process, information regarding adsorption equilibria is important.[15]

ADSORPTION ISOTHERMS

Adsorption can be best described by means of isotherms, which gives the information about the amount of adsorbate on the adsorbent. Adsorption isotherm studies can be used to assess the efficiency of adsorbent to remove adsorbate from aqueous solutions. To optimize the design of the adsorption system it is necessary to correlate the equilibrium data by either theoretical or empirical equations to that of practical data Some adsorption experiments were carried out previously by shaking constant mass of adsorbent with a constant volume of methylene blue solutions with increasing dye concentrations. pH of the solutions were adjusted by adding 0.1 N HCl and 0.1 N NaOH. pH plays an important role because the hydrogen ion concentration affects the extent of ionization of dyes and surface properties of adsorbent.[15]

LANGMUIR ISOTHERM

Langmuir proposed a theory to describe adsorption of gas molecules onto the solid surface. This adsorption isotherm has found success in explaining many other real sorption processes involving monolayer adsorption. The Langmuir isotherm has several assumptions: intermolecular forces decrease rapidly with distance, predicting the existence of monolayer coverage of adsorbate at the outer surface of the adsorbent; adsorption takes place only at specific homogeneous sites on the surface of the adsorbent, all the sites on the adsorbent are identical and energetically equivalent and once a dye

molecule occupies a site, no further adsorption can take place at that site. These assumptions are seldom true because of the imperfections existing on the surface of the adsorbent.[18] The Langmuir equation is expressed as

$$\frac{C_2}{n_2^s} = \frac{1}{n^s b} + \frac{C_2}{n^s}$$

where C_2 is the equilibrium solute concentration

n_2^s is the number of moles of solute

n^s is the moles of adsorption sites per gram of adsorbent

b is a constant

A plot of $\frac{C_2}{n_2^s}$ versus C_2 gives a straight line of slope of $1/n^s$ and intercept of $1/n^s b$[19].

AIMS OF THIS WORK

SA, ST and AST samples are prepared by heating and subsequently oxidizing the precursors MCl_n (M = Si, Al, Ti, etc.). These precursors show differences in reactivity and hence the surface compositions of the mixed fumed oxides vary from the overall composition of the primary particles. The distribution of precursors on heating also affects the distribution of corresponding oxides on the surface. This is important because the adsorption and catalytic behavior of the materials is affected by the changes in the surface composition of the mixed oxides.

Our first aim is to characterize surface silanols in a series of oxides; silica, alumina, titania and mixed oxides such as silica/alumina (SA), silica/titania (ST), alumina/silica/titania (AST) at different contents of silica, alumina, titania and at different temperatures by means of FTIR spectroscopy. This is done by using transmission and

reflectance FTIR spectroscopic techniques. Transmission FTIR spectra are used to determine the composition of oxides and mixed oxides. Diffuse reflectance FTIR spectra are used to characterize surface silanols. In order to insure that the OH stretching vibrations detected in the FTIR are only from surface hydroxyl groups, thermogravimetric analysis is performed on all the samples.

New catalytic active sites are generated on the surface of silica/titania samples as a result of formation of Si-O-Ti bonds. Previous investigations have shown an increase in the Si-O-Ti band up to 20 wt % of titania. Therefore, our second aim is to characterize mixing of phases in mixed oxides, especially in ST samples i.e., quantitative characterization of the Si-O-Ti band at 960 cm^{-1}, as a function of Si content.[20]

After knowing the surface silanol content, our next aim is to modify ST samples with organofunctional silanes in order to enhance adsorption for improved photocatalytic decomposition reactions. For the purpose of enhancing the adsorption for photocatalytic decomposition reactions, modification of pure silica with organofunctional silanes is done first by reacting silica with various organofunctional silanes in refluxing toluene medium. Then the adsorption behaviour of methylene blue on silica and modified silicas is studied in order to choose a functional group for methylene blue decomposition with ST samples. Adsorption isotherms of methylene blue on modified silicas are obtained for this purpose. From these studies, the functional group for modification on to the ST samples and for methylene blue decomposition experiments is chosen. After choosing a specific functional group, the next step is modification of an ST sample with organosilane, for enhanced adsorption properties. Preliminary photocatalytic reactions

with ST 20 samples are performed in order to test the hypothesis of improved

performance after surface modification with organosilane.

CHAPTER II

MATERIALS AND METHODS

MATERIALS

Samples	Si (wt %)	Al (wt %)	Ti (wt %)
Pure silica (A 500)	100	-	-
Alumina	-	100	-
Titania	-	-	100
SA 1	99	1	-
SA 3	97	3	-
SA 8	92	8	-
SA 23	77	23	-
SA 30	70	30	-
SA 75	25	75	-
ST 2	98	-	2
ST 9	91	-	9
ST 14	86	-	14
ST 20	80	-	20
ST 40	60	-	40
ST 63	37	-	63
ST 65	35	-	65
ST 94	6	-	94
AST 50	28	22	50
AST 71	8	21	71
AST 82	6	12	82
AST 87	4	9	87
AST 88	8	4	88

Table 1: Samples used for analysis

The samples shown in **Table 1** were obtained from the Institute of Surface Chemistry, Kalyush, Ukraine. Cab-O-Sil® used for adsorption experiments was obtained from Cabot corporation (Tuscola, IL). Methylene blue, manufactured by National Aniline and Chemical laboratories, NY, USA was used as received. Millipore water, buffer of pH 7 having the contents sodium phosphate dibasic and potassium phosphate monobasic obtained in capsule form were dissolved in water. This was obtained from Micro essential laboratory, Brooklyn, NY. Organofunctional silanes, 3-mercaptopropyltrimethoxy silane, 3-cyanopropyltrimethoxysilane, 3-thiocyanatopropyltriethoxysilane, 3-aminopropyltrimethoxysilane and hexamethyldisilazane obtained from Gelest, Inc, Morrisville, PA were used as received.

FTIR SPECTROSCOPY

A Digilab FTS-3000 FTIR spectrometer equipped with a liquid-nitrogen-cooled MCT (mercury-cadmium-telluride) detector was used to obtain reflectance FTIR spectra. The same spectrometer utilizing a DTGS (deuterated triglysine sulfate) detector was used to obtain transmission infrared spectra. The optical accessory used for diffuse reflectance (DRA-2CN) and variable temperature cell (HVC-DRP) were obtained from Harrick Scientific (Ossining, NY, USA). The sample temperature was monitored and controlled with a temperature controller obtained from Omega Engineering. A 5% (w/w) of the fumed and mixed fumed oxides was dispersed in 95% (w/w) of ground and dried KCl. The dispersion was heated to 200°C and 300°C for a minimum of 15 min before the spectral data acquisition. The sample height was adjusted in the accessory to obtain the most intense interferogram with the purpose of attaining high signal-to-noise ratio. Interference due to adsorbed water and atmospheric CO_2 is diminished by pumping N_2

through the FTIR sample compartment during sample analysis. Spectra of the samples were acquired at 4 cm^{-1} nominal resolution by co-addition of 64 scans and subjected to 9 point quartic smoothing in order to reduce problems from incomplete ratioing of vapor phase water in the FTIR spectrometer. The spectra of the samples dispersed in KCl are ratioed against that of pure KCl, and the % reflectance data is converted to Log (1/R) to approximate absorbance spectra. The obtained reflectance spectra were converted to Kubelka Munk units.[31] KM units were used to relate the reflectance of a diluted sample of infinite depth to sample concentration. Kubelka Munk units can be mathematically written as

$$KM = \frac{(1-R)^2}{2R}$$

where R is the reflectance of the spectra.

Transmission FTIR spectra were obtained by placing a small amount of sample between two NaCl plates and the plates rotated to disperse the particles. Spectra were obtained at 4 cm^{-1} nominal resolution by co-addition of 16 scans.

THERMOGRAVIMETRIC ANALYSIS

A TGA Q50, obtained from TA Instruments, was used for analyzing the weight loss of the sample. For this purpose, approximately 5 mg of the sample was loaded on a platinum pan and the sample was heated at 10°C/min up to 800°C. Nitrogen gas is purged into the furnace at a flow rate of 40 – 60 ml/min. The thermograms of the samples obtained are converted to derivative weight % to accurately know the point at which the maximum weight loss occurs. The furnace was allowed to cool for 10 min by purging nitrogen gas after each experiment.

SILYLATION REACTIONS

Silica was reacted with organosilanes in refluxing toluene medium for a minimum of 2 hours in the presence of butyl amine catalyst and filtered. The filtered product was washed with toluene and dried in vacuum for 2 hrs at 150°C. These were resuspended in millipore water for 30 min to facilitate cross linking and vacuum dried at 150°C. These various modified silicas were used as adsorbents for performing the adsorption experiments.

ADSORPTION EXPERIMENTS

Methylene blue solutions with concentrations of 80, 70, 60, 50, 30, 20, 10, 5 and 1 ppm were prepared from analytical grade reagent and millipore water. All the solutions were adjusted to pH 7 by adding 0.1 N HCl and 0.1 N NaOH. A standard curve for methylene blue was obtained using 0.25, 1, 2, 4, 5 and 10 ppm concentrations at pH 7. The calibration curve is used to calculate the amount of methylene blue in solution at equilibrium and the amount adsorbed on the adsorbent. Adsorbents (cyano, thiocyano, amino, thiol and HMDS modified silicas) weighing 25 mg were placed in a conical flask each containing various concentrations of methylene blue and shaken on a mechanical shaker overnight prior to the analysis to determine the methylene blue concentration remaining in solution. All the measurements for the adsorption isotherms are obtained at 660 nm corresponding to the maximum absorbance of methylene blue.

UV/Vis SPECTROPHOTOMETER

A Shimadzu UV-vis spectrophotometer (Model UV-3100) was used to measure methylene blue solution concentrations in the adsorption and photocatalytic experiments. Methylene blue solutions used for obtaining the absorbance values were separated from

the adsorbents by means of centrifugation. Some of the highest concentration solutions were diluted for obtaining absorbance values. The obtained absorbance values were used for plotting adsorption isotherms using the standard curve equation at 660 nm.

PHOTOCATALYTIC EXPERIMENTS

Photocatalytic activity experiments are designed in order to know the photodegradation of methylene blue in the presence of photocatalyst. ST 20 and SCN modified ST 20 are used as adsorbents. 0.2 g of powdered adsorbents and 0.2 L of methylene blue solution was added to a glass beaker and the solution stirred with a magnetic stirrer bar. UV light irradiation was provided with a 275 W mercury lamp. Samples of ~ 5 ml volume were withdrawn at fixed time intervals and the concentration of methylene blue was obtained from the UV-Vis spectrophotometer at 660 nm. Methylene blue solutions were separated from the adsorbents by means of centrifugation. Blank reactions were performed in the absence of UV light.

CHAPTER III

RESULTS AND DISCUSSION

Thermogravimetric analysis is performed on all the SA, ST and AST samples in order to determine the loss of water with increasing temperature. The obtained thermograms show similar weight loss curves and hence only a few are shown here (Figures 3, 4 and 5). The weight loss up to 200°C can be attributed to the evaporation of weakly adsorbed water. At above 300°C, the weight loss can be attributed to the loss of strongly adsorbed water or to the condensation of surface hydroxyl groups of silica or titania. The weight is completely constant at around 600°C. From these thermograms, it can be said that these materials possess good thermal resistance. Since all the samples show similar weight loss, it can be said that the amount of alumina or titania incorporated onto the silica surface have no effect on the thermal stability of these materials. Derivative weight loss curve are obtained in order to know the temperature at which the weight loss is maximum. From the derivative curves it is seen that much of the weight loss occurred at around 100°C.

The diffuse reflectance FTIR spectrum of pure silica A 500, demonstrates a sharp silanol peak at 3740 cm^{-1}(Figure 6). SA samples up to alumina wt% of 30 show a silanol peak at ~3740 cm^{-1} (Figures 6-11). All the spectra show similar characteristic peaks as that of pure silica up to alumina wt% of 30, but with 75 wt% of alumina, the spectra approaches that of pure alumina and the intensity of the silanol peak is very low. The silanol peak is seen at the same wavenumber for all the SA samples at 200 and 300°C. It is important to study the silanol groups, because they will be used to react with organosilanes to immobilize various functional groups to the surface. Some small peaks

observed in the 3600-3700 cm^{-1} region (Figures 6-11) correspond to weakly hydrogen bonded silanols. SA samples do not show any individual bands in the IR which can be assigned to bridging hydroxyls such as AlOH, Al-O(H)-Si. The reason for not observing these bands may be due to the formation of hydrogen bonds with adsorbed water, the heterogeneity of the amorphous samples, or the low concentration of these surface groups. The OH stretching vibrations in the 3650-3400 cm^{-1} region (Figures 6-11) correspond to surface hydrogen bonded hydroxyls with water molecules of the neighbouring hydroxyls of the same particle or an adjacent particle. Since the FTIR spectra are recorded at 200 and 300°C, the heating might have caused the formation of denser contacts between adjacent particles.

Diffuse reflectance FTIR spectra of ST samples exhibit a sharp silanol peak at 3740 cm^{-1}. ST samples up to titania wt% of 65 show a silanol peak at ~3740 cm^{-1}, (Figures 12-19) but at 94 wt% of titania, the spectra approached that of pure titania, and the silanol peak is not seen (Figures 15 and 19). Bands seen in the 3600-3700 cm^{-1} are expected to correspond to bridging hydroxyls, but because of the low concentration of these groups and possible interference from the vapor phase water rotation bands, it is not possible to assign specific bands to bridging surface hydroxyls. It is interesting to note that these bands are more visible at 300°C (Figures 16-19) compared to 200°C (Figures 12-15) because of less perturbation due to surface adsorbed water. A band at 3300-3200 cm^{-1} corresponds to surface hydroxyls and strongly adsorbed water molecules (Figures 12-19). These hydroxyls may be present in very narrow micropores which undergo hydrogen bonding interactions.

Diffuse reflectance FTIR spectra of AST samples exhibit a sharp silanol peak only for AST 50 having silica wt% of 28 (Figure 20). The other AST samples do not show sharp silanol peaks because of the low silica content in those samples (Figures 20-23). Bands are observed in the 3600-3700 cm^{-1} region as observed for the SA and ST samples which are expected to correspond to bridging hydroxyls, but because of the low concentration of these groups and possible interference from the vapor phase water rotation bands, it is not possible to assign specific bands to bridging surface hydroxyls. The band at 3300-3200 cm^{-1} corresponds to surface hydroxyls and strongly adsorbed water molecules. These hydroxyls may be present in very narrow micropores which undergo hydrogen bonding interactions.

The silanol content is determined for SA and ST samples, as these groups will react with organosilanes. The silanol content of SA and ST samples can be measured from the integrated band areas of diffuse reflectance spectra. The relative amounts of silanols for the SA and ST samples is estimated from the ratio of Si-OH band area at ~3740 cm^{-1} to that of Si-O-Si combination vibration band area at 1860 cm^{-1} (Figures 24-27).[12, 13] The band position at ~3740 cm^{-1} does not vary with the titania or alumina content, which indicates that this band does not contain significant contributions from other OH species in the sample. The band position is consistently at 3742 cm^{-1} for SA samples and 3738 cm^{-1} for ST samples. Small differences in the Si-O combination vibration range at 1860 cm^{-1} for SA and ST samples is observed (Figures 28 and 29). SA 75 and ST 94 shows a significant difference compared to A 500 and approaches that of pure alumina and pure titania, respectively. The band at 1860 cm^{-1} is used as an internal standard to eliminate the effects of different sample weights and, therefore, differences in

spectral intensities. The percentage of silica is taken into account in calculating the band area ratios. For example, the band area of Si-OH when divided by band area of Si-O-Si multiplied with 1.02 gives the band area ratio at 98 wt% of silica. The calculations for other samples are done in the same way by considering the silica percentage. The plots show a decrease in silanol content with an increase in alumina and titania contents though the trend is not smooth at low alumina and titania contents (Figures 24-27). From this it can be said that there is a non linear dependence of silica phase as the content of alumina and titania increases. The spectra of AST also show small differences in the Si-O combination vibration at 1860 cm^{-1}(Figure 30). AST 71, AST 82, AST 87 and AST 88 show significant differences compared to A 500 and approaches that of pure alumina or pure titania.

In the case of ST samples, ST 20 exhibits minimal loss in Si-OH content, yet there is significant TiO$_2$. Thus, this is a good candidate for photocatalytic studies because there is sufficient TiO$_2$ to exhibit photocatalysis and sufficient Si-OH groups to functionalize the surface.

FTIR spectra in the Si-O stretching vibration range of SA, ST and AST samples show small differences at 1100 cm^{-1} and 800 cm^{-1} (Figures 31-33). All the SA samples show similar spectra in the 1100 cm^{-1} and 800 cm^{-1} region except SA 75 which shows significant differences compared to A 500. The spectrum of SA 75 approaches that of pure alumina because of less silica content (Figure 31). Among AST samples, only AST 50 shows similar Si-O stretching vibrations in the 1100 and 800 cm^{-1} region as that of A 500 (Figure 32). ST samples at high contents of titania show a significant difference at 800 cm^{-1}. The spectrum of ST 94 approaches that of pure titania as it has more titania

content (Figure 33). A new band appears at 960 cm^{-1} for some of the ST samples which corresponds to Si-O-Ti linkages.

For the purpose of quantitatively measuring the content of Si-O-Ti linkages in the ST samples, integrated absorbance values from transmission FTIR spectra are used. The relative amounts of Si-O-Ti bands in the ST samples is obtained from the ratio of Si-O-Ti vibration band at 1000-870 cm^{-1} region to that of Si-O stretching vibration region (870-760) at 800 cm^{-1} (Figure 34), (1920-1820) at 1860 cm^{-1} (Figure 35) and (1290-980) at 1100 cm^{-1} (Figure 34). The Si-O stretching vibrations at 800, 1100 and 1860 cm^{-1} are taken as internal standards to avoid the differences in sample weights and spectral intensities. The percentage silica content is taken into account in calculating the band area ratios. For example, the band area at 960 cm^{-1} region when divided by the band area at 800 cm^{-1} region multiplied by 1.25 gives a band area ratio for a material containing 80 % silica. The calculations for other samples are done in the same way by taking into account the silica percentage. From the three plots of Si-O-Ti band area ratio versus % silica (Figures 36-38) it is seen that ST 20 has the largest contribution for Si-O-Ti bonds, in agreement with previous work.[8] ST 20 (80% silica and 20% titania) has a greater degree of phase intermixing and hence a greater concentration of Si-O-Ti bonds are observed. From the above observations, it can be said that there is a nonlinear dependence of Si-O-Ti bonds as the total content of titania increases.

Transmission FTIR spectra of Cab-O-Sil® and Cab-O-Sil® surface modified with various organofunctional silanes are obtained in order to confirm the presence of silane groups on the modified silica surface. The FTIR spectrum of silica surface modified with 3-cyanopropyltrimethoxysilane shows the loss of silanol peak, indicating the reaction of

silanol group with the organosilane and siloxane bond formation (Figure 39). The propyl groups attached to the Cab-O-Sil® are identified by the C-H stretching band in the 2980 – 2820 cm^{-1} region which show the attachment of organic moiety to the surface of silica. The band for cyano stretching vibration is seen at 2256 cm^{-1}.

The FTIR spectrum of Cab-O-Sil® surface modified with 3-thiocyanopropyltriethoxysilane also shows the loss of silanol peak, indicating the reaction of silanol group with organosilane and siloxane bond formation. The band for thiocyano stretch is seen at 2166 cm^{-1} region. The C-H stretching band in the 3000-2800 cm^{-1} region shows the propyl groups attached to the surface of silica (Figure 40).

The FTIR spectrum of 3-mercaptopropyltrimethoxysilane modified onto Cab-O-Sil® show the loss of silanol peak indicating the reaction of silica with silane and formation of siloxane bond. The C-H stretching band seen in the 3000-2800 cm^{-1} region shows the attachment of silica surface to the organic moiety. A very weak band for thiol stretching vibration is barely detectable at 2575 cm^{-1} (Figure 41).

The FTIR spectrum of 3-aminopropyltrimethoxysilane modified on Cab-O-Sil® also shows the loss of silanol peak at 3740 cm^{-1}. The appearance of C-H stretching bands in the 3000-2800 cm^{-1} region are observed, as are N-H stretches (3400 – 3300 cm^{-1}, and the N-H deformation band at approximately 1550 cm^{-1} (Figure 42).[28]

The FTIR spectrum of Cab-O-Sil® modified with HMDS also shows the silanol peak loss at 3740 cm^{-1} which is in agreement with previous work[26] and methyl peaks at 2964 and 2912 cm^{-1} (Figure 43). The loss of silanol peak indicates the reaction of silane with the surface hydroxyl groups.

After modification of the silica surface with organofunctional silanes, the aim is to study the adsorption behaviour of methylene blue (adsorbate) on silica and modified silicas (adsorbents). These studies inform the choice of an appropriate organosilane for surface functionalization in order to enhance methylene blue adsorption and ultimately photocatalytic decomposition.

At constant pH, the adsorption isotherms are plotted using the concentration of methylene blue in solution, C_2 and the amount of methylene blue adsorbed on the adsorbent, n_2^s to represent the equilibrium. The equilibrium relationship obtained depends on the concentration of adsorbate in the fluid phase and the concentration adsorbed on the adsorbent at constant pH.

Figure 44 shows the calibration curve obtained using methylene blue concentrations, 0.25, 1, 2, 4, and 5 ppm at pH 7. The equation displayed in this figure is used for the calculation of amount of adsorbate in the solution and on the adsorbent. The amount of methylene blue adsorbed on the adsorbent is obtained by subtracting the amount of methylene blue present in solution after adsorption from the amount of methylene blue present in the original solution. Table 2 shows the data corresponding to methylene blue adsorption onto Cab-O-Sil® at pH 7. Figure 45 shows the adsorption isotherm of methylene blue adsorption onto Cab-O-Sil® at pH 7. The shape of an isotherm determines the nature of adsorption. The isotherms have been classified according to Giles et.al.[27] into four main groups: S, L, H and C. According to his classification the isotherm of methylene blue adsorption on Cab-O-Sil® displays an S shaped curve. This S shape indicates the adsorption of molecules vertically on the surface.[27] The S shape of the curve shows less amount of solute taken up by the adsorbent

at lower concentrations. At this point there is more chance for solute molecules to find a suitable site on the adsorbent.

Table 3 shows the data corresponding to methylene blue adsorption onto cyano modified Cab-O-Sil®. Figure 46 shows the adsorption isotherm of methylene blue adsorption onto the silica surface modified with cyano groups at pH 7. According to the classification of Giles *et.al*[27], this isotherm shows an L curve pattern.[22] An L shaped curve indicates the adsorption of solute molecules flat on the surface. The L shape indicates more solute is taken up by the adsorbent and almost all the sites on the adsorbent are filled. Hence, it becomes difficult for the solute molecules to find a vacant site available for adsorption. The initial portion of this curve shows good strength of adsorption compared to Cab-O-Sil® and amine treated Cab-O-Sil® (Figure 51). The good strength shows that the solute has a high affinity for adsorption in dilute solutions. The plateau portion of the curve shows less extent of adsorption compared to Cab-O-Sil®, amine, thiocyano and thiol modified Cab-O-Sil® and more extent of adsorption compared to HMDS modified Cab-O-Sil® (Figure 51). The long plateau of the curve indicates monolayer adsorption on the surface of the adsorbent.

Table 4 shows the data corresponding to methylene blue adsorption onto thiocyano modified Cab-O-Sil®. Figure 47 shows the adsorption isotherm of methylene blue adsorption onto the silica surface modified with the thiocyano groups at pH 7. According to the classification of Giles *et.al*, the shape of the curve looks like a special L curve pattern. The initial portion of this curve shows higher strength of adsorption compared to Cab-O-Sil®, cyano and amino modified Cab-O-Sil®. The plateau portion of the curve shows greater extent of adsorption compared to cyano and HMDS modified

Cab-O-Sil® (Figure 51). Here, the solute has high affinity for adsorbent in dilute solutions. In dilute solutions, the solute is almost completely adsorbed and only less measurable amounts remain in the solution. The plateau portion of the curve represents monolayer coverage on the surface of the adsorbent.

Table 5 shows the data corresponding to methylene blue adsorption onto thiol modified Cab-O-Sil®. Figure 48 shows the adsorption isotherm of methylene blue adsorption onto the silica surface modified with the thiol groups at pH 7. The initial portion of the curve shows higher strength of adsorption compared to Cab-O-Sil®, amino and cyano modified Cab-O-Sil®. The plateau portion of the curve shows a greater extent of adsorption compared to cyano, thiocyano and HMDS modified Cab-O-Sil® (Figure 51). Here the solute molecules have a high affinity for the adsorbent in dilute solutions. At the beginning of the initial portion of the curve a short plateau portion or an inflection is seen indicating the point of first degree saturation of the surface, indicating monolayer coverage. From this it can be said that all the possible sites in the original surface are filled and further adsorption occurs only on the new surfaces. A condensed monolayer formed on the top of the first is seen from the second plateau of the curve. The extent of coverage seen from the second plateau of the curve indicates the formation of a complete monolayer.

Table 6 shows the data corresponding to methylene blue adsorption onto amine treated Cab-O-Sil®. Figure 49 shows the adsorption isotherm of methylene blue adsorption onto the silica surface modified with the amine groups at pH 7. This isotherm shows a greater extent of adsorption compared to cyano, thiocyano, thiol and HMDS modified Cab-O-Sil® but poor strength of adsorption compared to thiol, thiocyano and

HMDS modified Cab-O-Sil® (Figure 51). At dilute concentrations, it can be seen that there is not much solute adsorbed on the surface of the adsorbent.

Table 7 shows the data corresponding to methylene blue adsorption onto HMDS modified Cab-O-Sil®. Figure 50 shows the adsorption isotherm of methylene blue adsorption onto the silica surface modified with HMDS at pH 7. The shape of the isotherm looks like a H curve pattern. The initial portion of the curve shows greater strength of adsorption compared to amine and cyano modified Cab-O-Sil®. The plateau portion of the curve shows lesser extent of adsorption compared to Cab-O-Sil®, cyano, thiocyano, and amine modified Cab-O-Sil® (Figure 51). From the initial portion of the curve it can be said that there is no measurable amount of solute left in the solution at dilute concentrations. The point of inflection indicates the monolayer coverage of the surface or first degree of saturation of the surface of adsorbent. All the possible sites on the surface of the adsorbent are filled and further adsorption occurs only at new sites. The second plateau of the curve or final portion indicates complete monolayer coverage.

In Figure 51 all the adsorption isotherms are plotted on the same scale. Thiocyano and thiol groups modified onto the Cab-O-Sil® shows similar and greater strength of adsorption compared to Cab-O-Sil®, cyano and HMDS modified silicas. Thiol groups modified onto Cab-O-Sil® shows greater extent of adsorption compared to cyano, thiocyano and HMDS modified silicas but lesser extent compared to amine treated Cab-O-Sil®. From these observations, thiocyano and thiol functional groups were chosen for methylene blue photocatalytic decomposition. In order to obtain quantitative data, the applicable isotherms were fit to the Langumir equation. Langmuir plots are best applicable to adsorption isotherms which show L type of adsorption behaviour.

The adsorption data for all the isotherms are analyzed by a regression analysis to fit the Langmuir isotherm model. A plot of $\frac{C_2}{n_2^s}$ versus C_2 gives a straight line of slope $1/n^s$ and intercept of $1/n^s b$. The correlation coefficient value tells us whether this type of linearization is appropriate for a given plot. Figure 52 shows the Langmuir fit for methylene blue adsorption onto cyano modified Cab-O-Sil®. The correlation coefficient value of 0.9807 is an indication of appropriate fit for this plot. A good fit of the Langmuir model indicates a homogeneous surface of the adsorbent having identical sites that are energetically equivalent and equally available for adsorbate molecules. A good fit also indicates the absence of interaction between adsorbate molecules and monolayer coverage of the adsorbate at the outer surface of the adsorbent.

Figure 53 shows the Langmuir plot for SCN modified Cab-O-Sil® at pH 7. The correlation coefficient value of 0.9819 suggests the data exhibit reasonable linearity. This plot also shows monolayer coverage of adsorbate on the outer surface of the adsorbent. Figure 54 shows Langmuir plot for SH modified Cab-O-Sil®. The correlation coefficient value of 0.9882 is an indication of appropriate fit for this plot. Figure 55 shows Langmuir plot for HMDS modified Cab-O-Sil®. The correlation coefficient value of 0.9761 shows a good fit of Langmuir model for this plot. From the above results it can be said that the Langmuir equation provides a reasonably accurate description of the experimental data. Equilibrium constant values are calculated from the slope and intercept obtained from the Langmuir plots and the activity of water is chosen as 55.5 M. The higher equilibrium constant values are indicative of greater strength of adsorption. From the observation of results in Table 8, it can be seen that thiol and thiocyano functional groups result in the largest equilibrium constants and hence greatest adsorption strength for methylene blue.

It was decided that these functional groups would be bonded onto the ST samples for methylene blue photodecomposition studies.

The FTIR spectra of ST 20 and 3-mercaptopropyltrimethoxysilane modified onto ST 20 are shown in Figure 56. The silanol peak at 3740 cm^{-1} is not seen in the transmission FTIR spectra of ST 20 because of interference from water, but silanols are present on the surface of ST 20 which can be seen from the diffuse reflectance FTIR spectra (Figures 13 and 17). The C-H stretching band seen in the 3000-2835 cm^{-1} region shows the attachment of the surface of ST 20 to the organic moiety. The band for thiol stretching vibration barely detectable at 2590 cm^{-1}, indicates the presence of thiol groups. The absorptivity of this band is quite low, making it difficult to detect.

The FTIR spectra of ST 20 and thiocyano groups modified onto ST 20 are shown in Figure 57. The spectrum of thiocyano groups modified over ST 20 shows the thiocyano stretch at 2166 cm^{-1} and C-H stretching band in the 3000-2890 cm^{-1} region.

In cases where ST samples are surface modified with organosilanes, it is possible that not only SiO-H groups are reacted, but also TiO-H groups. While the former is desirable, the latter would be harmful to photocatalytic activity since the TiO-H groups are photocatalytic active sites. Therefore prior to using the surface modified ST 20 for photocatalysis, it is important to eliminate the surface modified TiO-H groups. Since the Ti-O-Si bond is hydrolyzable due to its polarity, the SCN modified ST 20 sample was exposed to water and dried prior to its use as a photocatalyst. In order to detect any loss of thiocyano groups after treatment with water, the spectra of SCN modified ST 20 are obtained before (i.e, after the reaction of organosilane with ST 20 in toluene medium and before resuspending in millipore water) and after treatment with water (i.e., after

resuspending the dried sample in millipore water for 30 min). The amount of thiocyano groups before and after treatment with water is obtained from the ratio of SCN band area at $2180 - 2140$ cm^{-1} region to that of Si-O-Si combination band at 1920-1800 cm^{-1} region. The band area ratios of SCN modified ST 20 before and after treatment with water are shown in Table 9. In order to know if there is any significant difference in the amount of thiocyano groups lost, a t-test is performed on these samples, assuming two samples with equal variances. t-calculated and t-test values obtained at 95% confidence level are shown in Table 10. The obtained t-calculated value, 2.49 is greater than the t-test value, 2.45 at 95% confidence level and hence there is significant difference in the two mean values. The probability of observing the two mean values and the two standard deviations by a random chance if the means are same is 4.6%, thus there is slightly greater than a 95% chance that some loss of organosilane results from the water treatment. It is likely that loss of thiocyano groups attached to Si-O-Ti linkages is responsible for this result.

Table 11 shows the data corresponding to methylene blue adsorption onto ST 20 at pH 7. Table 12 shows the data corresponding to methylene blue adsorption onto thiol groups modified over ST 20. The adsorption isotherms of methylene blue adsorption onto ST 20 and thiol modified ST 20 at pH 7 are shown in Figure 58. The isotherm of SH modified ST 20 shows less amount of adsorption at initial concentrations. The reason for this behaviour is because of its hydrophobicity to water; it was observed that thiol-modified ST 20 was sufficiently hydrophobic that it did not disperse in water, affecting its adsorption behavior towards the methylene blue dissolved in the aqueous phase.

Table 13 shows the data corresponding to methylene blue adsorption onto thiocyano modified ST 20 at pH 7. Adsorption isotherms for ST 20 and thiocyano groups modified onto ST 20 are shown in Figure 59. At initial concentrations, up to 5 ppm initial concentration of methylene blue in solution, a slightly greater strength of adsorption is seen for thiocyano groups modified onto ST 20, but the extent of adsorption is greater for ST 20.

Isotherm data linearized assuming Langmuirian behavior for ST 20 is shown in Figure 60. The Langmuir plot for SCN modified ST 20 is shown in Figure 61. Equilibrium constant values are calculated from the slope and intercept obtained from the Langmuir plots (Table 14). The equilibrium constant value of thiocyano groups modified onto ST 20 is more which indicates greater strength of adsorption (Table 14). It should be noted that these data in Table 14 are not highly reliable since these isotherms are far from exhibiting ideal behavior.

Table 15 shows the data corresponding to methylene blue adsorption onto ST 20 using the conc 0.5-5 ppm at pH 7. Table 16 shows the data corresponding to methylene blue adsorption onto SCN modified ST 20 using the conc 0.5-5 ppm at pH 7. Adsorption isotherms of methylene blue adsorption onto ST 20 and thiocyano modified ST 20 at initial concentrations ranging from 0.5-5 ppm are shown in Figure 62. From the plots, it is seen that thiocyano groups modified onto ST 20 shows greater strength of adsorption for methylene blue than ST 20. As adsorption is an important step for photocatalytic decomposition process to take place, the most strongly adsorbed organosilane i.e., SCN modified ST 20 is chosen for photocatalytic studies of methylene blue at pH 7.

Photodegradation of methylene blue is performed in the presence of pure silica in order to know if photocatalysis occurs in the presence of titania. Figure 63 shows the amount of methylene blue present in solution after photocatalysis in the presence of pure silica and ST 20. This plot shows that there is more amount of methylene blue present in solution in the presence of pure silica compared to ST 20. The loss of methylene blue in pure silica is presumably from adsorption alone, while that in ST 20 is from a combination of adsorption and photocatalysis. This would explain why there is a greater loss of methylene blue with ST 20 than pure silica.

Photodegradation of methylene blue is performed on ST 20 and SCN modified ST 20 in order to evaluate their photocatalytic activity. In monitoring the reaction progress by visible spectrophotometry of the solution, all that is measured is the methylene blue concentration in solution. However methylene blue can be depleted in two ways: 1) catalytic photodecomposition reaction; and 2) surface adsorption. So, in order to take adsorption into account, blank reactions are performed in the absence of UV light using the methylene blue concentration of 5 ppm. The data obtained from the blank reactions provides information on the contribution from adsorption only, since photocatalysis does not occur in the absence of UV light. Figure 64 shows the amount of methylene blue present in solution as a function of time in the absence of UV light. Table 17 shows the amount of methylene blue present in solution in the presence and absence of UV irradiation. The amount of methylene blue adsorbed on the photocatalyst is obtained by subtracting the amount of methylene blue present in solution after adsorption from the amount of methylene blue present in original solution. Figure 65 shows the concentration of methylene blue present in solution after irradiation with UV light as a function of time.

From Figures 64 and 65, it is seen that more amount of methylene blue is present in solution for SCN modified ST 20 than ST 20, i.e., less methylene blue is adsorbed on SCN modified ST 20 than ST 20. This result obtained doesn't correlate with the adsorption isotherm data obtained using the concentrations 0.5-5ppm (Figure 62) because both the experiments are not done using the same conditions.

Experiments done in the presence of UV light gives information about the amount of methylene blue decomposed. The amount of methylene blue reacted is obtained by subtracting the absorbance values obtained in the photocatalytic degradation reaction at a given time t, from the absorbance values obtained for the blank reaction at the same time t. The obtained absorbance values when calibrated using the standard curve equation gives the amount of methylene blue reacted. The photocatalytic equilibrium concentration of methylene blue solution is obtained directly by the absorbance measurement.

Tables 18 and Table 19 show the photocatalytic data of ST 20 and SCN modified ST 20 in the presence of methylene blue at pH 7. Figure 66 shows the degradation curves of methylene blue with ST 20 and SCN modified ST 20 at pH 7. It shows that the amount of methylene blue reacted in the presence of SCN modified ST 20 is greater than that of ST 20. These results are consistent with the data in Figure 62 which indicates that methylene blue adsorption is greater for SCN modified ST 20 than ST 20 under the reaction conditions studied (although, strangely and unfortunately, not conditions for obtaining the adsorption isotherms). Applying the data analysis described above, it is found that the amount of methylene blue decomposed for SCN modified ST 20 increased up to 10 minutes but after 10 minutes the amount decomposed decreased. This result is

not believable since MB is not expected to be regenerated during the experiment. Clearly the role of adsorption has not been adequately taken into account. Nevertheless if these results are to be believed even qualitatively, they show that surface modification has increased the rate of MB photocatalysis on these modified silica-titania samples.

In order to know if the organic residues are still present on the surface of SCN modified ST 20 after UV irradiation, photocatalysis is performed in the presence of water at pH 7. The adsorbent left after the reaction is filtered and dried in vacuum at 140°C. FTIR spectra of this adsorbent (SCN modified ST 20) is obtained. Figure 67 shows the FTIR spectra of SCN modified ST 20 and SCN modified ST 20 after photocatalytic decomposition in the presence of water at pH 7. From the spectra it is seen that the organic groups are still present even after irradiating with UV light. Thus the concept of applying surface modification methods on a silica-titania mixed oxide to enhance adsorption and therefore catalytic activity is a viable concept.
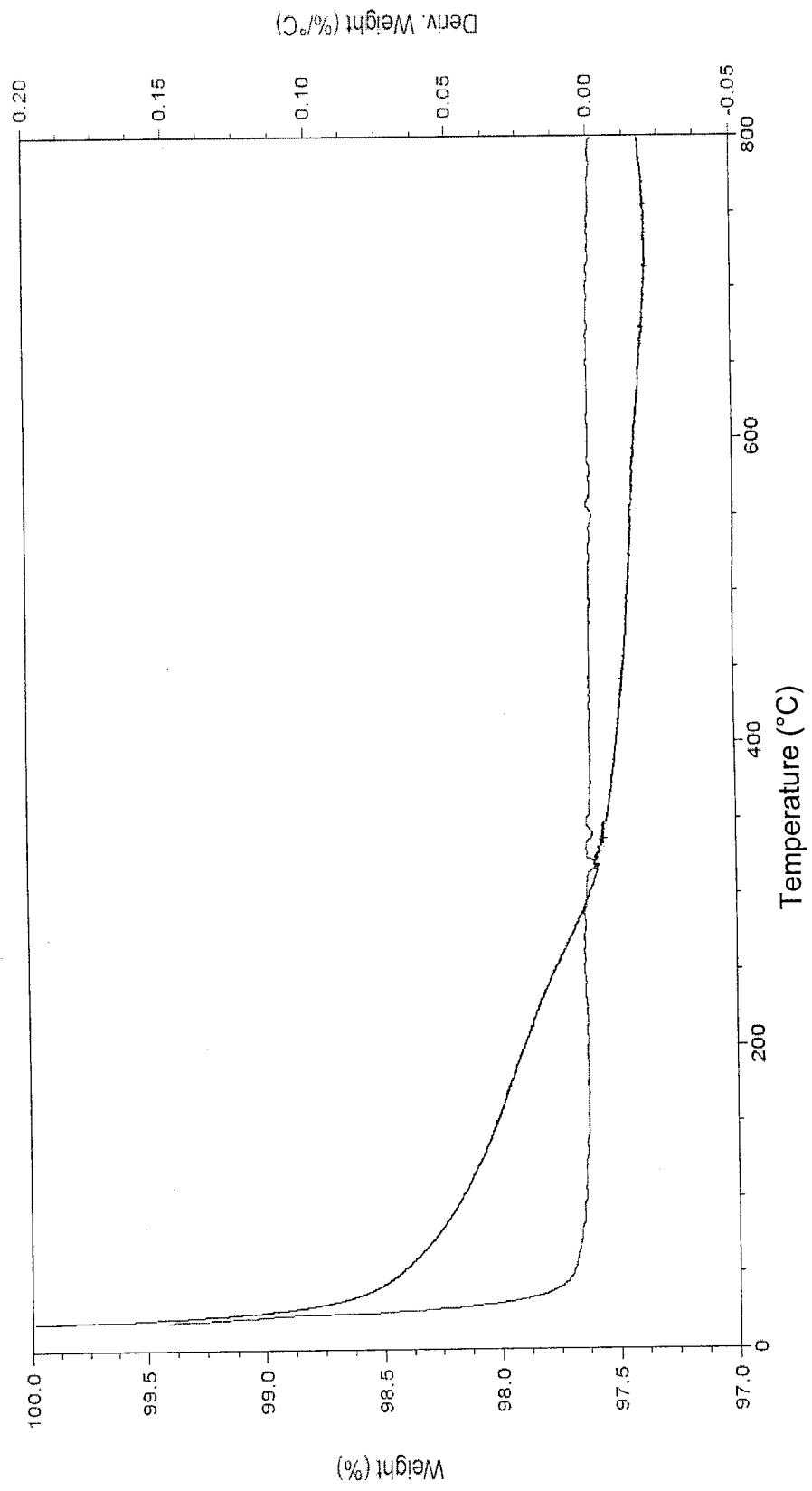
Figure 3: Thermogram of SA 8
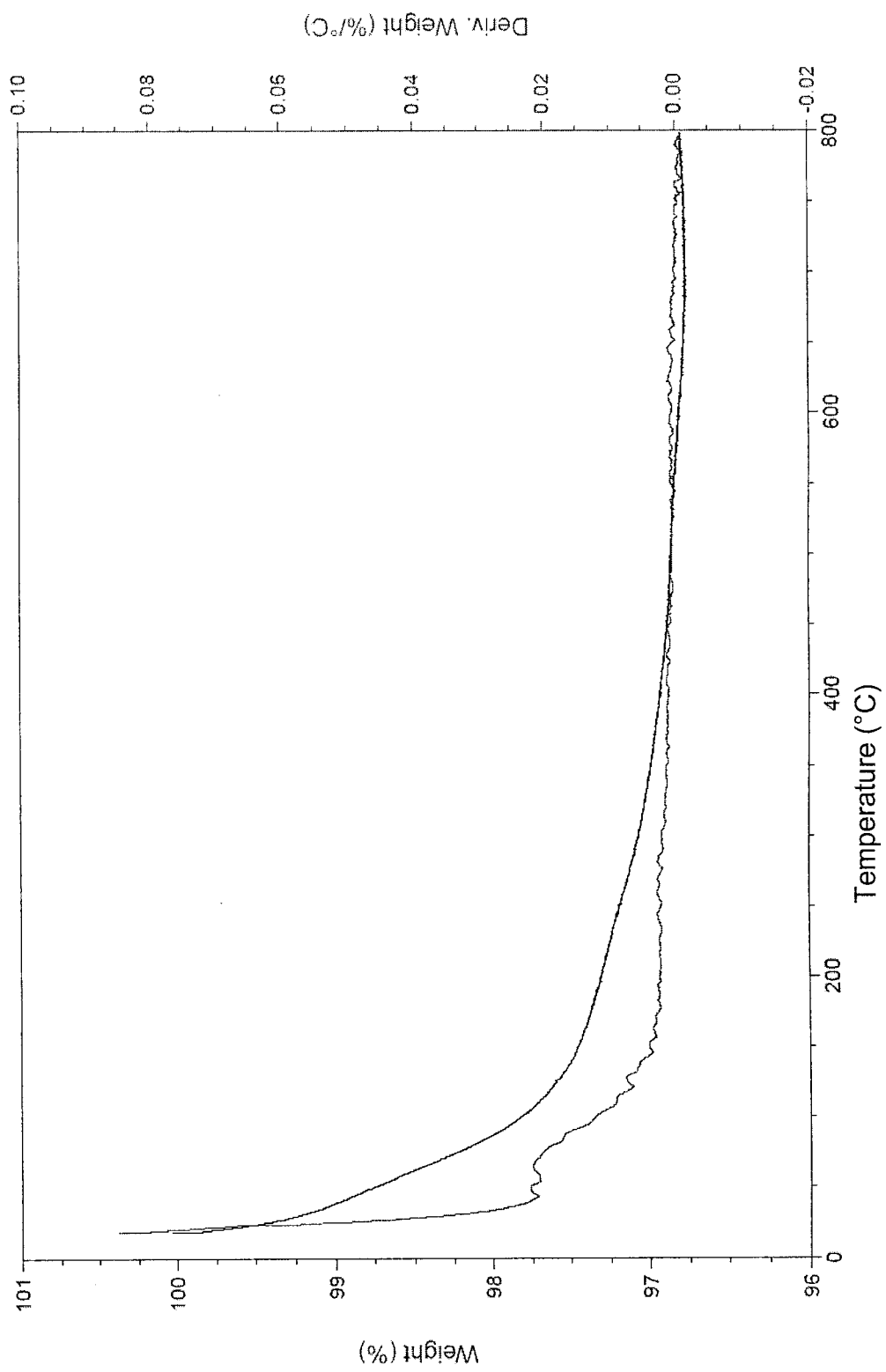
Figure 4: Thermogram of ST 14
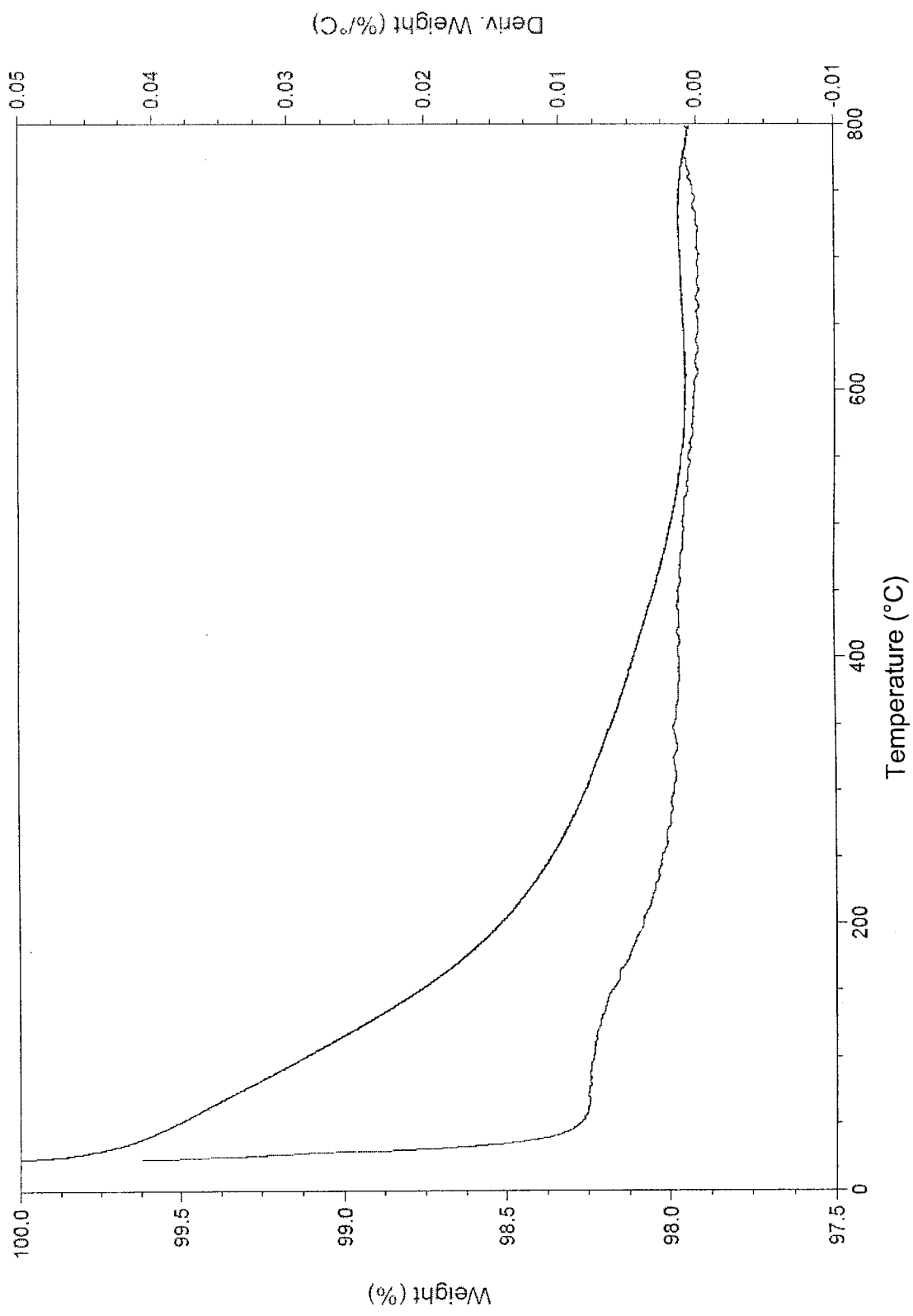
Figure 5: Thermogram of AST 88
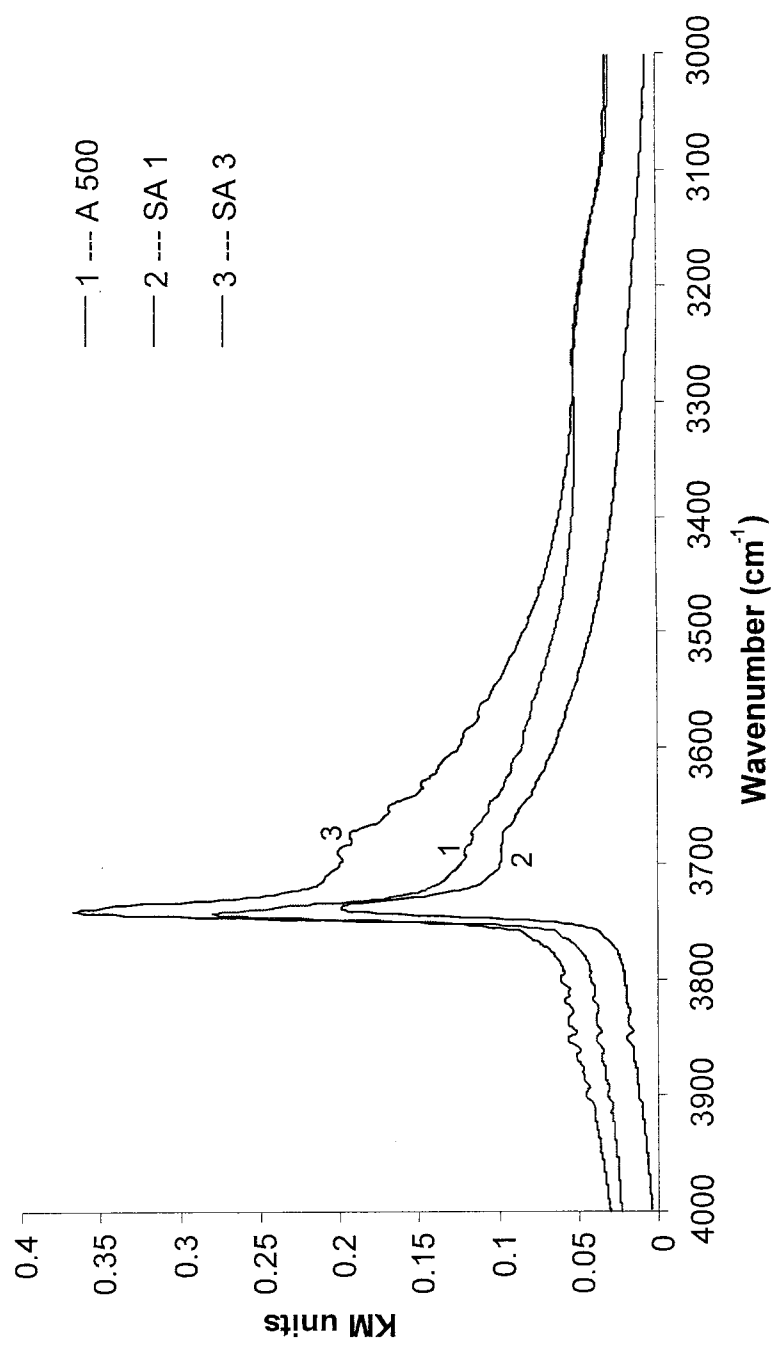
Figure 6: FTIR spectra of 1) A 500, 2) SA 1, 3) SA 3 at 200°C.
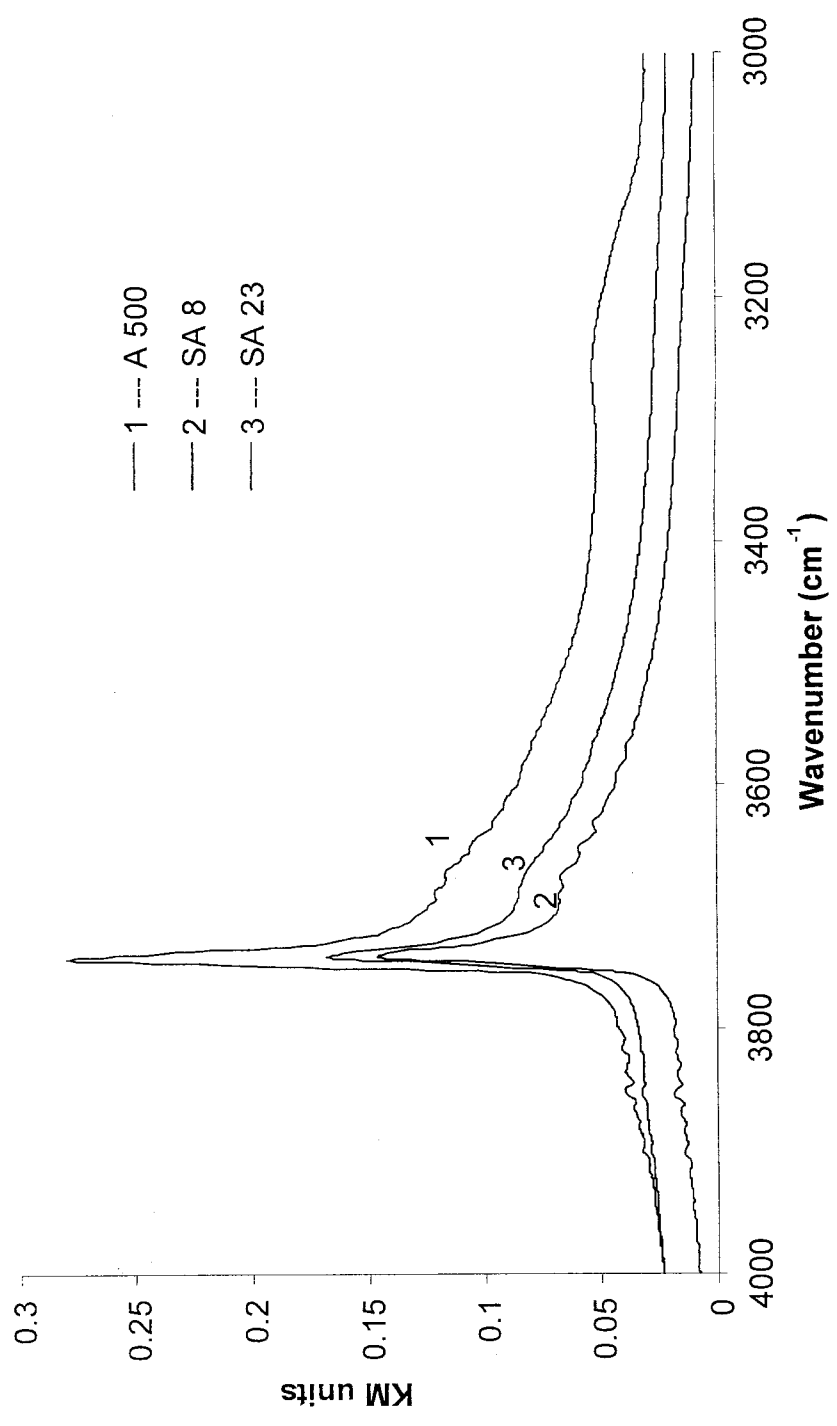
Figure 7: FTIR spectra of 1) A 500, 2) SA 8, 3) SA 23 at 200°C
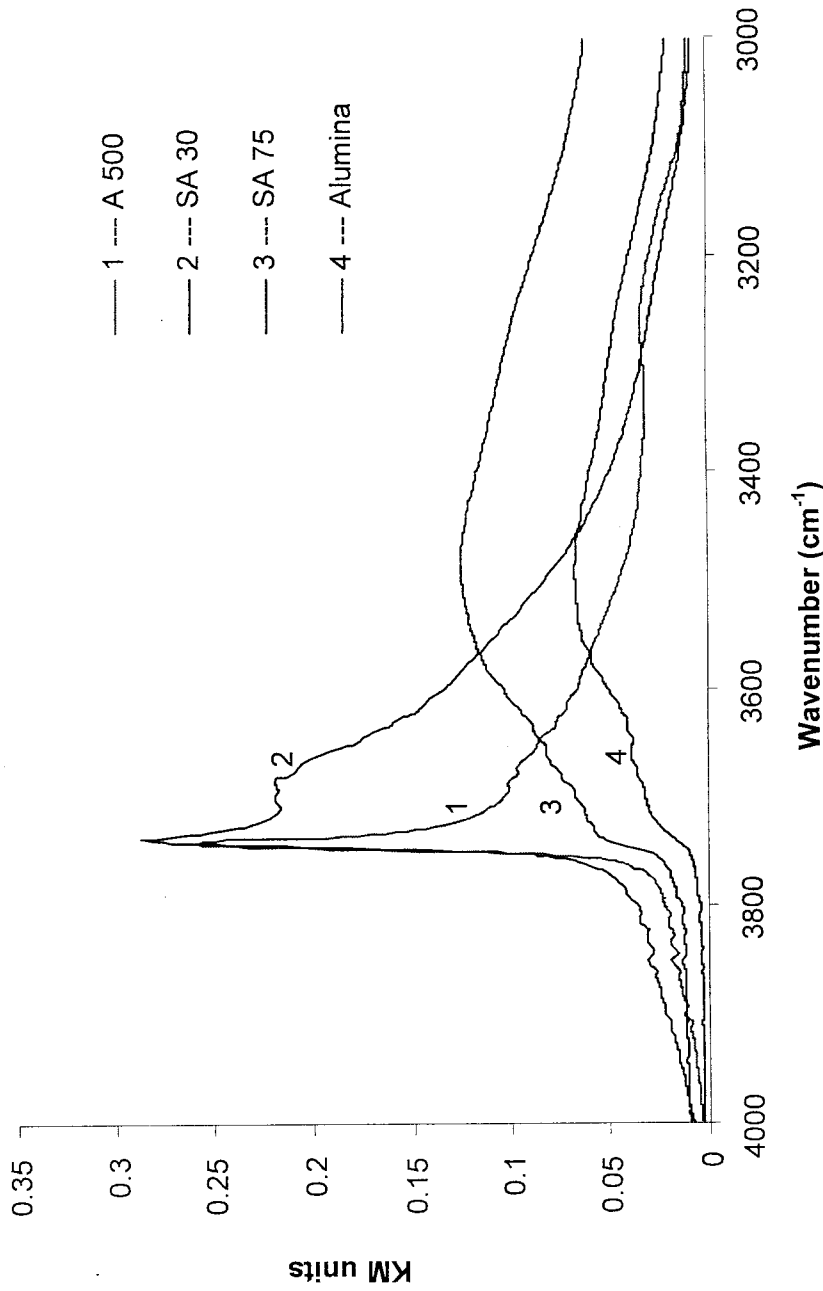
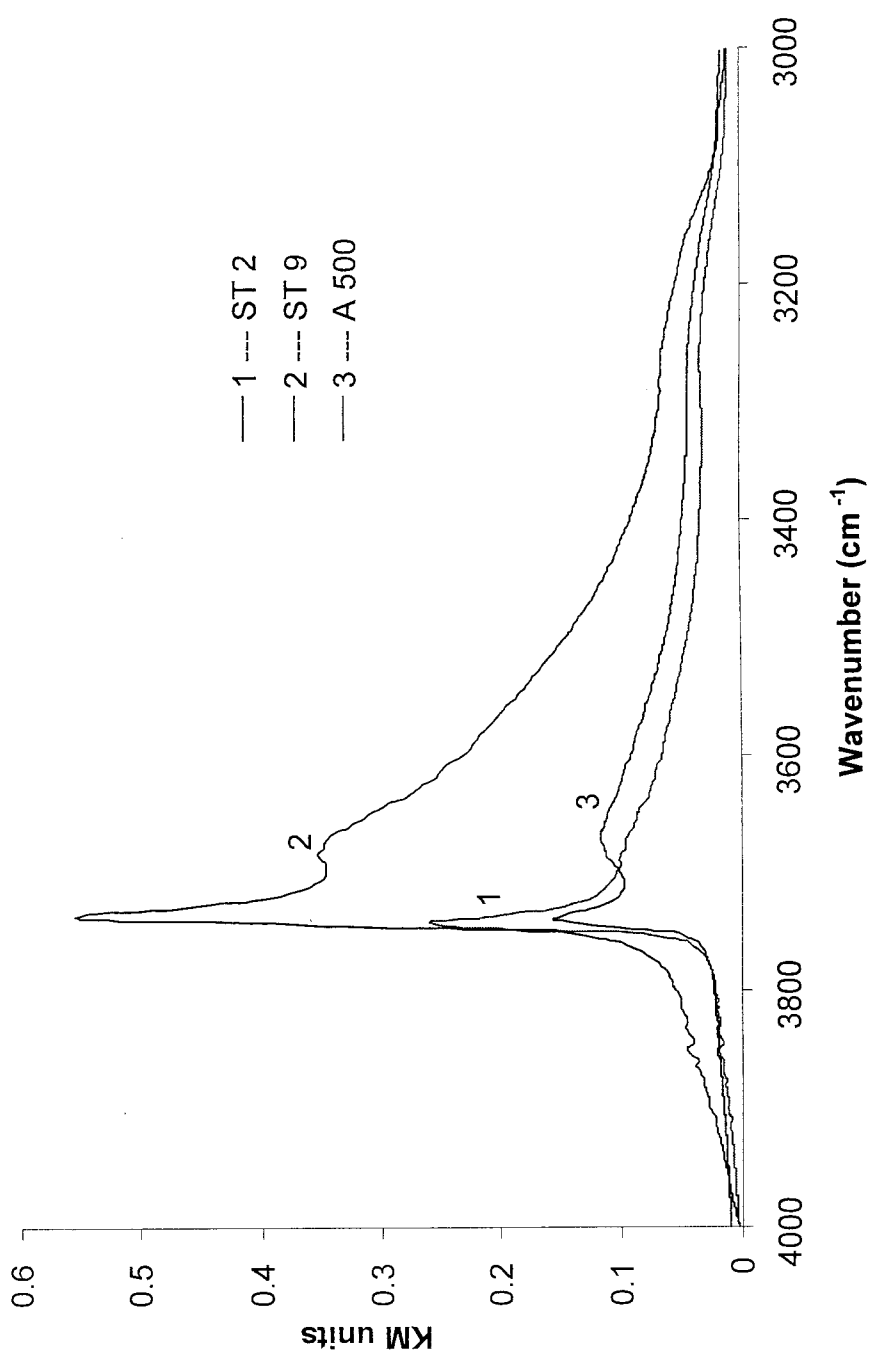Figure 8: FTIR spectra of 1) A 500, 2) SA 30, 3) SA 75, 4) Alumina at 200°C
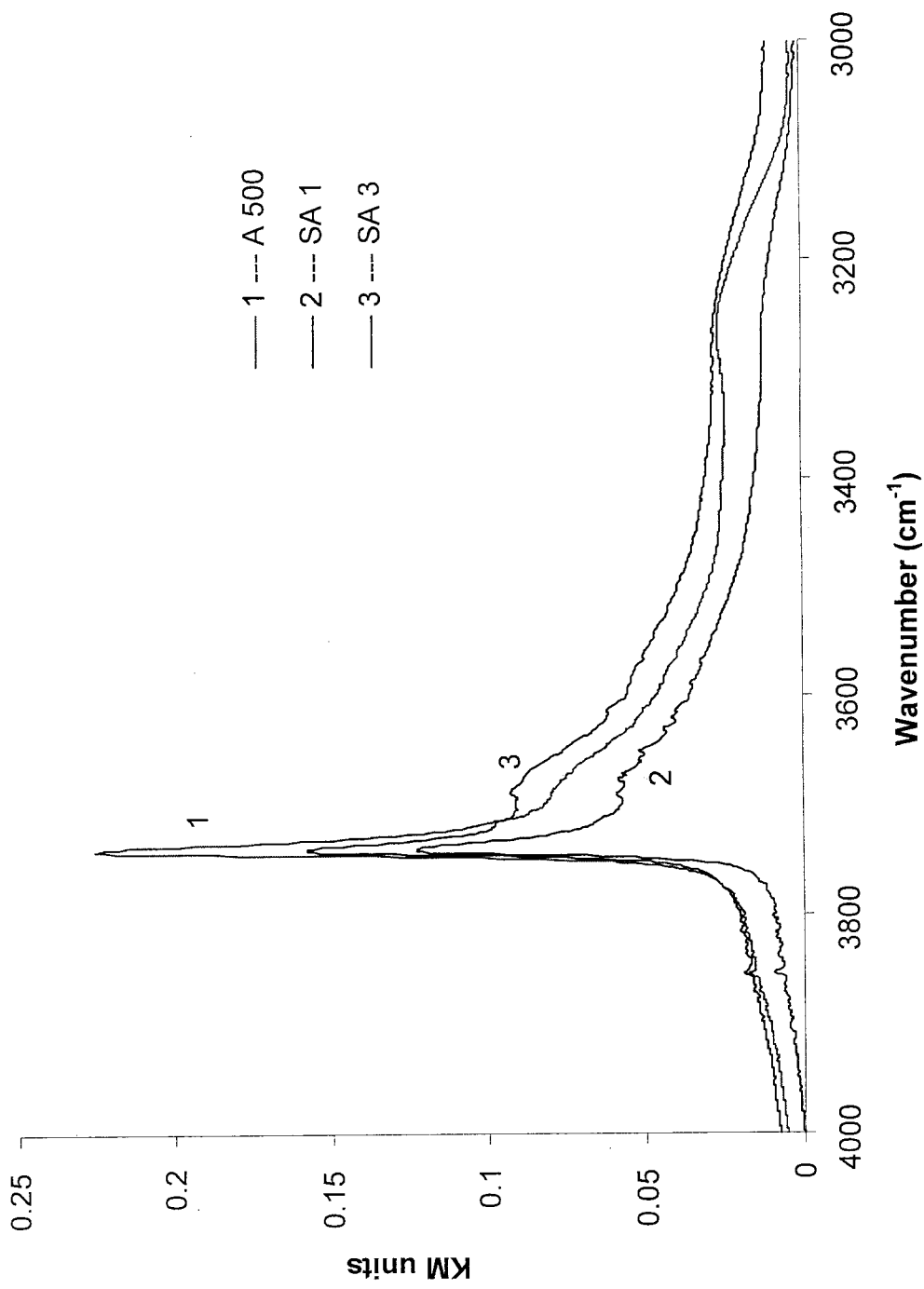
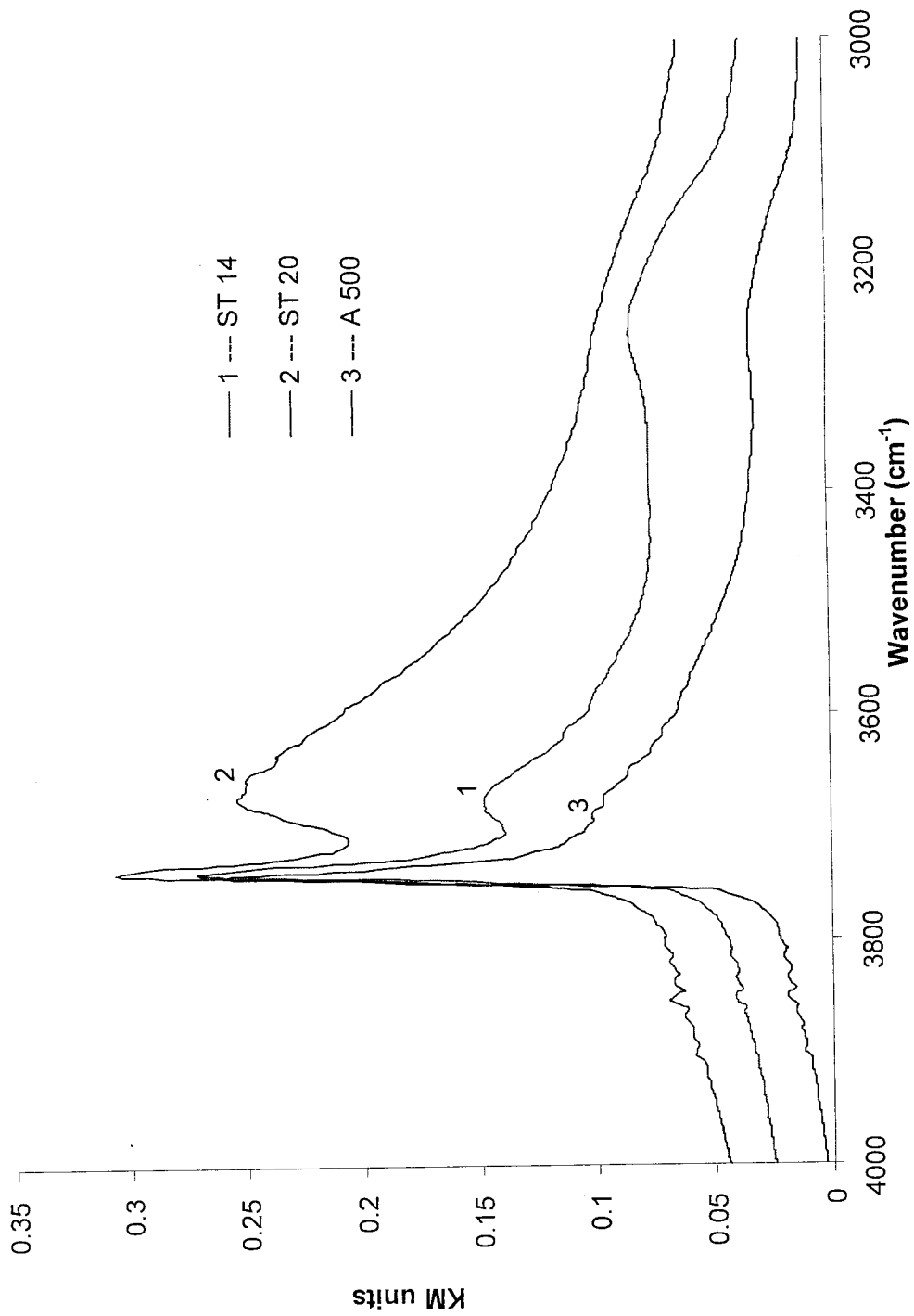Figure 9: FTIR spectra of 1) A 500, 2) SA 1, 3) SA 3 at 300°C
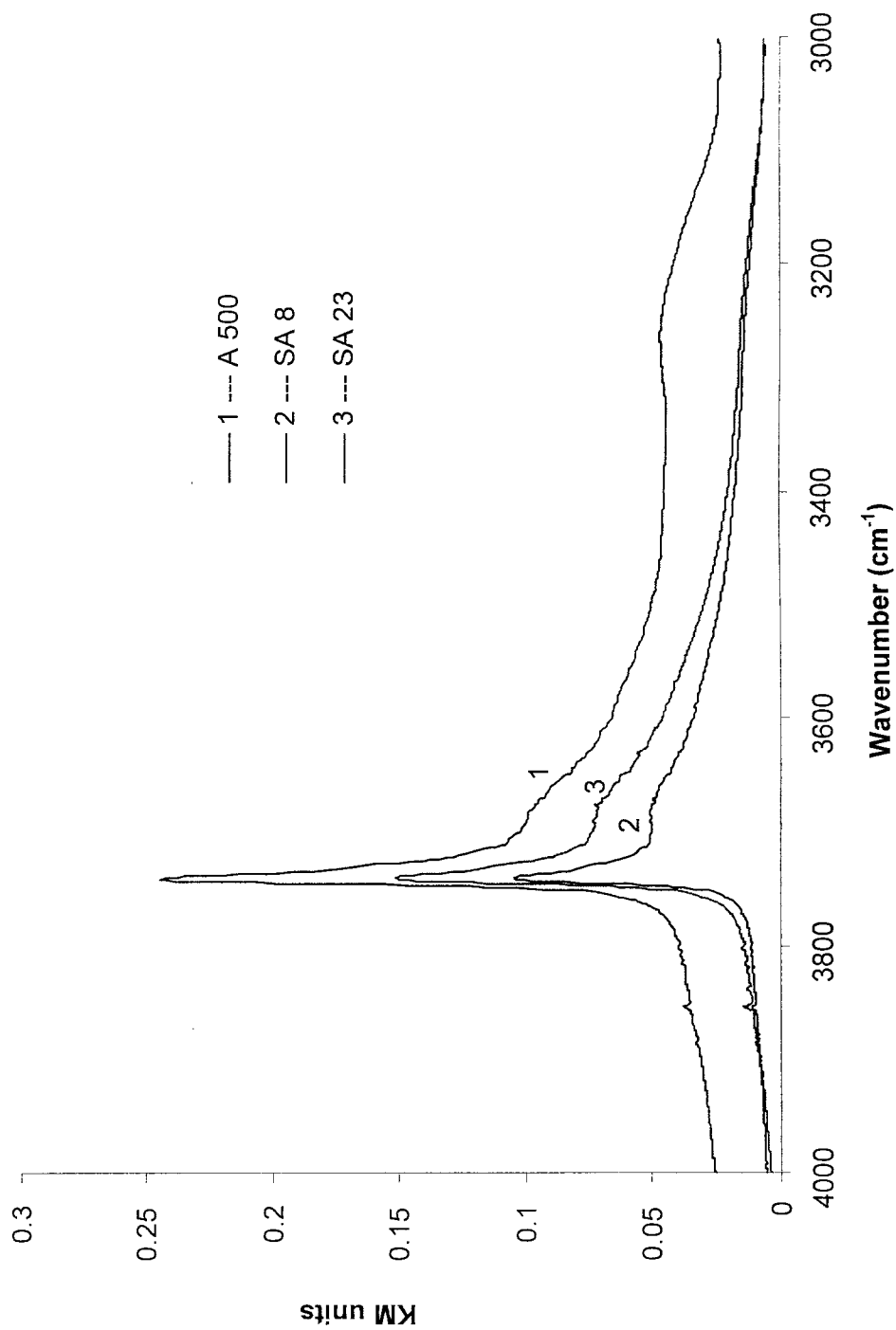
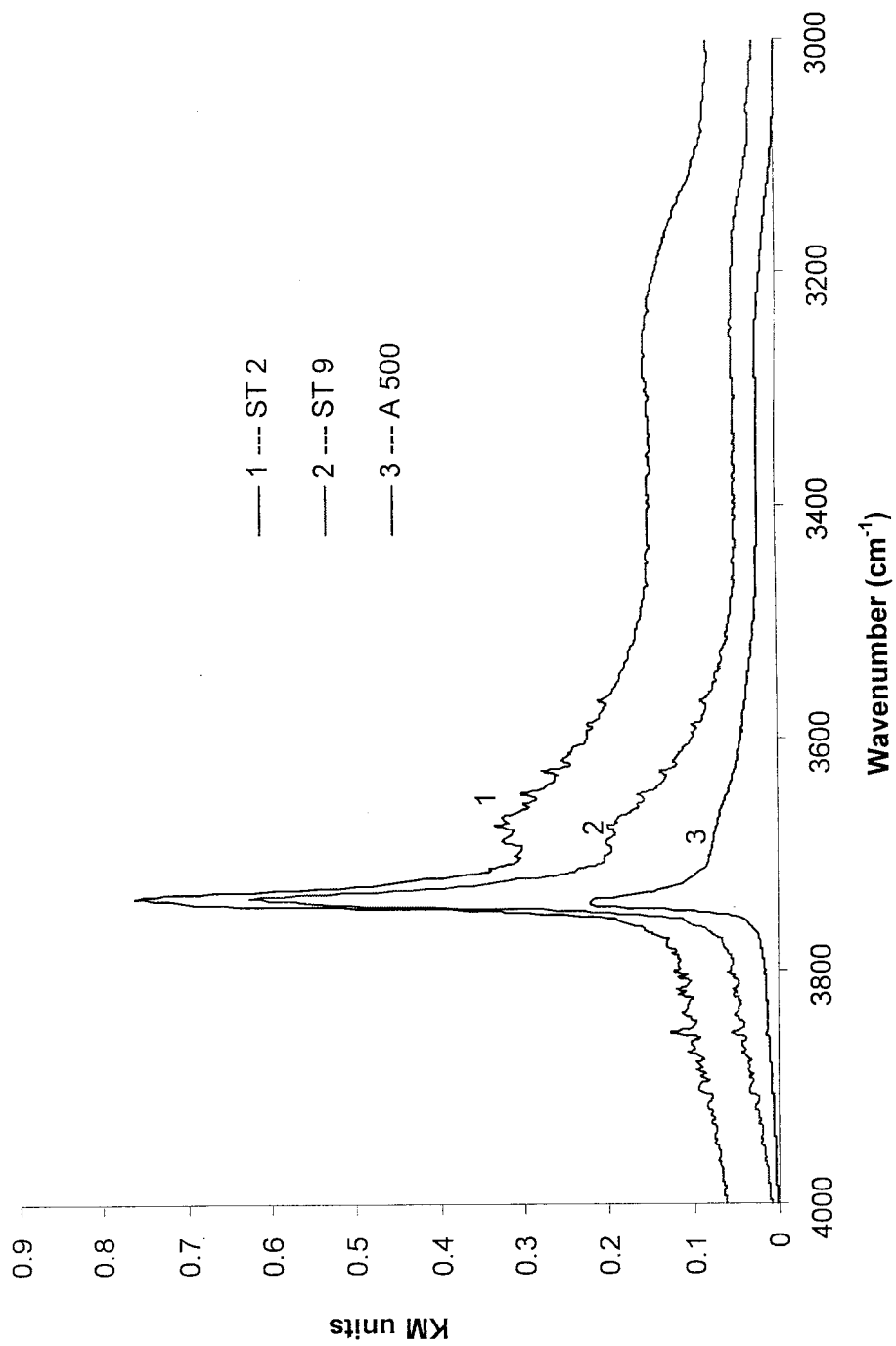Figure 10: FTIR spectra of 1) A 500, 2) SA 8, 3) SA 23 at 300°C
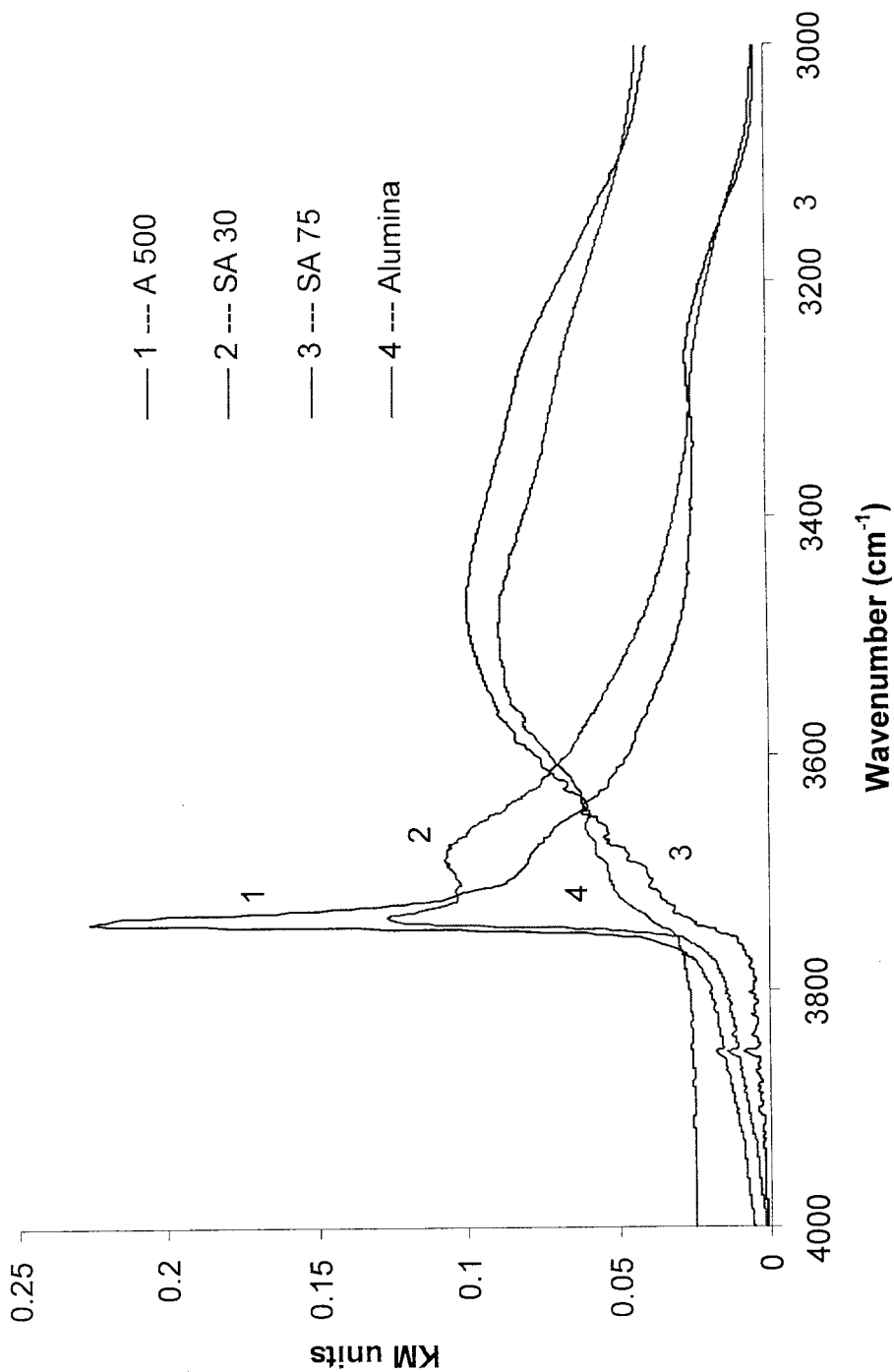
Figure 11: FTIR spectra of 1) A 500, 2) SA 30, 3) SA 75, 4) Alumina at 300°C

Figure 12: FTIR spectra of 1) ST 2, 2) ST 9, 3) A 500 at 200°C

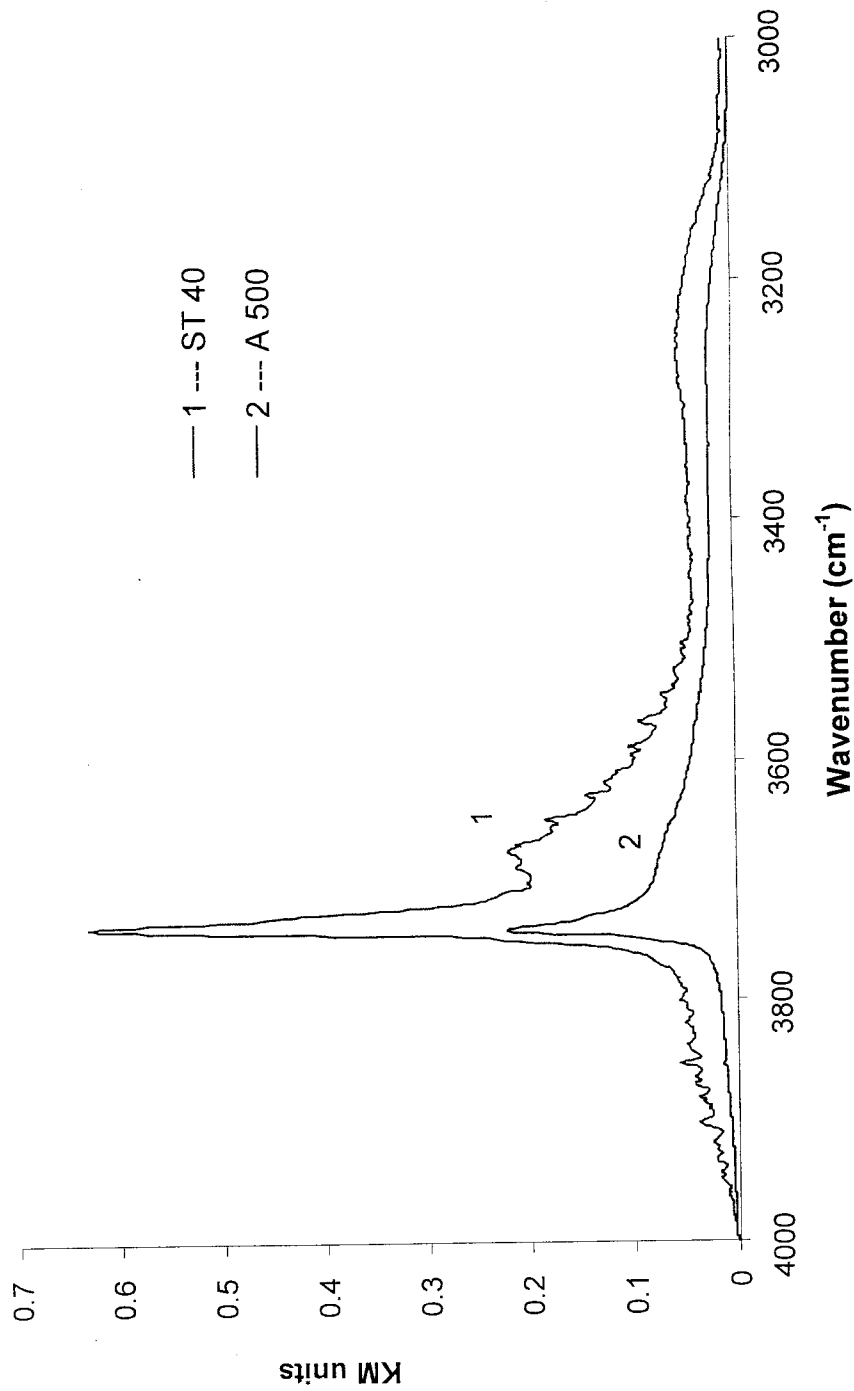Figure 13: FTIR spectra of 1) ST 14, 2) ST 20, 3) A 500 at 200°C
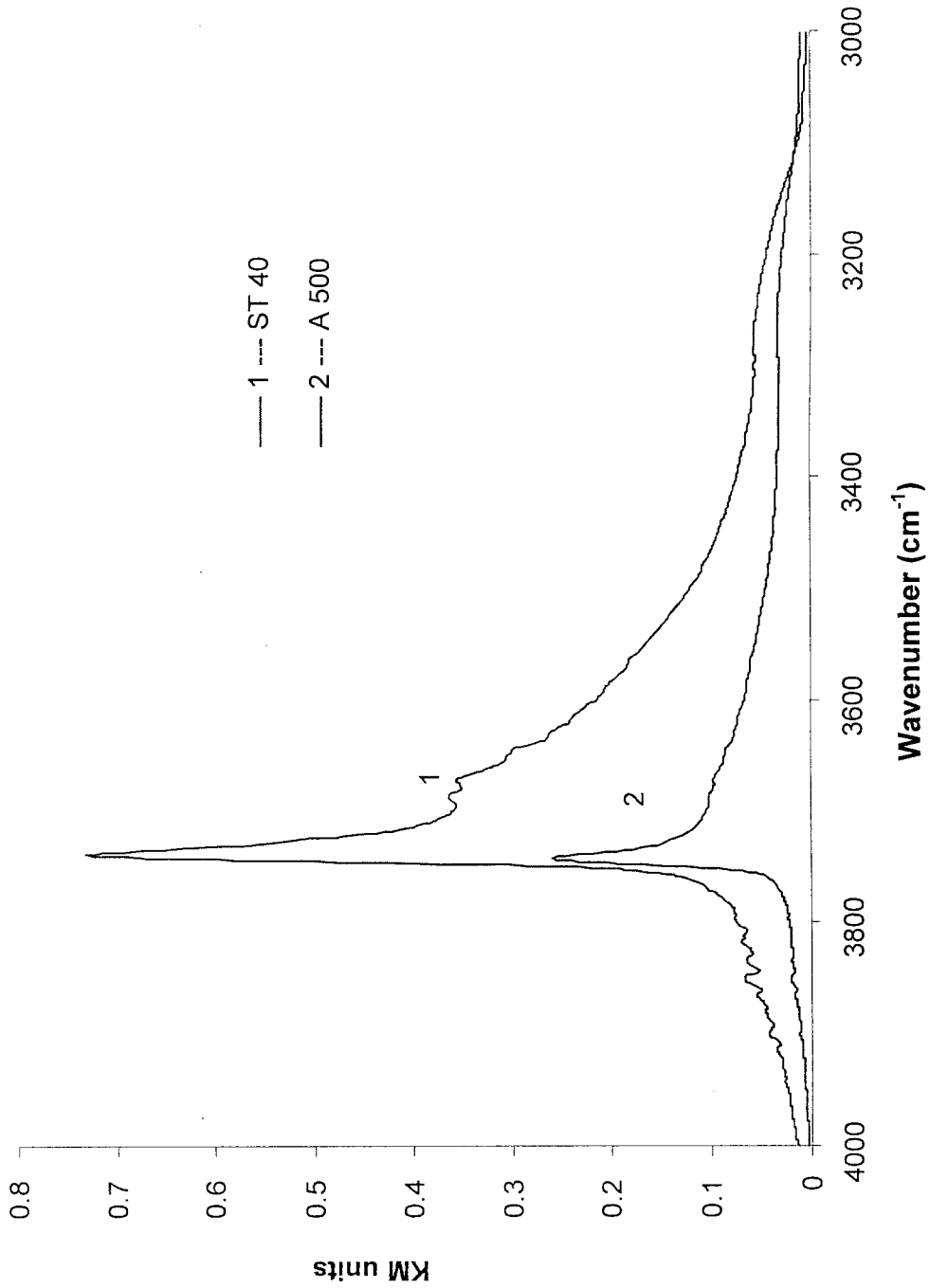
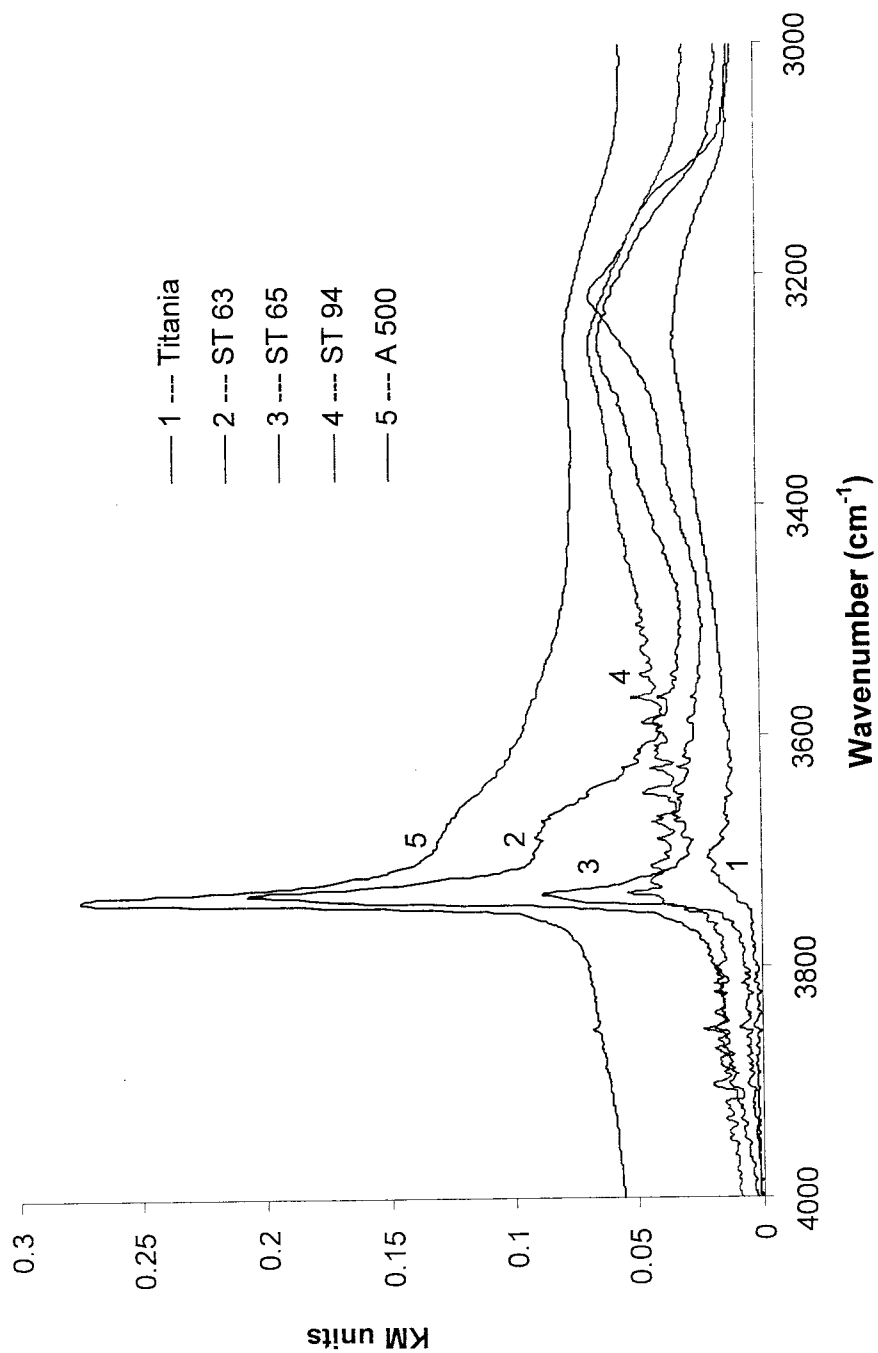Figure 14: FTIR spectra of 1) ST 40, 2) A 500 at 200°C
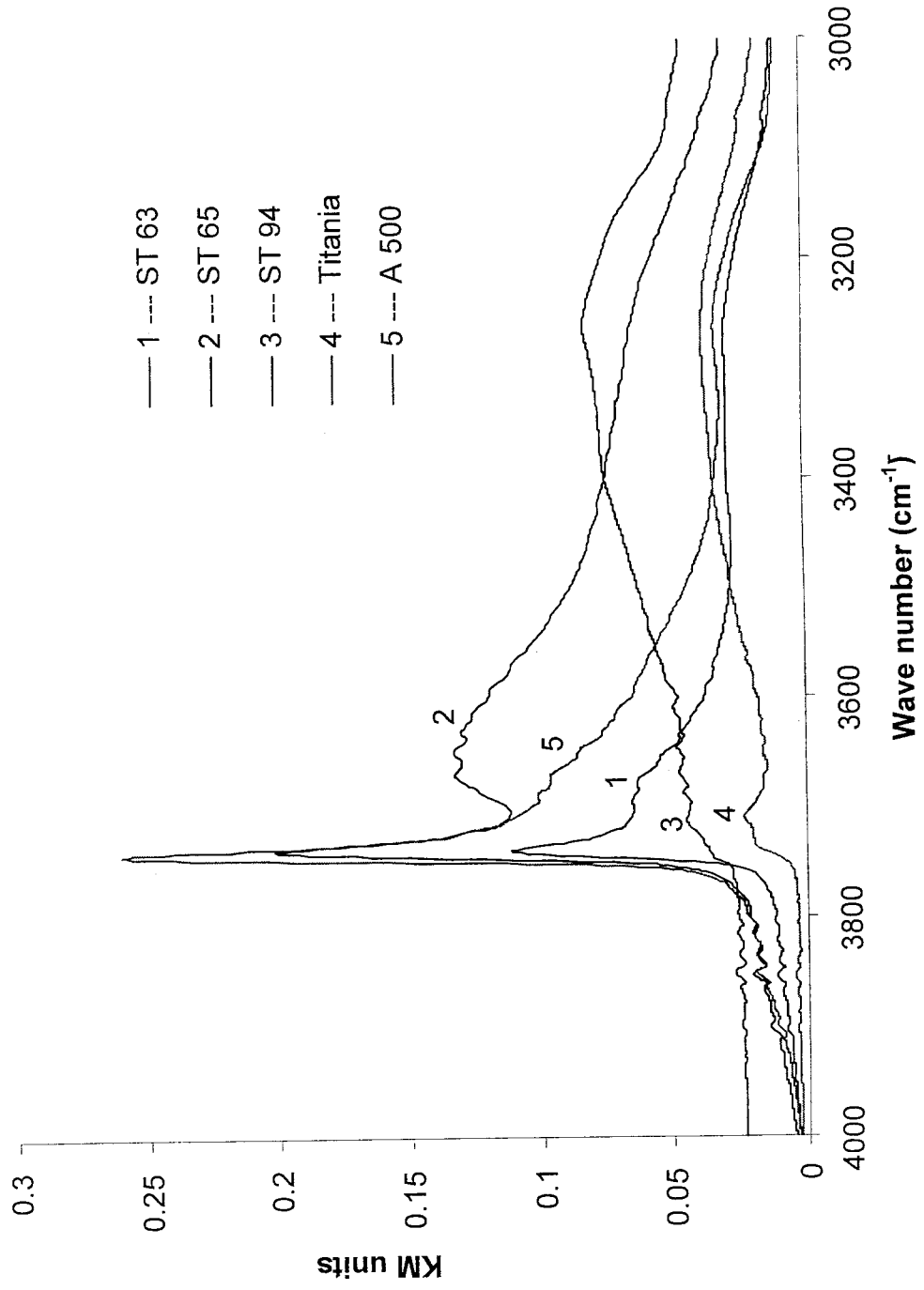
Figure 15: FTIR spectra of 1) ST 63, 2) ST 65, 3) ST 94, 4) Titania, 5) A 500 at 200°C

Figure 16: FTIR spectra of 1) ST 2, 2) ST 9, 3) A 500 at 300°C
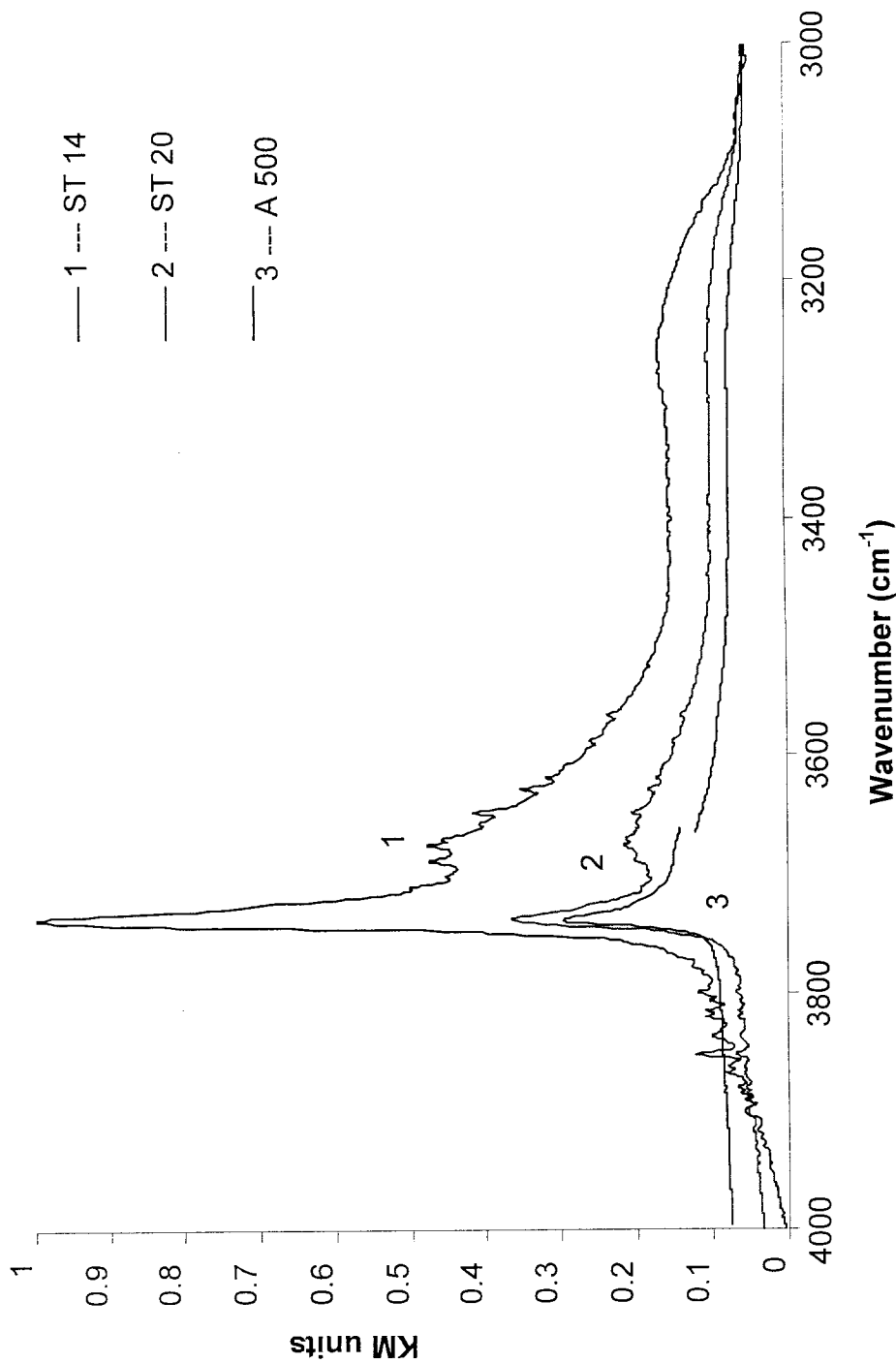
Figure 17: FTIR spectra of 1) ST 14, 2) ST 20, 3) A 500 at 300°C

Figure 18: FTIR spectra of 1) ST 40, 2) A 500 at 300°C

Figure 19: FTIR spectra of 1) Titania, 2) ST 63, 3) ST 65, 4) ST 94, 5) A 500 at 300°C
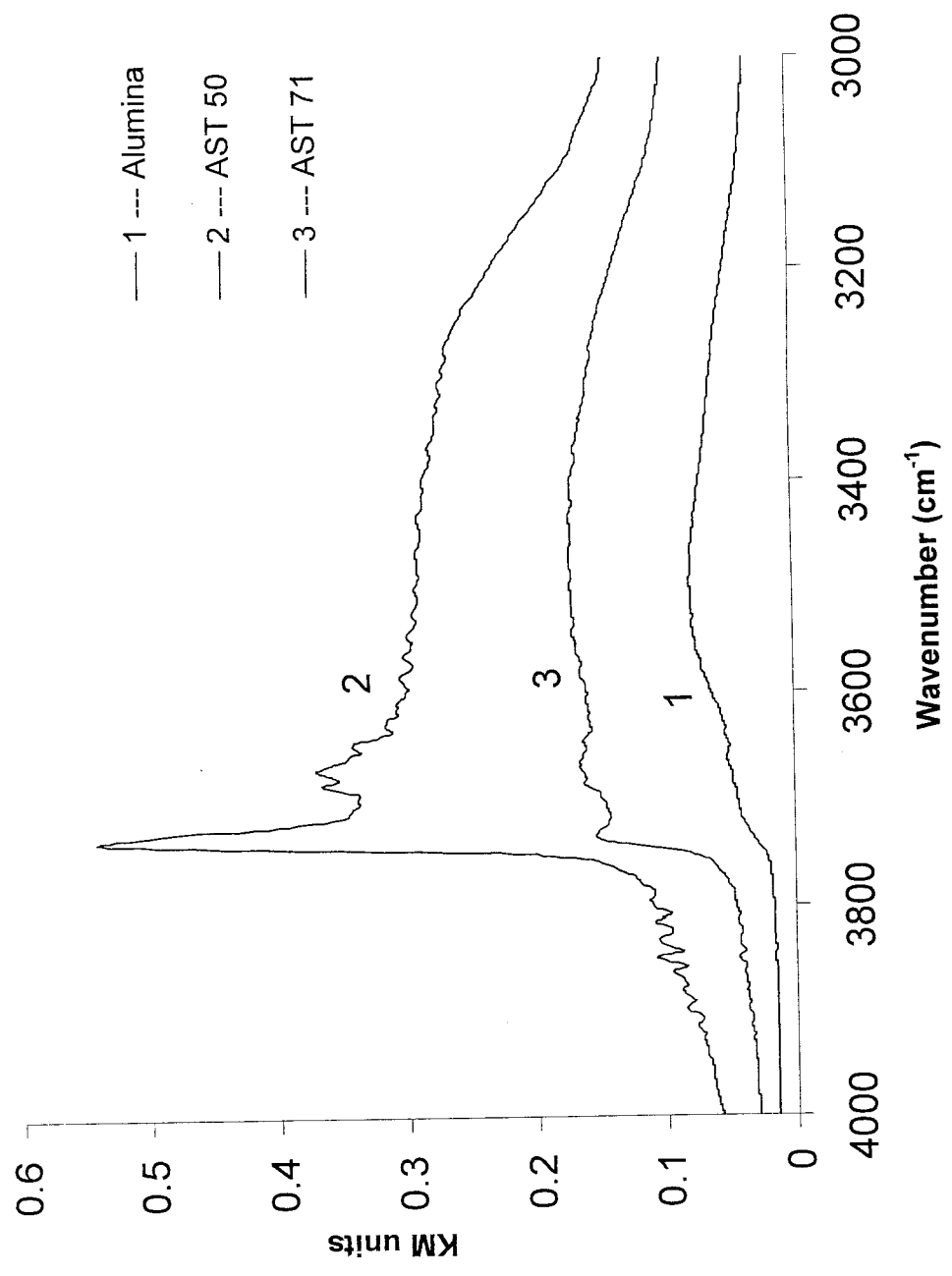
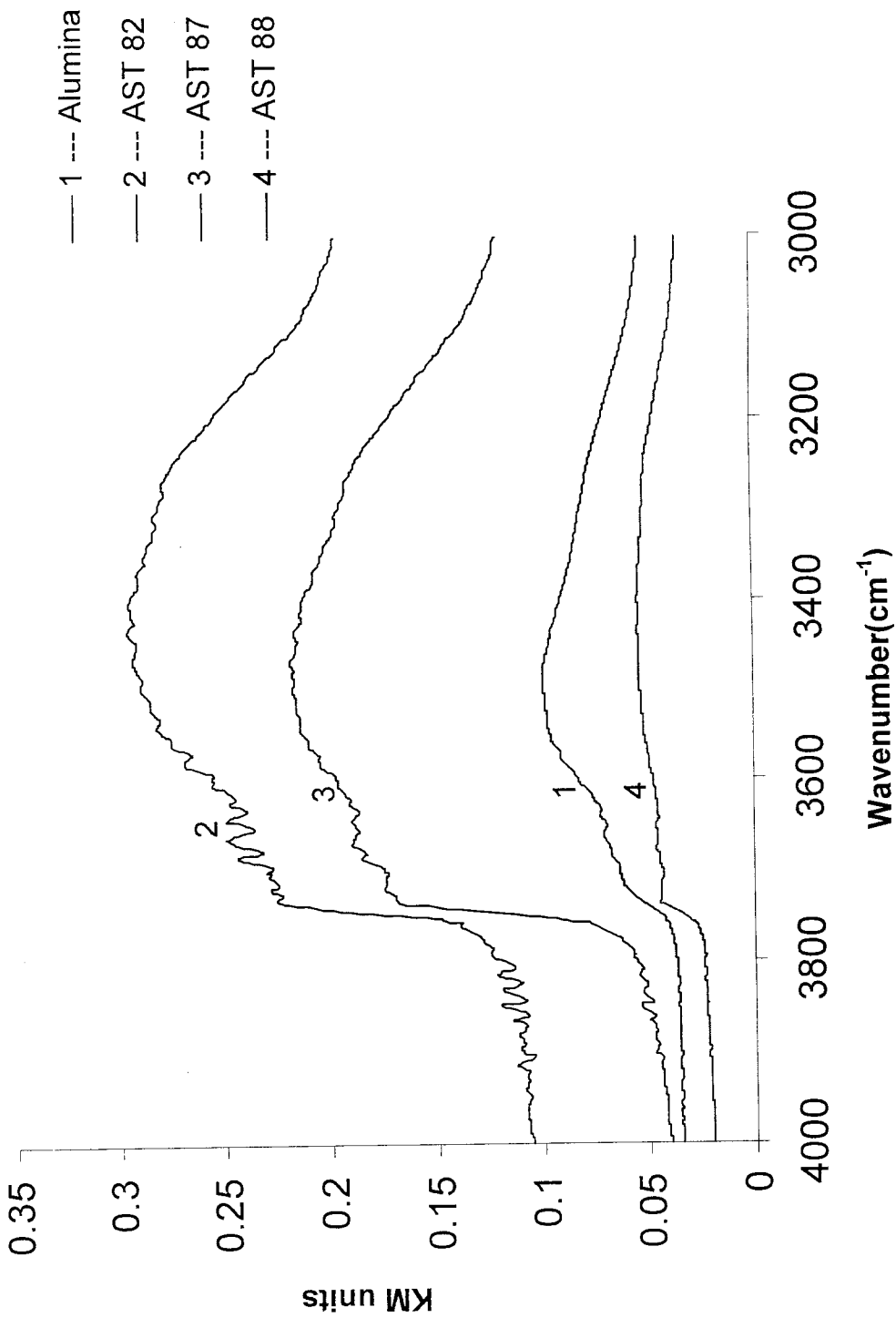Figure 20: FTIR spectra of 1) Alumina, 2) AST 50, 3) AST 71 at 200°C

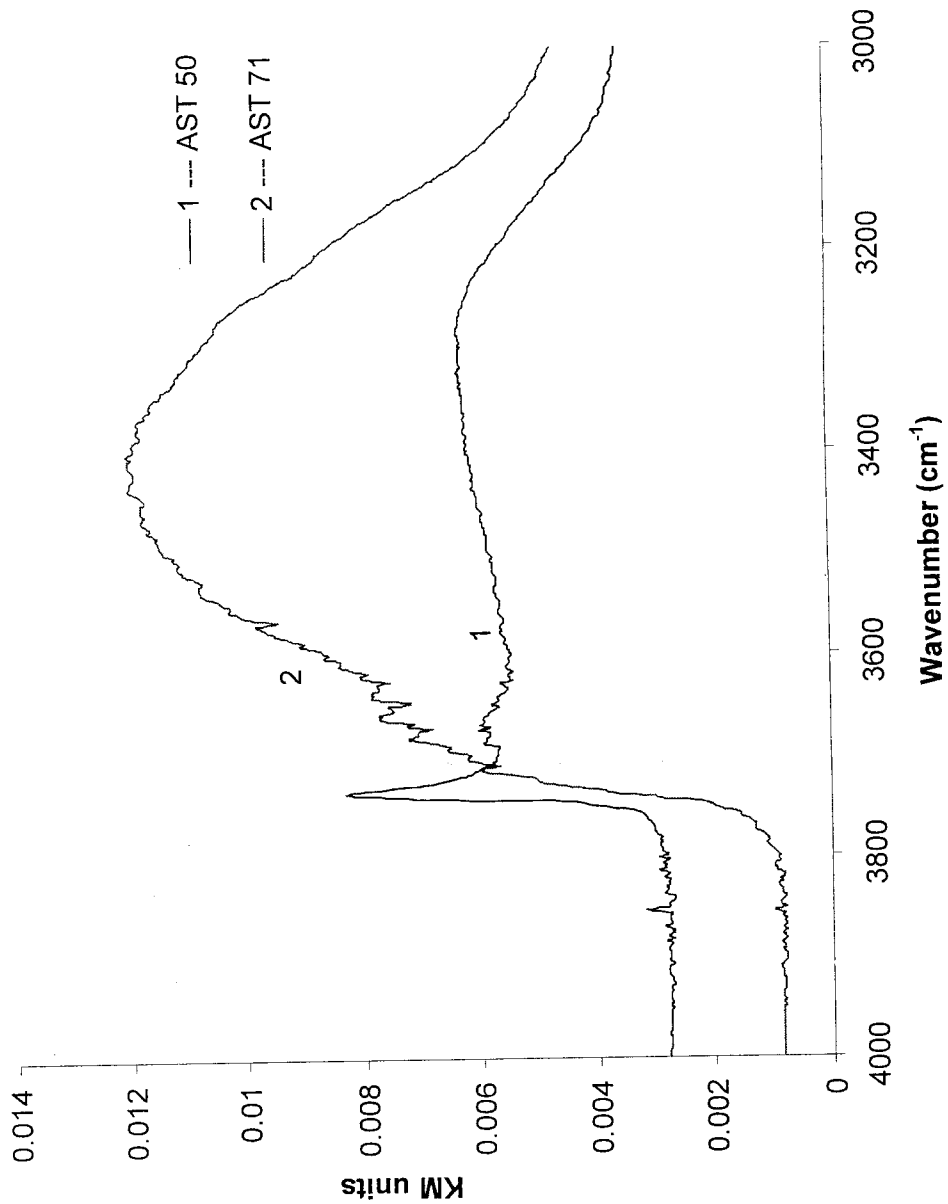Figure 21: FTIR spectra of 1) Alumina, 2) AST 82, 3) AST 87, 4) AST 88 at 200°C

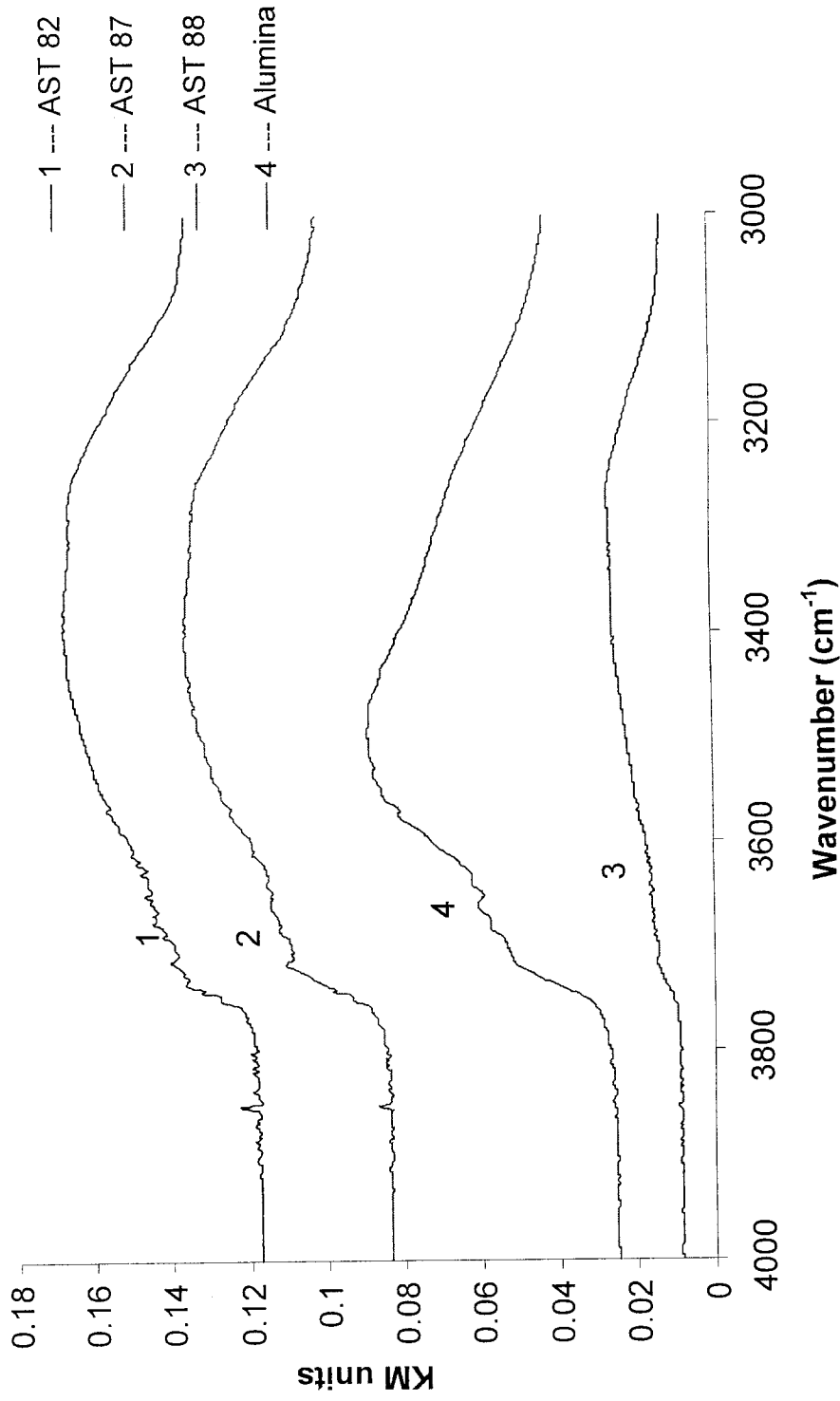Figure 22: FTIR spectra of 1) AST 50, 2) AST 71 at 300°C

Figure 23: FTIR spectra of AST 82, AST 87, AST 88 and Alumia at 300°C
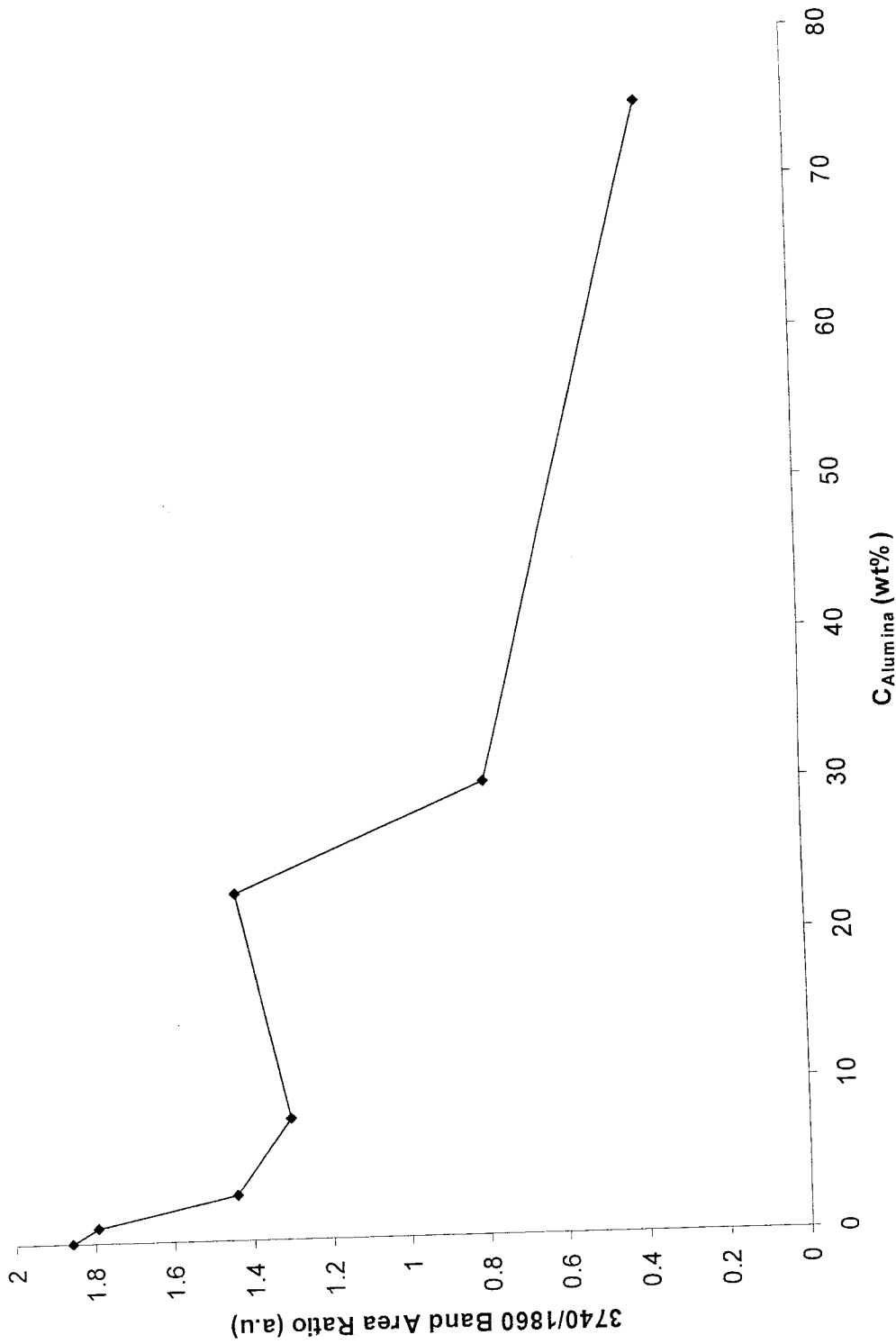
Figure 24: Relative amounts of silanols as a function of the total content of alumina in SA samples at 200°C
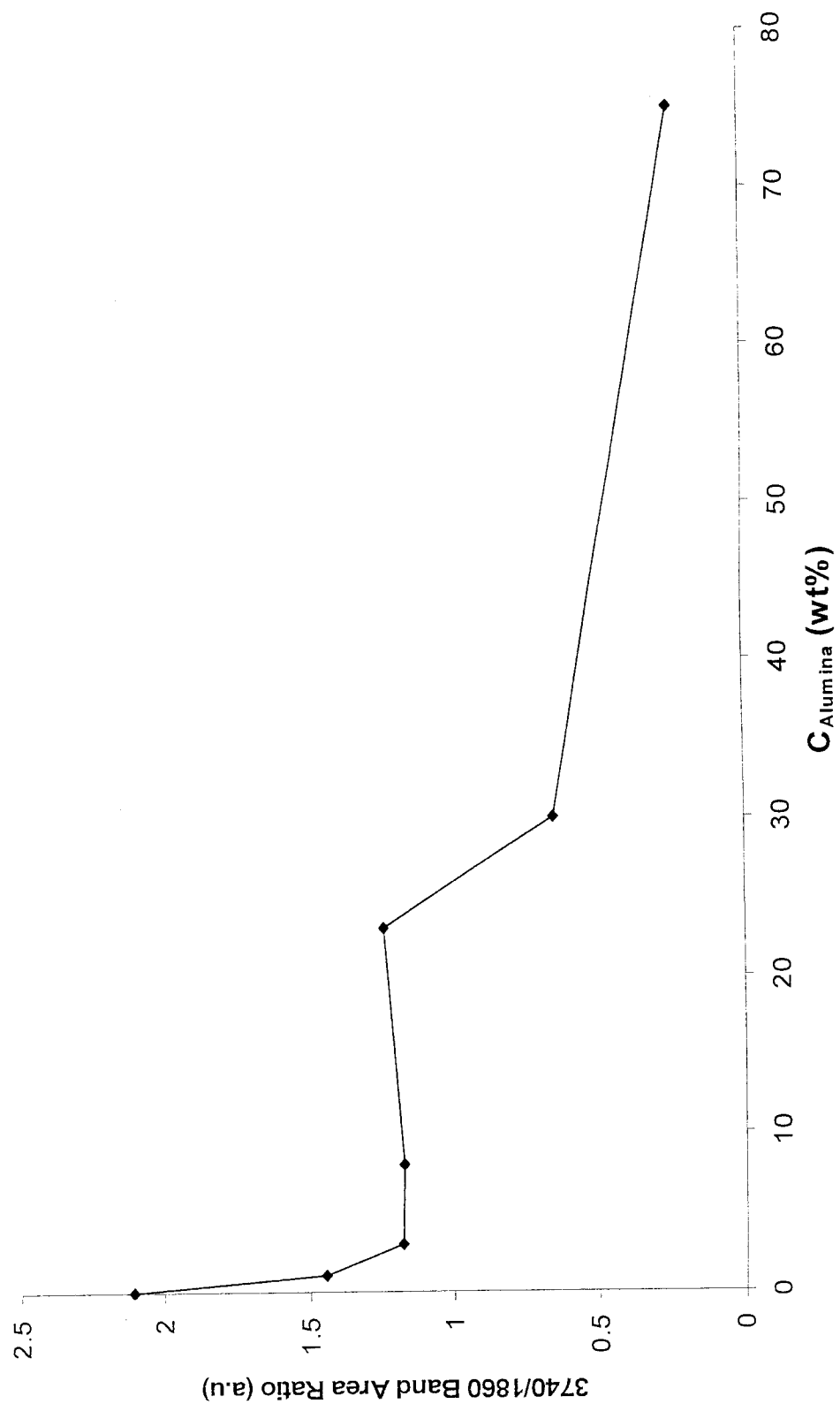
Figure 25: Relative amounts of silanols as a function of the total content of alumina in SA samples at 300°C
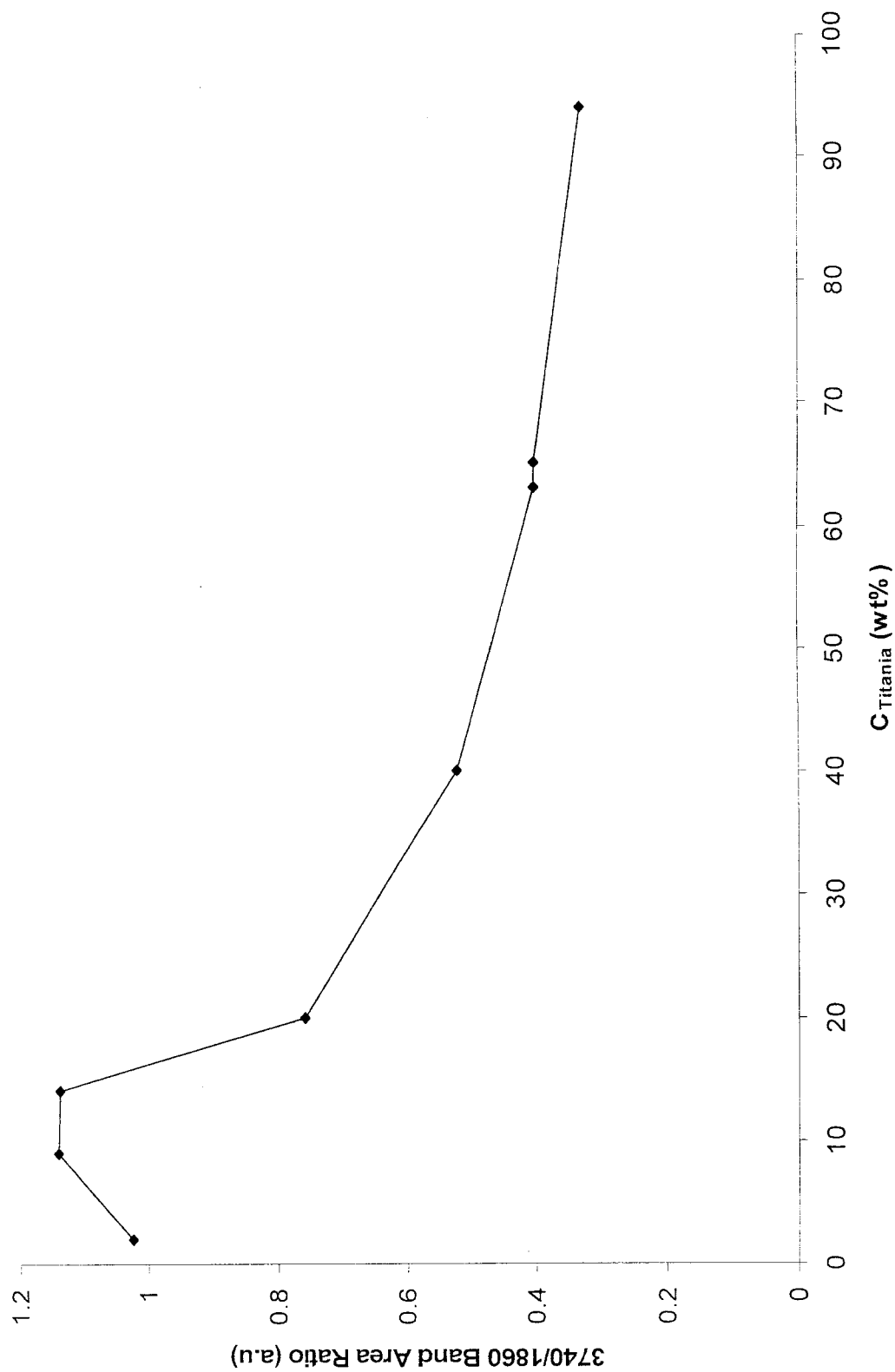
Figure 26: Relative amounts of silanols as a function of the total content of titania in ST samples at 200°C
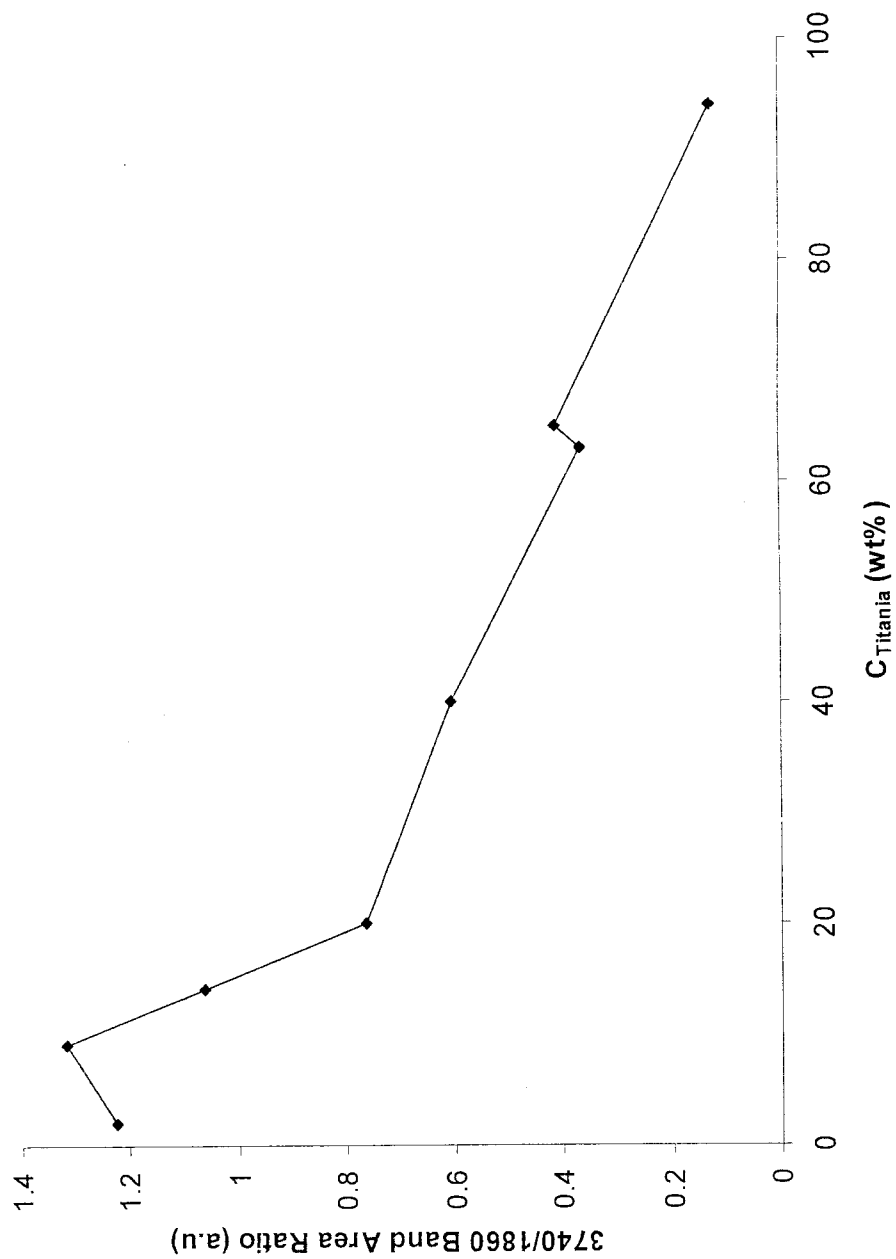
Figure 27: Relative amounts of silanols as a function of the total content of titania in ST samples at 300°C
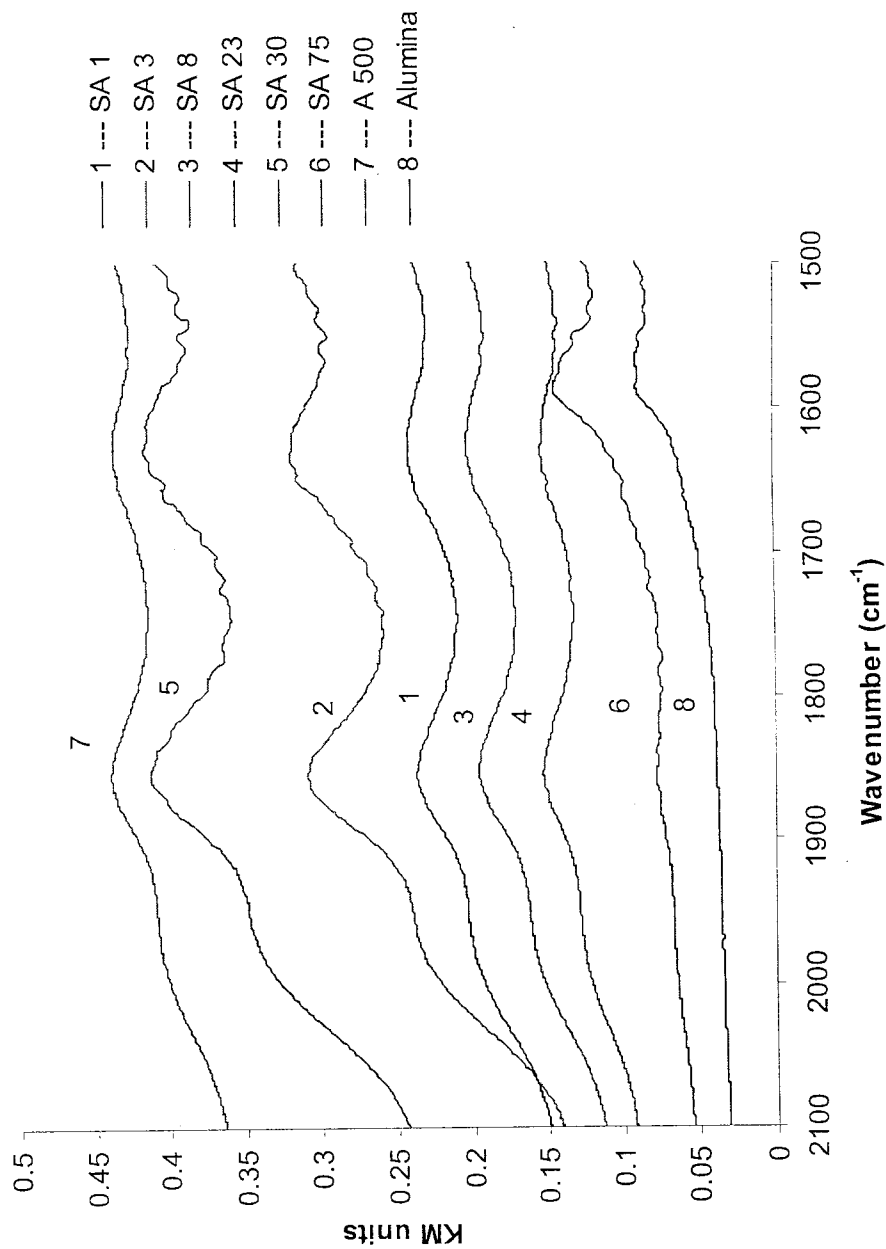
Figure 28: FTIR spectra of Si-O stretching vibration at 1860 cm^{-1} region for 1) SA 1, 2) SA 3, 3) SA 8, 4) SA 23, 5) SA 30, 6) SA 75, 7) Alumina, 8) A 500 at 200°C
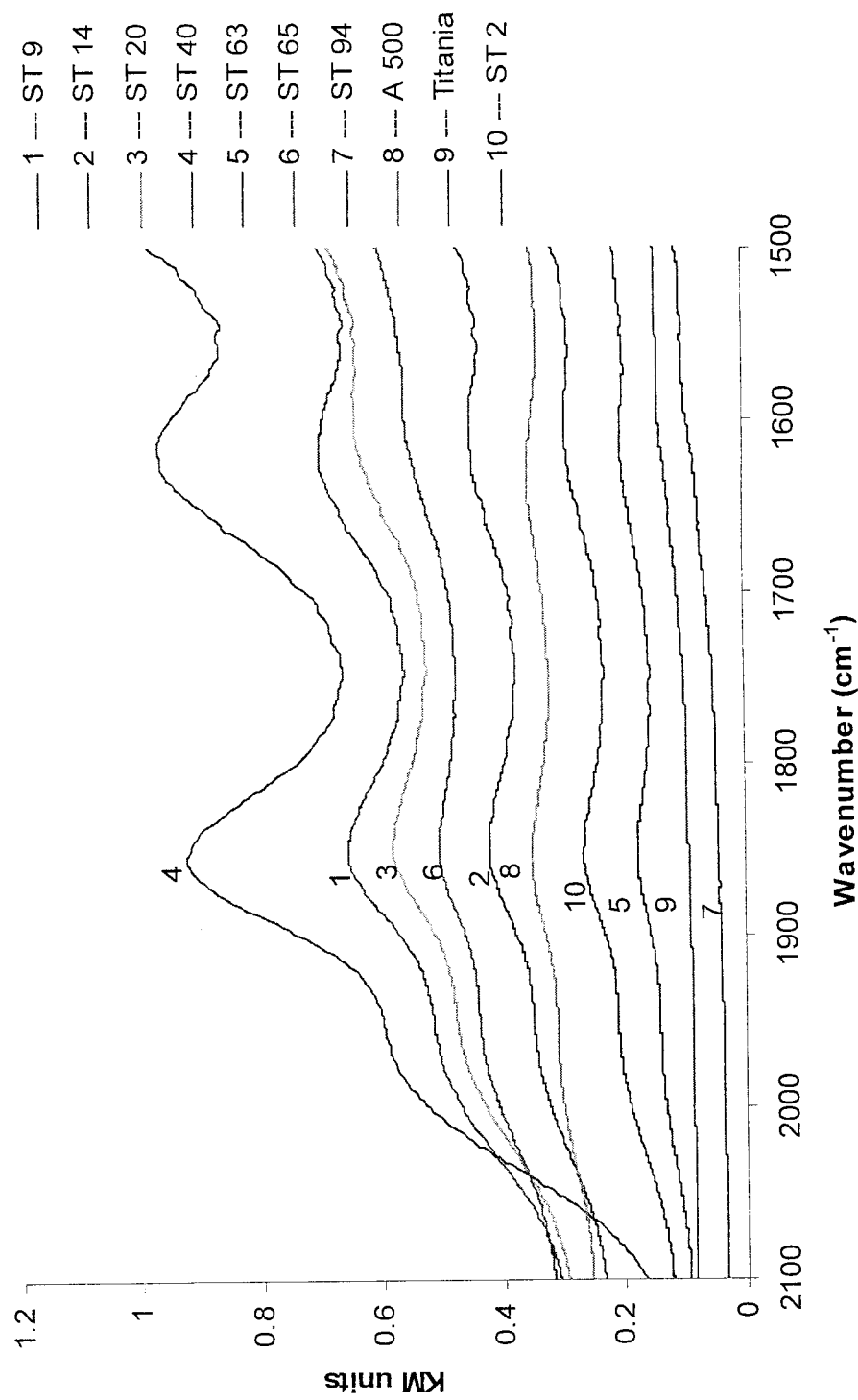
Figure 29: FTIR spectra of Si–O stretching vibration at 1860 cm^{-1} of 1) A 500, 2) ST 2, 3) ST 9, 4) ST 14, 5) ST 20, 6) ST 40, 7) ST 63, 8) ST 65, 9) ST 94, 10) Titania at 200°C.
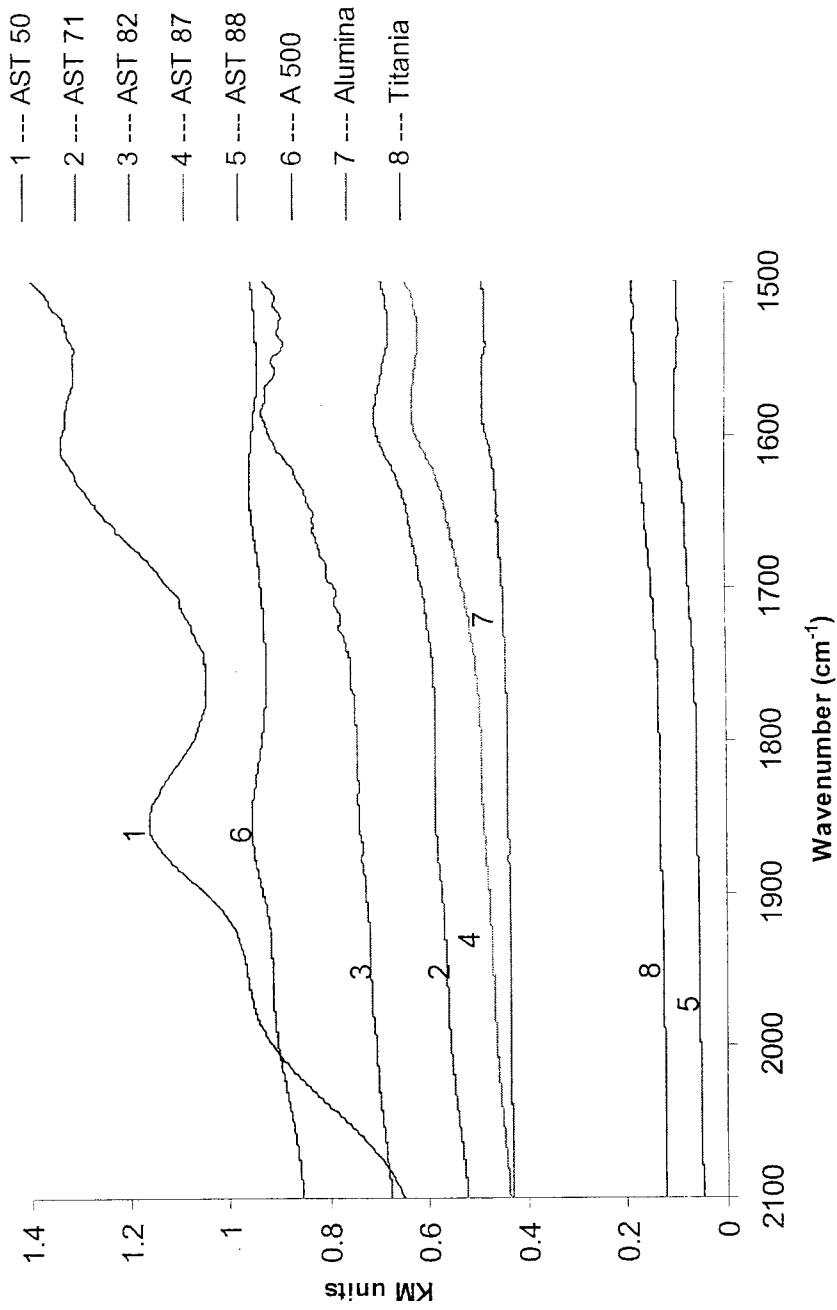
Figure 30: FTIR spectra of Si-O stretching vibration at 1860 cm^{-1} of 1) AST 50, 2) AST 71, 3) AST 82, 4) AST 87, 5) AST 88, 6) A 500, 7) Alumina, 8)Titania at 200°C
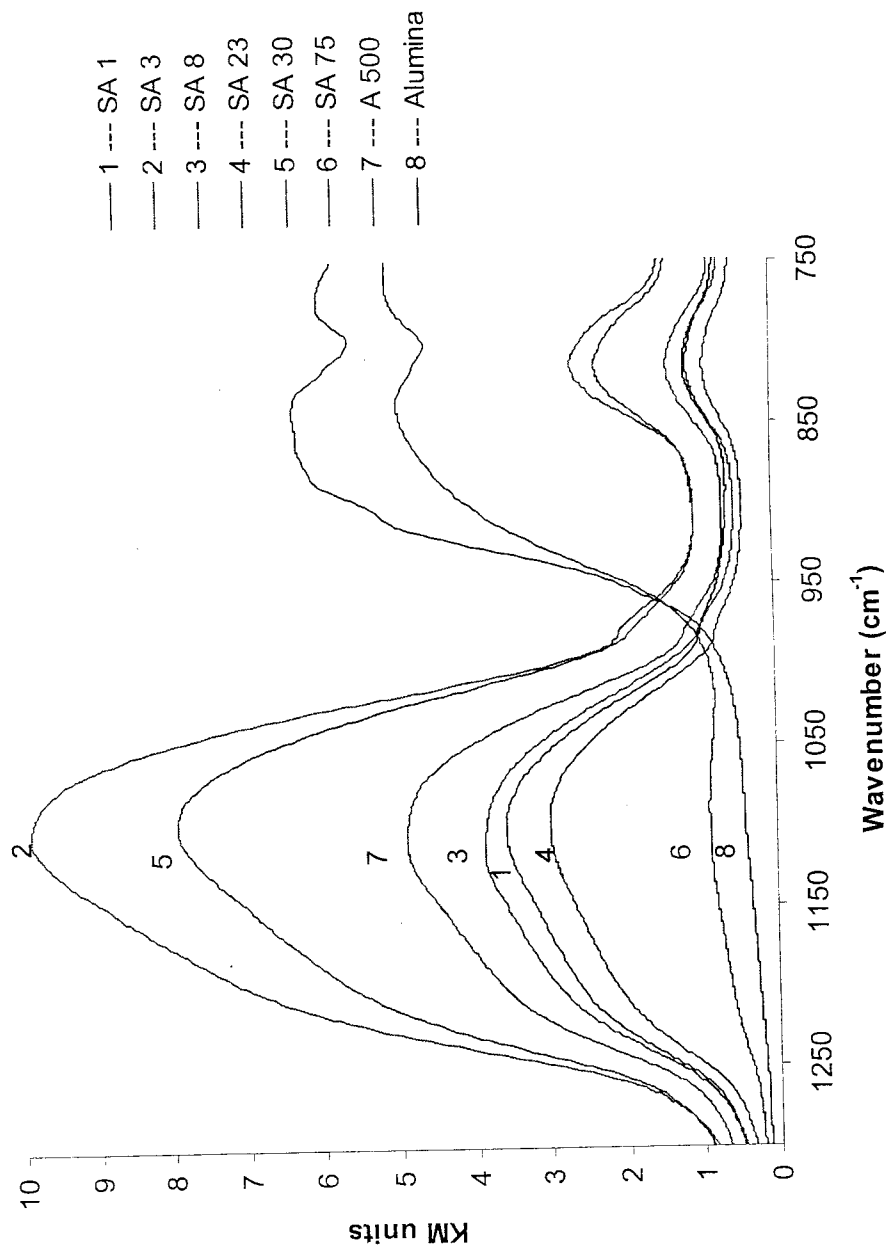
Figure 31: FTIR spectra of Si-O stretching vibration at 800 cm^{-1} and 1100 cm^{-1} for 1) SA 1, 2) SA 3, 3) SA 8, 4) SA 23, 5) SA 30, 6) SA 75, 7) Alumina and 8) A 500 acquired at 200° C
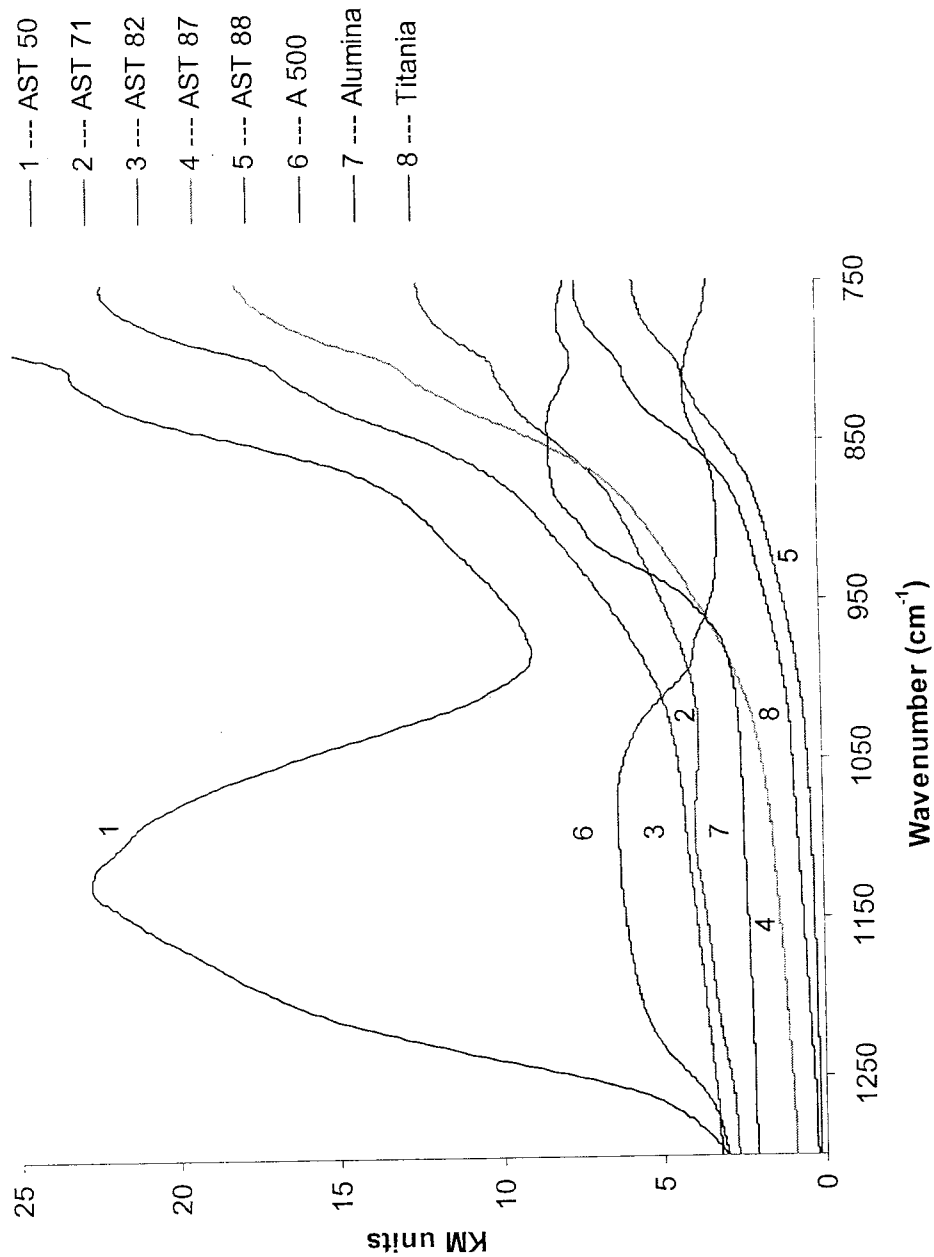
Figure 32: FTIR spectra of Si-O stretching vibration at 1100 cm^{-1} for 1) AST 50, 2) AST 71, 3) AST 82, 4) AST 87, 5) AST 88, 6) A 500, 7) Alumina and 8) Titania acquired at 200° C
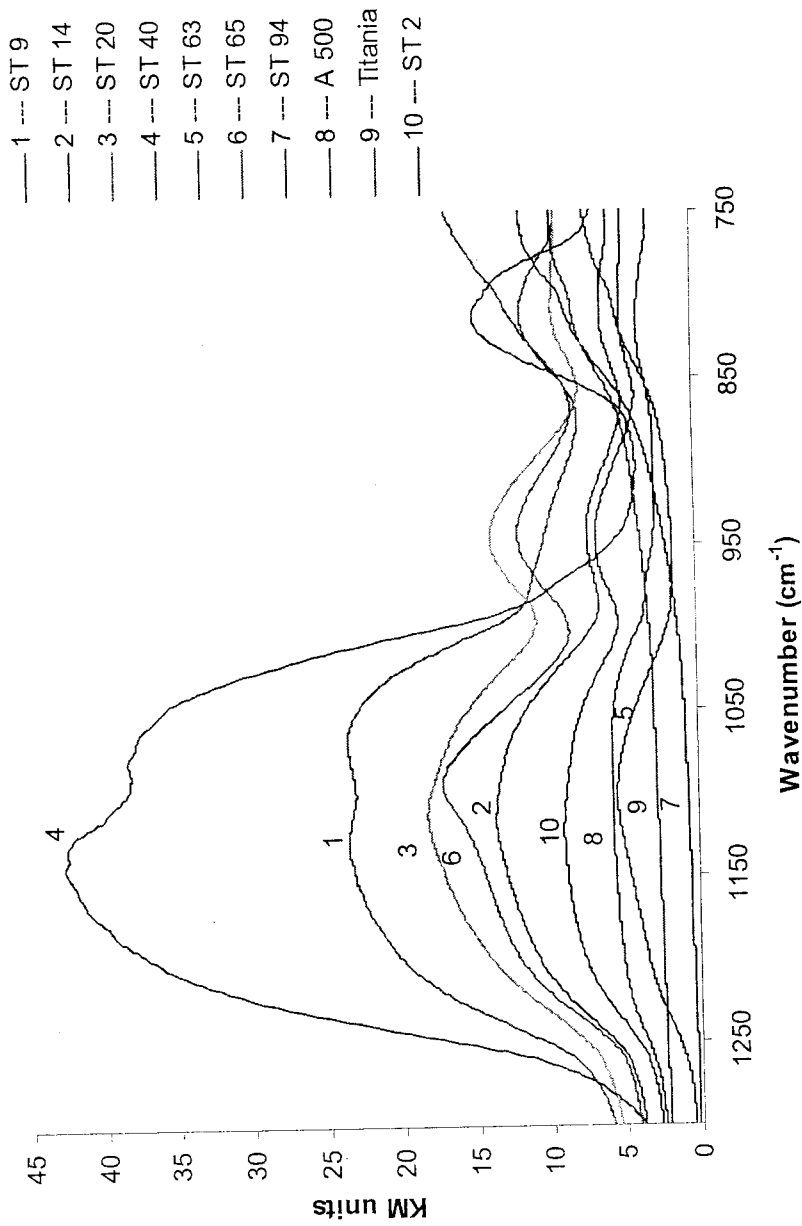
Figure 33: FTIR spectra of Si-O stretching vibration at 800 cm^{-1} and 1100 cm^{-1} and Si-O-Ti stretching vibration at 960 cm^{-1}

for 1) A 500, 2) ST 2, 3) ST 9, 4) ST 14, 5) ST 20, 6) ST 40, 7) ST 63, 8) ST 65, 9) ST 94 and 10) Titania at 200° C
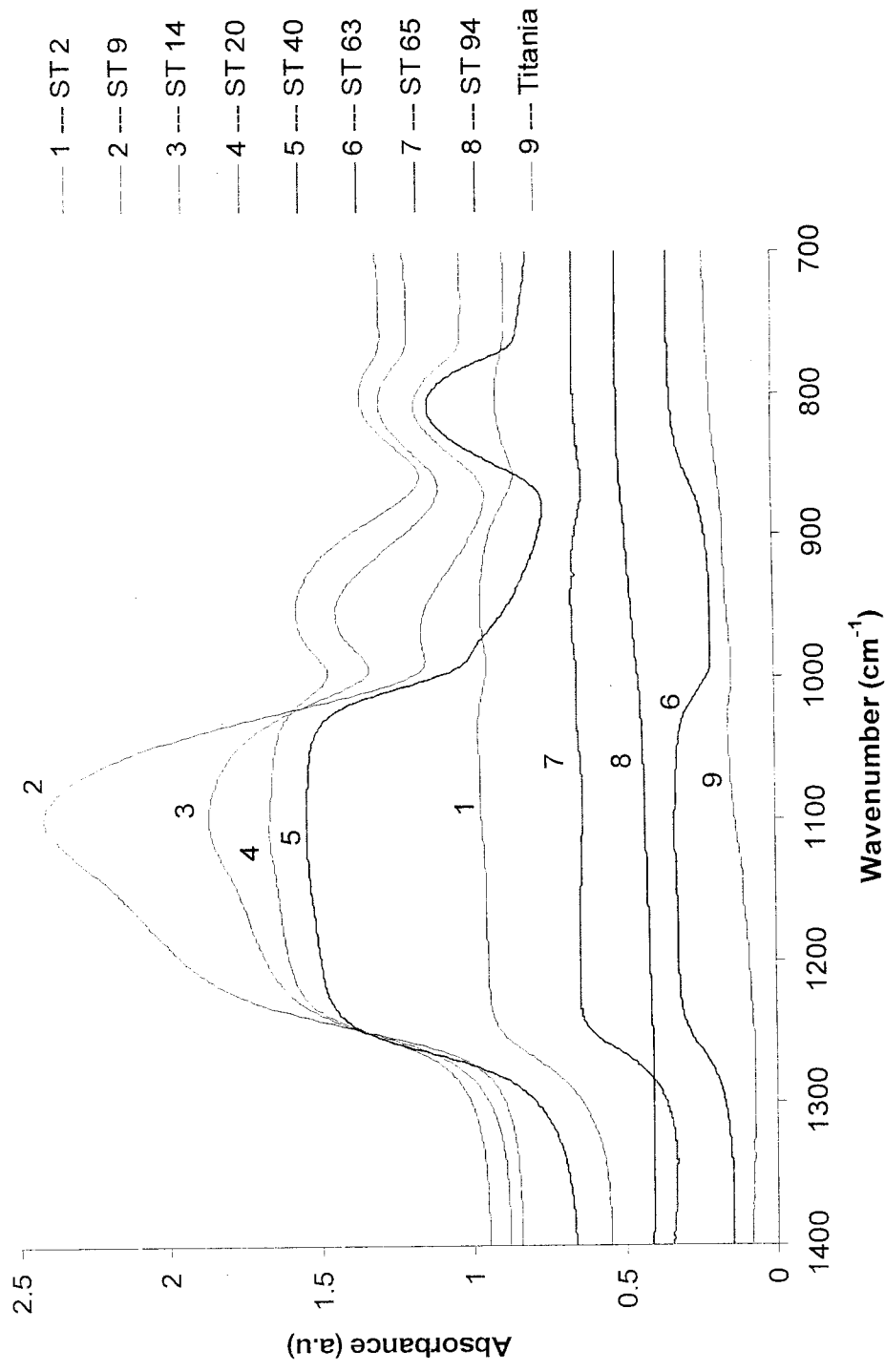
Figure 34: Transmission FTIR spectra of Si-O stretching vibration at 800 cm^{-1} and 1100 cm^{-1} and Si-O-Ti stretching vibration at 960 cm^{-1} for 1) ST 2, 2) ST 9, 3) ST 14, 4) ST 20, 5) ST 40, 6) ST 63, 7) ST 65, 8) ST 94 and 9) Titania.
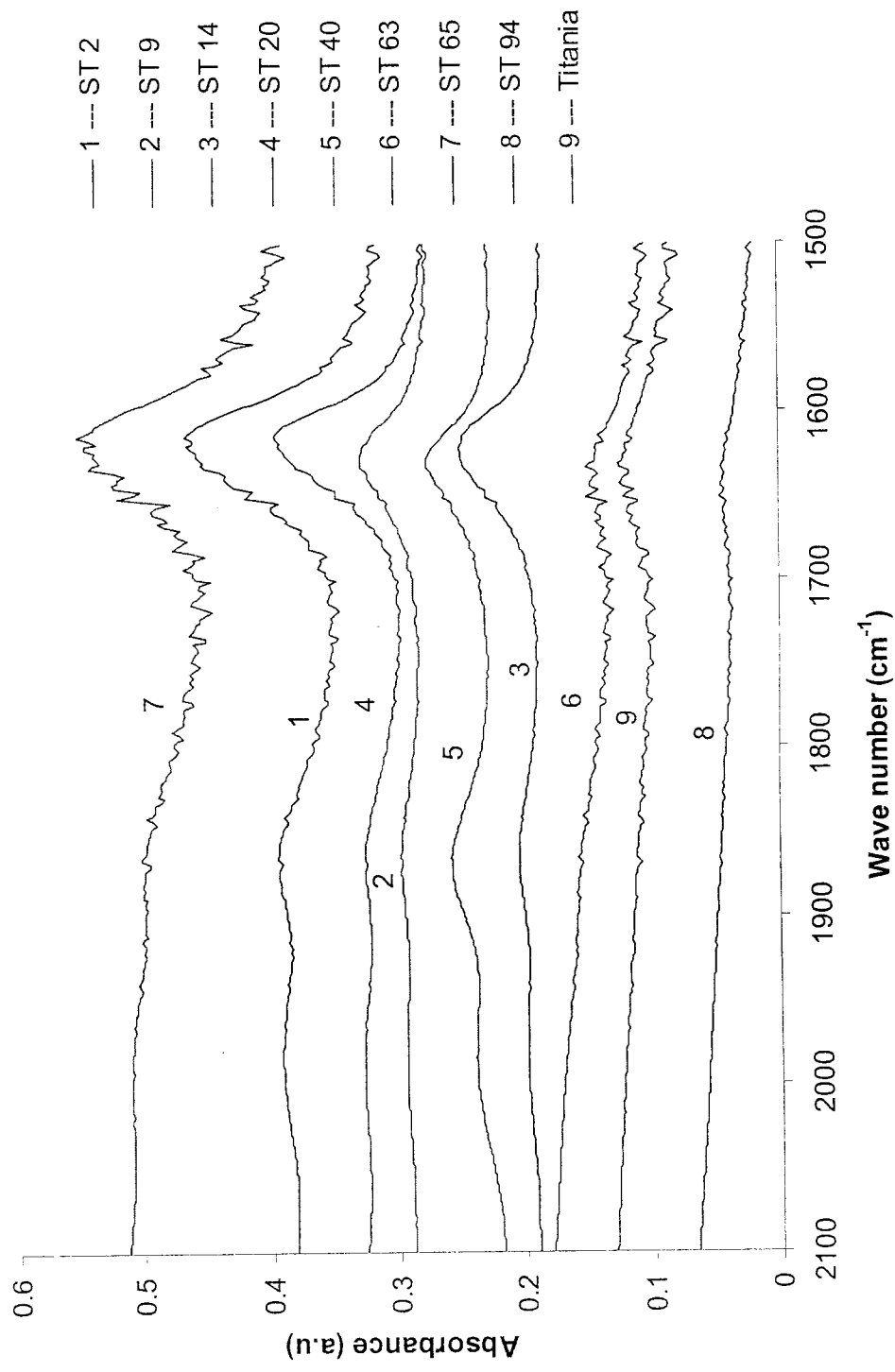
Figure 35: Transmission FTIR spectra of Si-O stretching vibration at 1860 cm^{-1} for 1) ST 2, 2) ST 9, 3) ST 14, 4) ST 20, 5) ST 40, 6) ST 63, 7) ST 65, 8) ST 94 and 9) Titania.
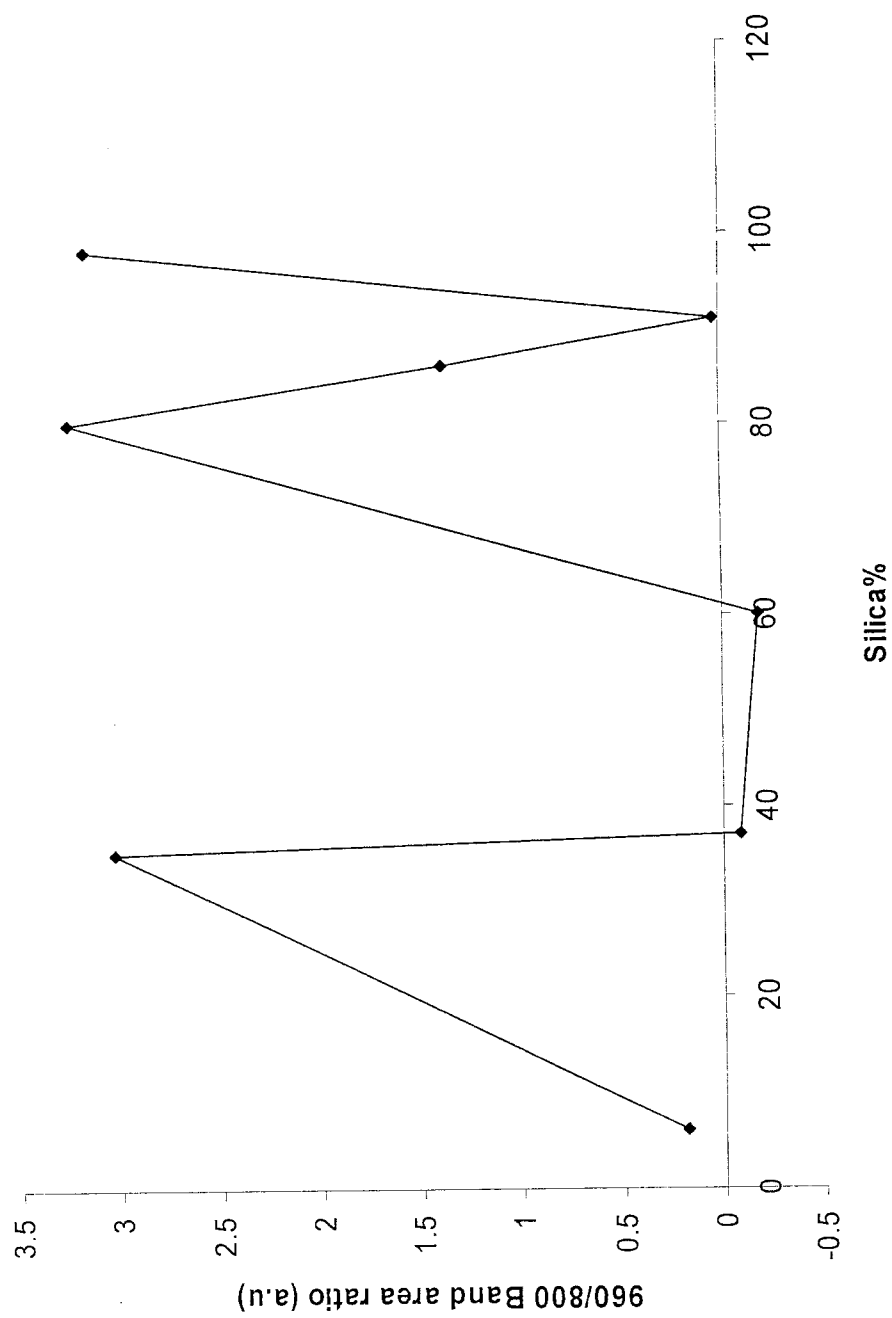
Figure 36: Relative amounts of Si-O-Ti bonds as a function of total content of silica in the ST samples
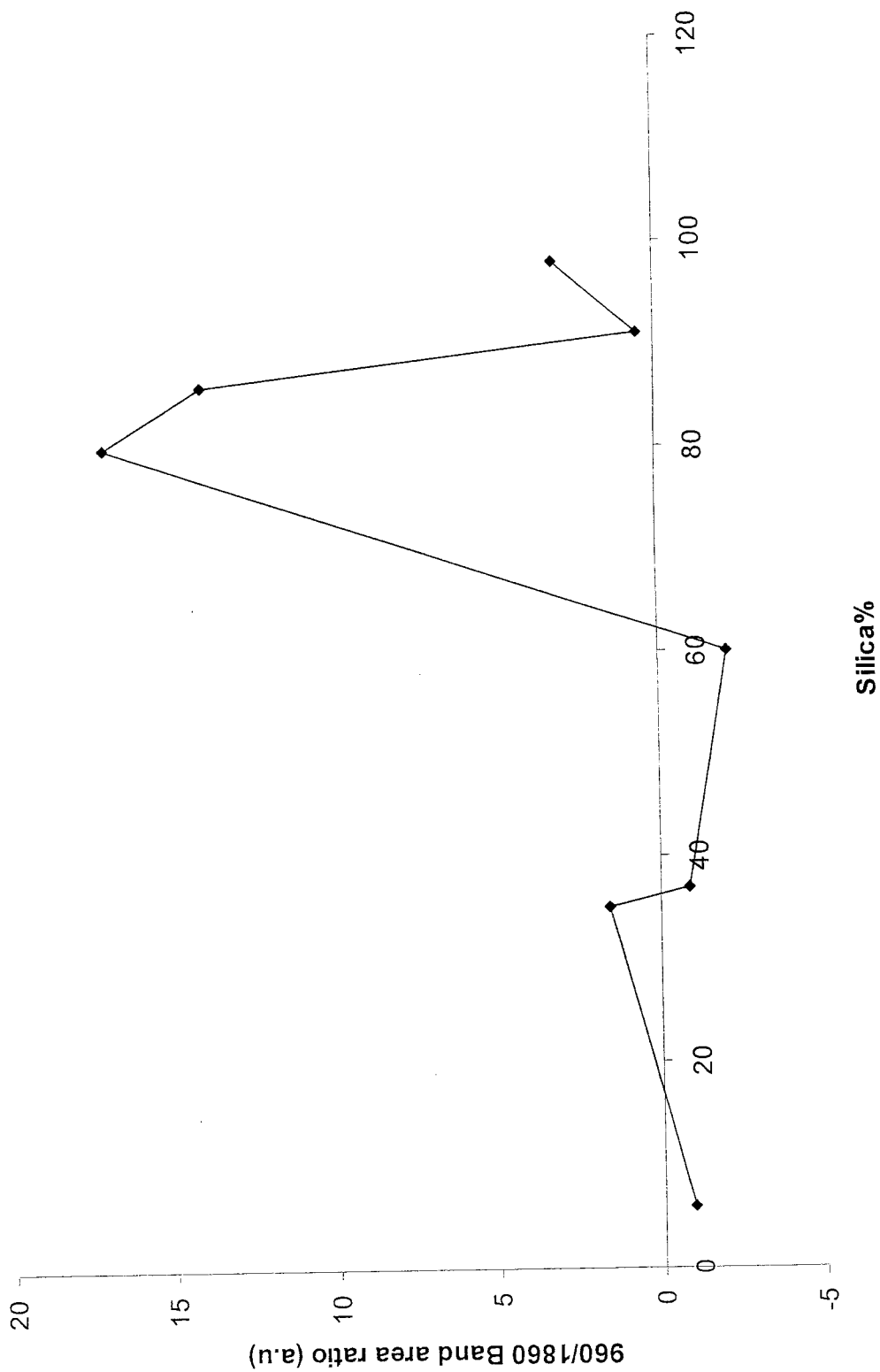
Figure 37: Relative amounts of Si-O-Ti bonds as a function of total content of silica in the ST samples
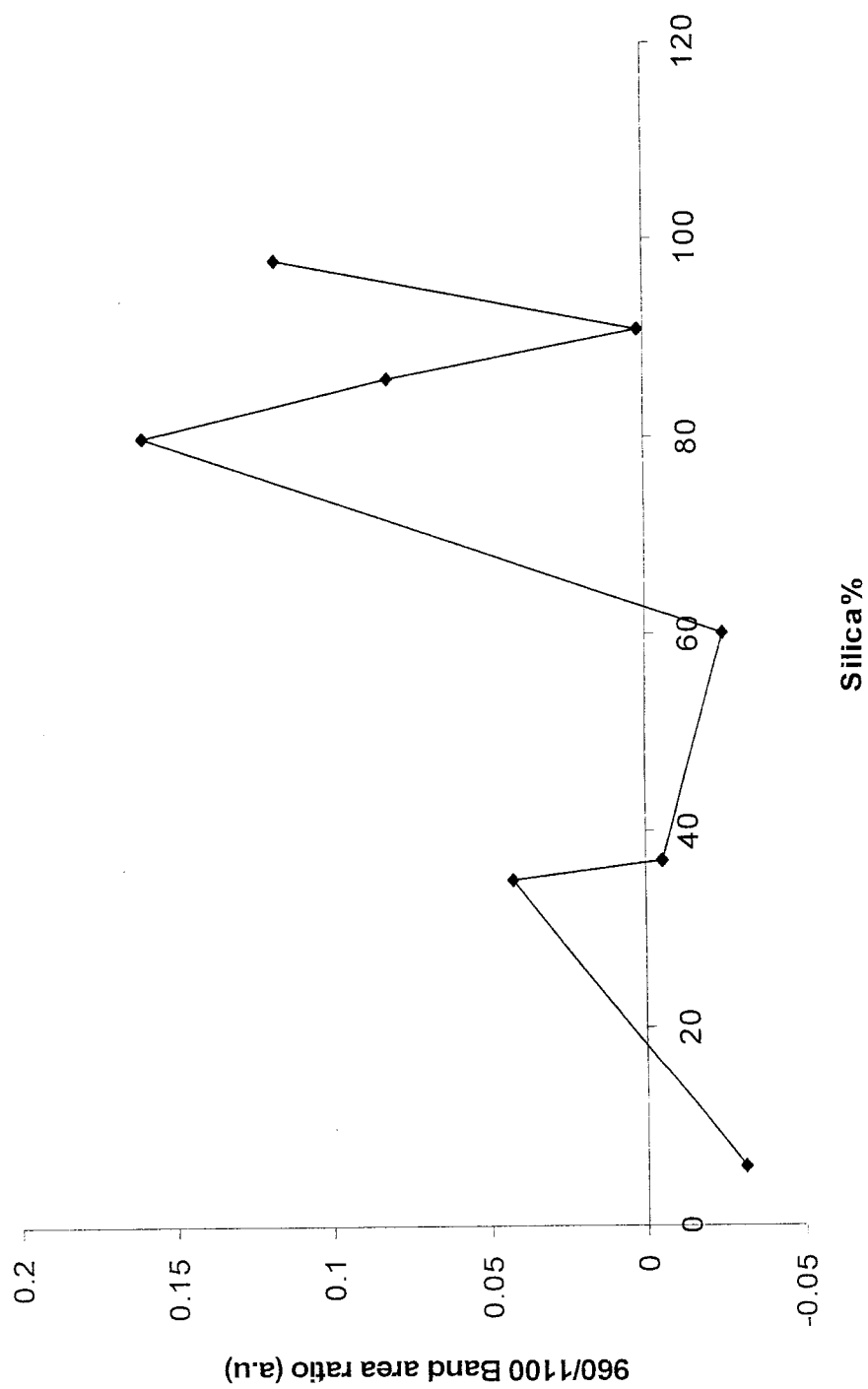
Figure 38: Relative amounts of Si-O-Ti bonds as a function of total content of silica in the ST samples
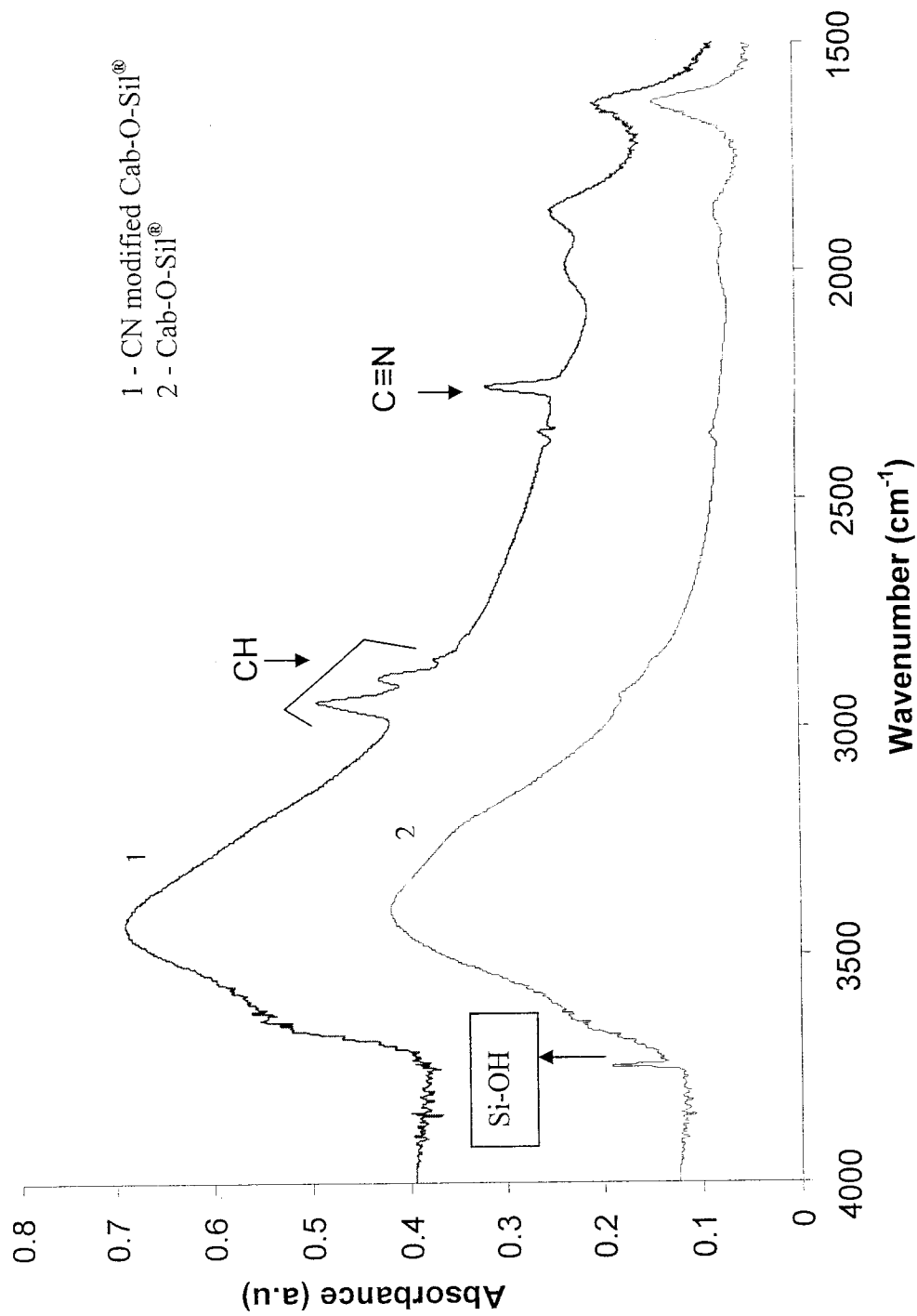
Figure 39: FTIR spectra of Cab-O-Sil® and cyano groups modified on to Cab-O-Sil®
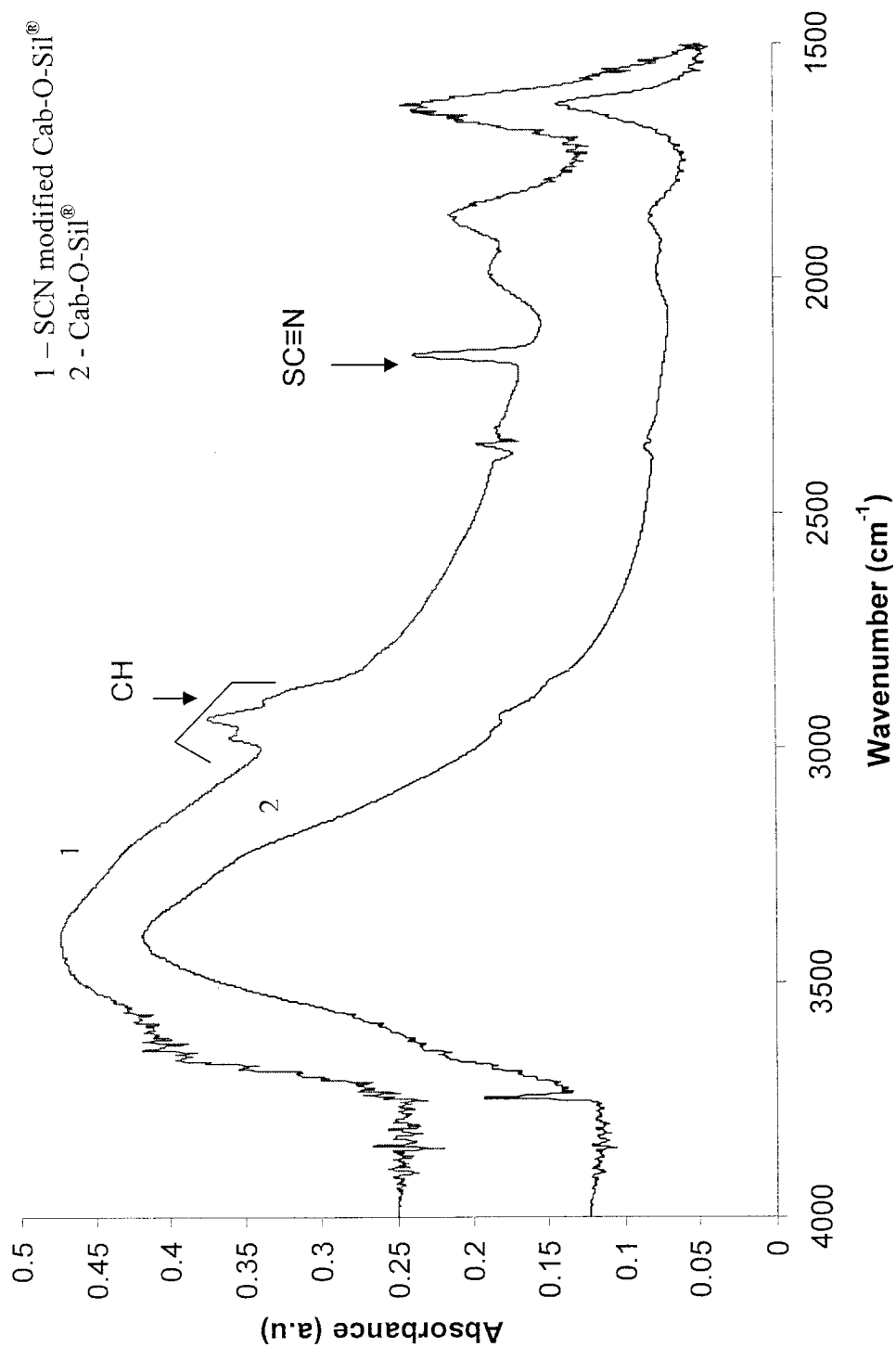
Figure 40: FTIR spectra of Cab-O-Sil® and thiocyano groups modified on to Cab-O-Sil®
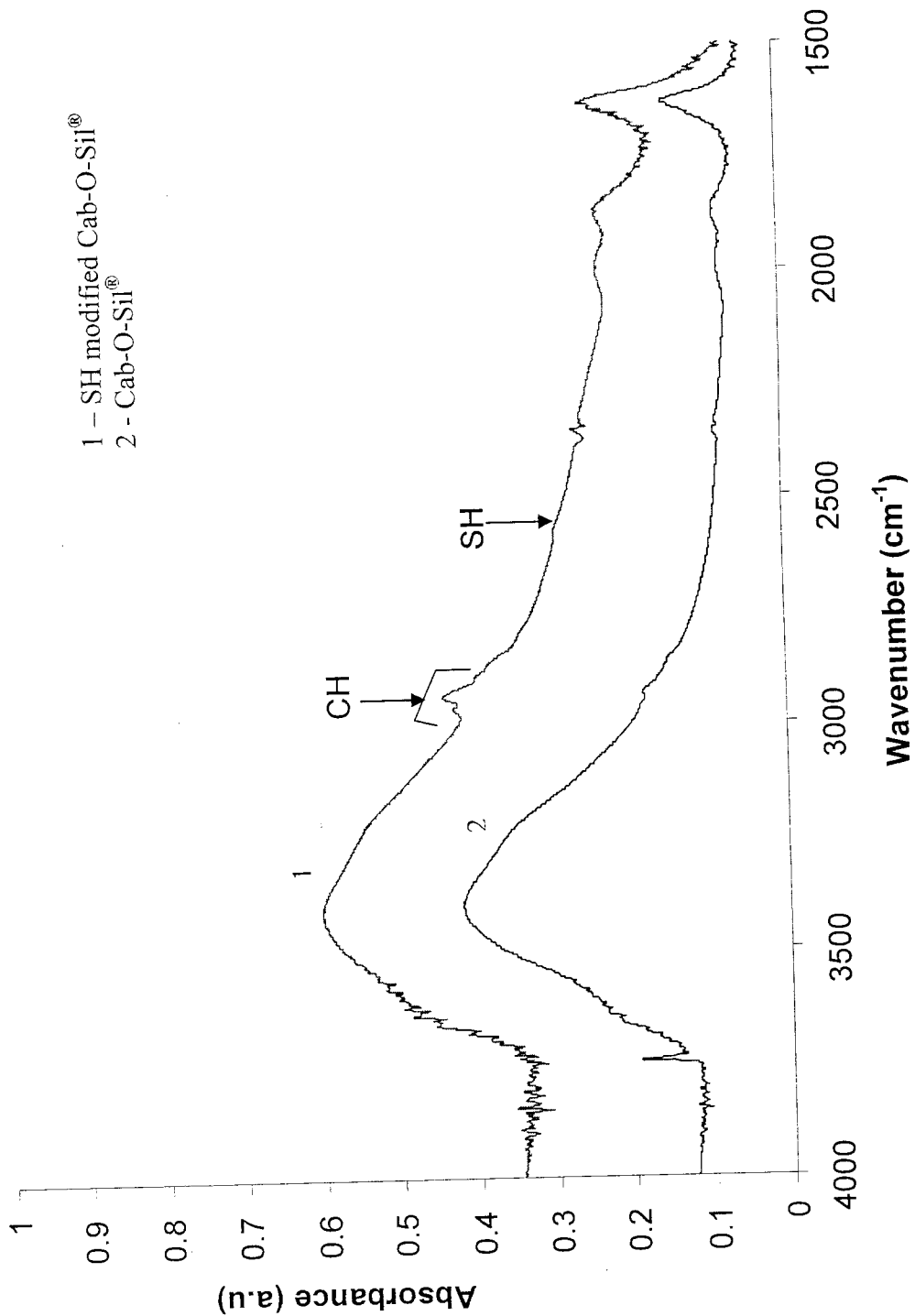
Figure 41: FTIR spectra of Cab-O-Sil® and thiol groups modified over Cab-O-Sil®
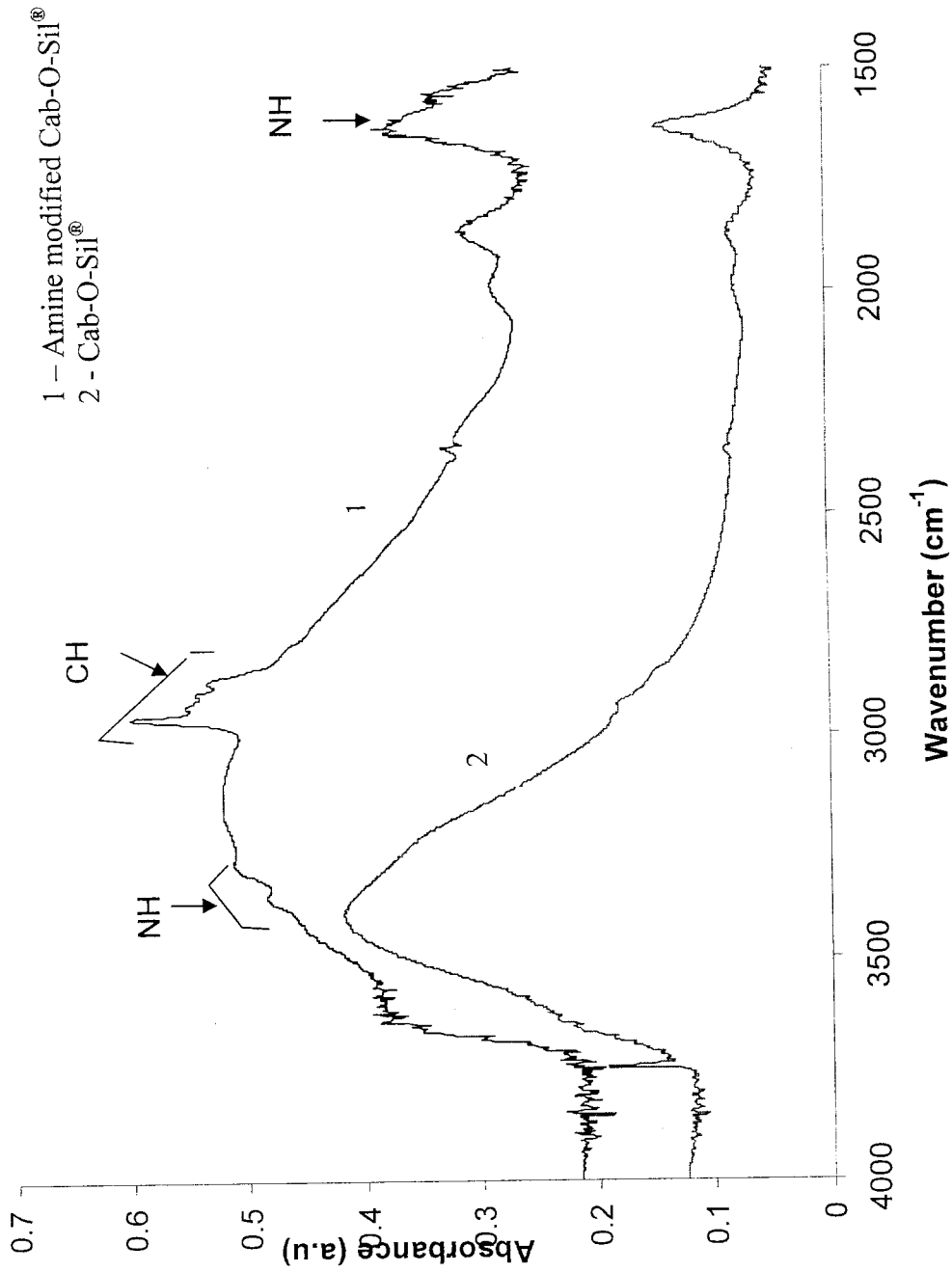
Figure 42: FTIR spectra of Cab-O-Sil® and amine treated Cab-O-Sil®
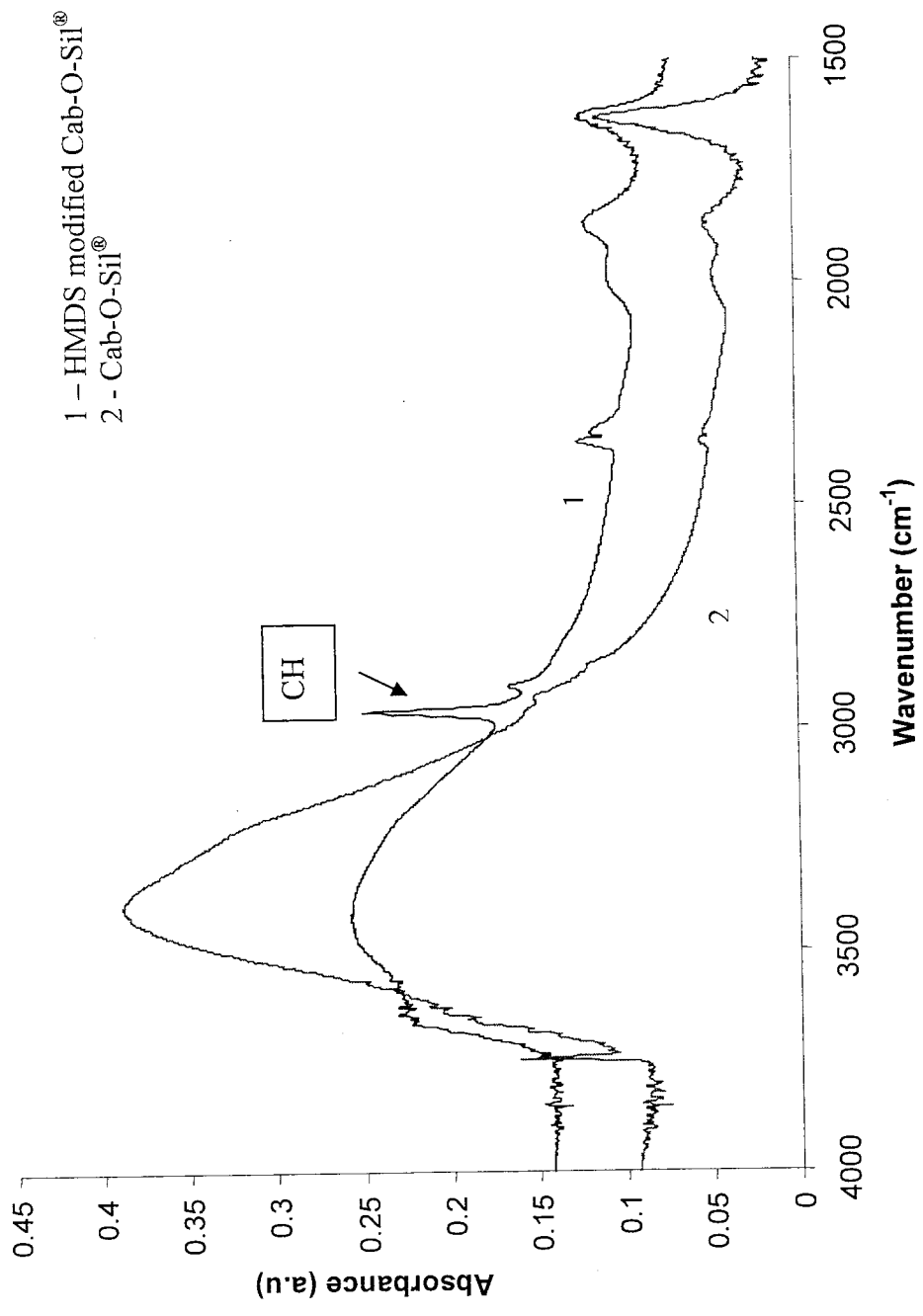
Figure 43: FTIR spectra of Cab-O-Sil® and HMDS modified on to Cab-O-Sil®

$$y = 0.2045x + 0.0445$$
$$R^2 = 0.9969$$
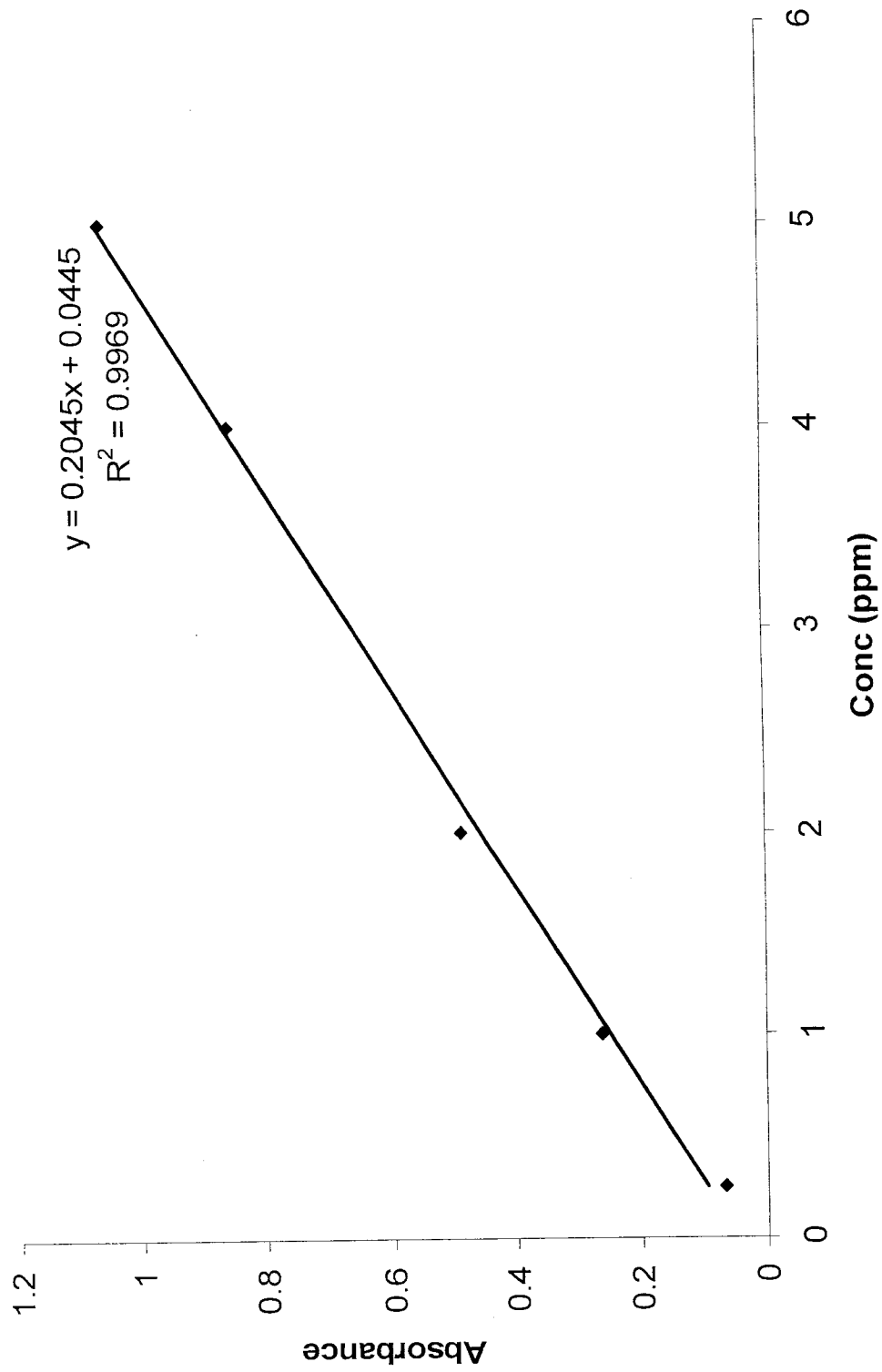
Figure 44: Standard curve for methylene blue obtained using the conc 0.25, 1, 2, 4 and 5 ppm at pH 7

S.No	Original conc of MB (ppm)	Mass of Cab-O-Sil® (g)	Equilibrium conc of MB (mMolar)	MB adsorbed on adsorbent mmol/g
1	80	0.0256	0.015861653	0.228765224
2	70	0.0251	0.009578145	0.208440679
3	60	0.0252	0.008156329	0.178007542
4	40	0.0254	0.004945778	0.118221302
5	30	0.0253	0.00639817	0.086359482
6	20	0.0255	0.005542023	0.05586989
7	10	0.0255	0.003753287	0.026971929
8	5	0.0253	0.002453779	0.013022282
9	1	0.0249	0.000558024	0.002578756

MB: Methylene blue

Table 2: Adsorption data for methylene blue adsorption onto Cab-O-Sil® at pH 7
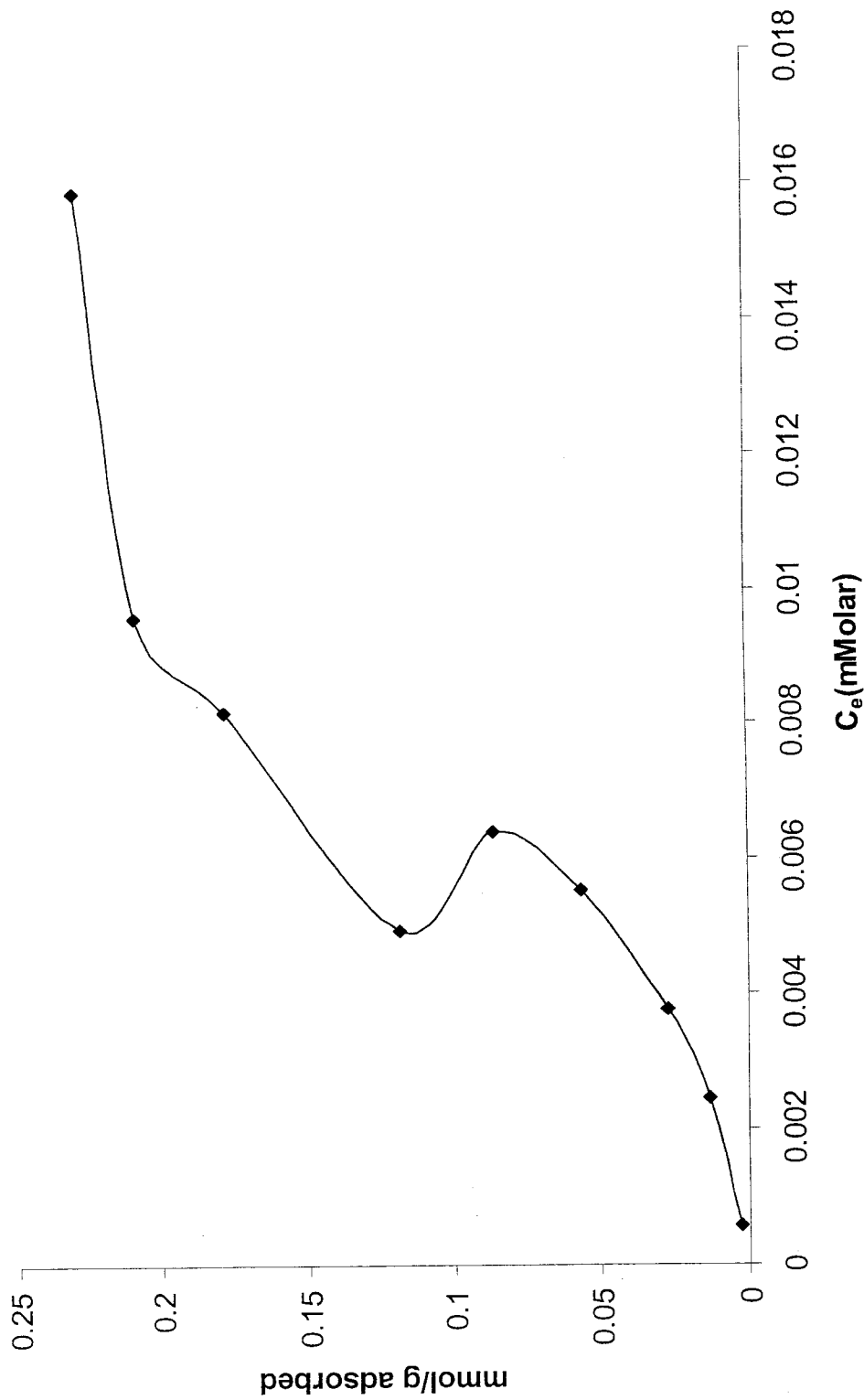
Figure 45: Adsorption isotherm of methylene blue adsorption onto Cab-O-Sil® at pH 7

S.No	Original conc of MB (ppm)	Mass of Cyano modified Cab-O-Sil® (g)	Equilibrium conc of MB (mMolar)	MB adsorbed on adsorbent mmol/g
1	80	0.0252	0.122115616	0.126985741
2	70	0.0249	0.07013526	0.149314586
3	60	0.025	0.035354286	0.152233646
4	40	0.0253	0.018919321	0.104880732
5	30	0.0249	0.012406488	0.081714335
6	20	0.0251	0.004273091	0.058024123
7	10	0.025	0.002484355	0.0287803
8	5	0.0248	0.000986098	0.014764344
9	1	0.025	2.29325E-05	0.003103533

Table 3: Adsorption data for methylene blue adsorption onto cyano modified Cab-O-Sil® at pH 7

Figure 46: Adsorption isotherm of methylene blue adsorption onto cyano treated Cab-O-Sil® at pH 7

S.No	Original conc of MB (ppm)	Mass of Thiocyano modified Cab-O-Sil® (g)	Equilibrium conc of MB (mMolar)	MB adsorbed on adsorbent mmol/g
1	80	0.0254	0.082365932	0.165109558
2	70	0.025	0.02923895	0.189613637
3	60	0.025	0.020065946	0.167521986
4	40	0.0254	0.013568402	0.109734468
5	30	0.0254	0.007819986	0.084620059
6	20	0.0251	0.002698392	0.059592548
7	10	0.0252	0.000542736	0.030478094
8	5	0.0256	3.82209E-05	0.015522862
9	1	0.0253	2.29325E-05	0.003066732

Table 4: Adsorption data for methylene blue adsorption onto thiocyano modified Cab-O-Sil® at pH 7

Figure 47: Adsorption isotherm of methylene blue adsorption onto thiocyano treated Cab-O-Sil® at pH 7

S.No	Original conc of MB (ppm)	Mass of Thiol modified Cab-O-Sil® (g)	Equilibrium conc of MB (mMolar)	MB adsorbed on adsorbent mmol/g
1	80	0.0252	0.076250596	0.172486753
2	70	0.025	0.025416865	0.193435722
3	60	0.0254	0.017772695	0.167140981
4	40	0.0249	0.013568402	0.111937971
5	30	0.0254	0.00280541	0.089555665
6	20	0.0248	0.001108405	0.061916236
7	10	0.0252	0.000619178	0.030402259
8	5	0.0251	0.000435718	0.015136066
9	1	0.0255	3.82209E-05	0.003027691

Table 5: Adsorption data for methylene blue adsorption onto thiol modified Cab-O-Sil® at pH 7
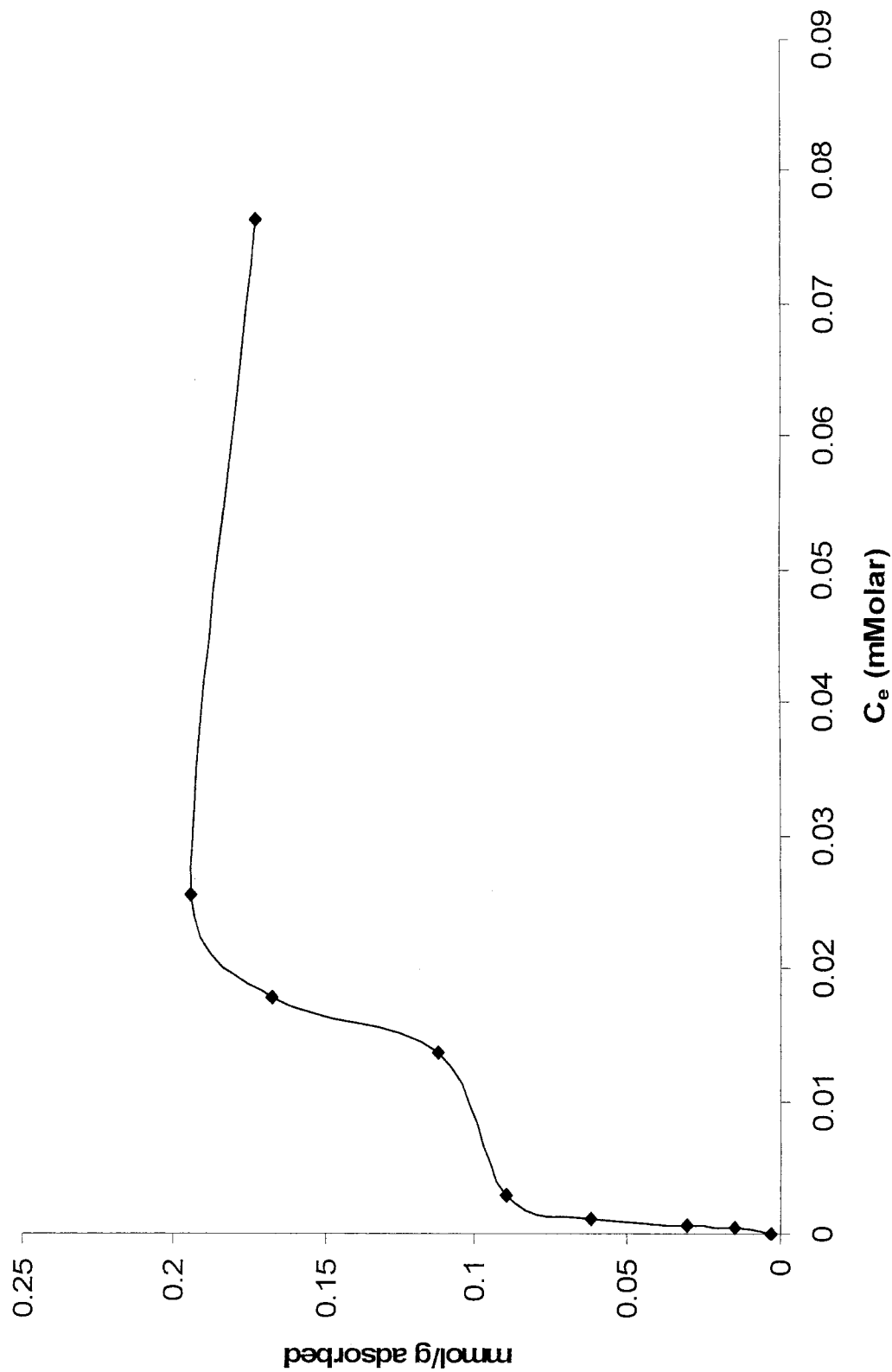
Figure 48: Adsorption isotherm of methylene blue adsorption onto thiol treated Cab-O-Sil® at pH 7

S.No	Original conc of MB (ppm)	Mass of Amine modified Cab-O-Sil® (g)	Equilibrium conc of MB (mMolar)	MB adsorbed on adsorbent mmol/g
1	80	0.0251	0.051024835	0.198299211
2	70	0.0256	0.016243861	0.197860084
3	60	0.0253	0.007548618	0.17790446
4	40	0.0256	0.005786637	0.116476547
5	30	0.0255	0.004609435	0.087435815
6	20	0.0251	0.003447521	0.058846404
7	10	0.0254	0.002224453	0.028582876
8	5	0.0257	0.002514932	0.012760113
9	1	0.0256	0.002178588	0.000925661

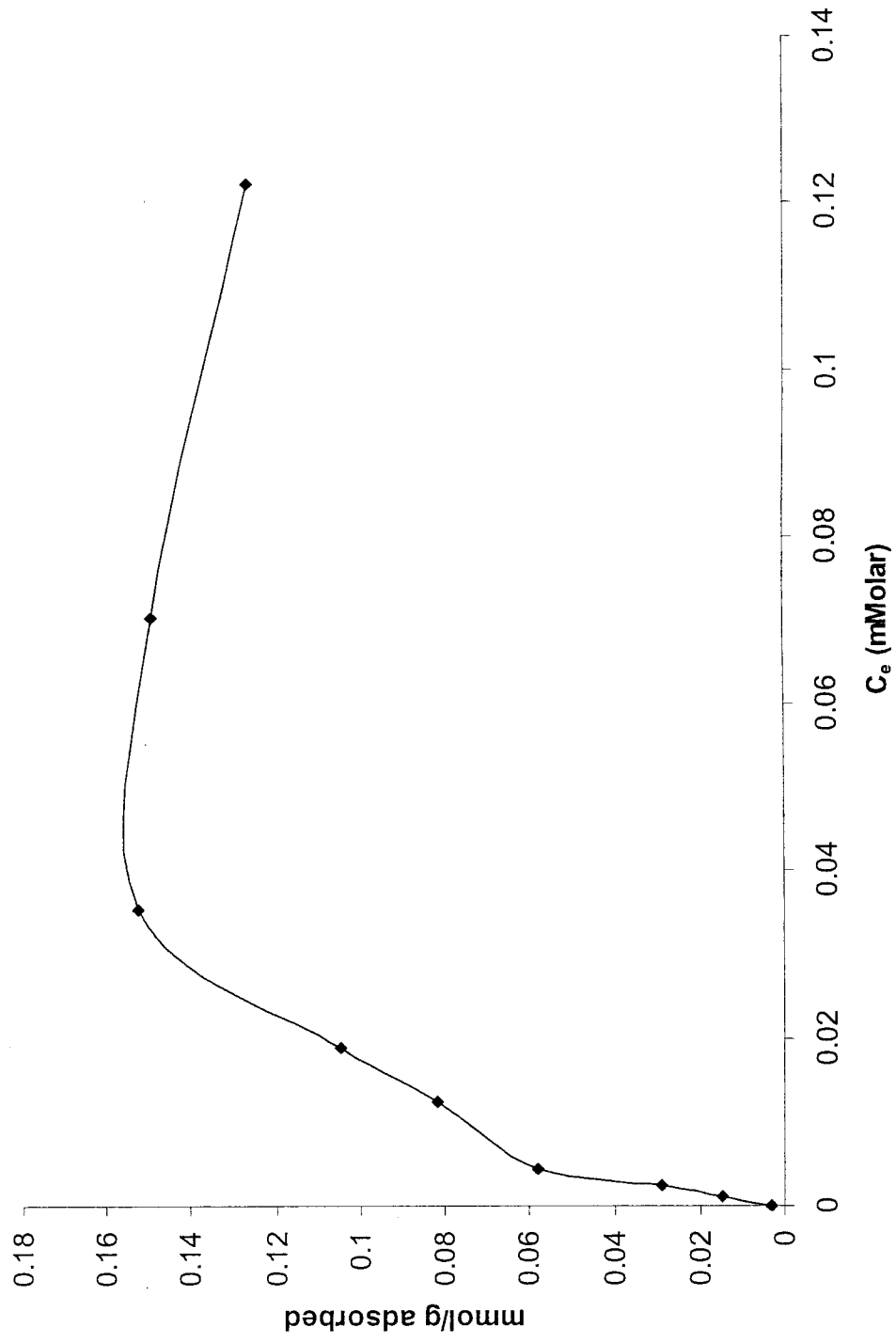Table 6: Adsorption data for methylene blue adsorption onto amine modified Cab-O-Sil® at pH 7

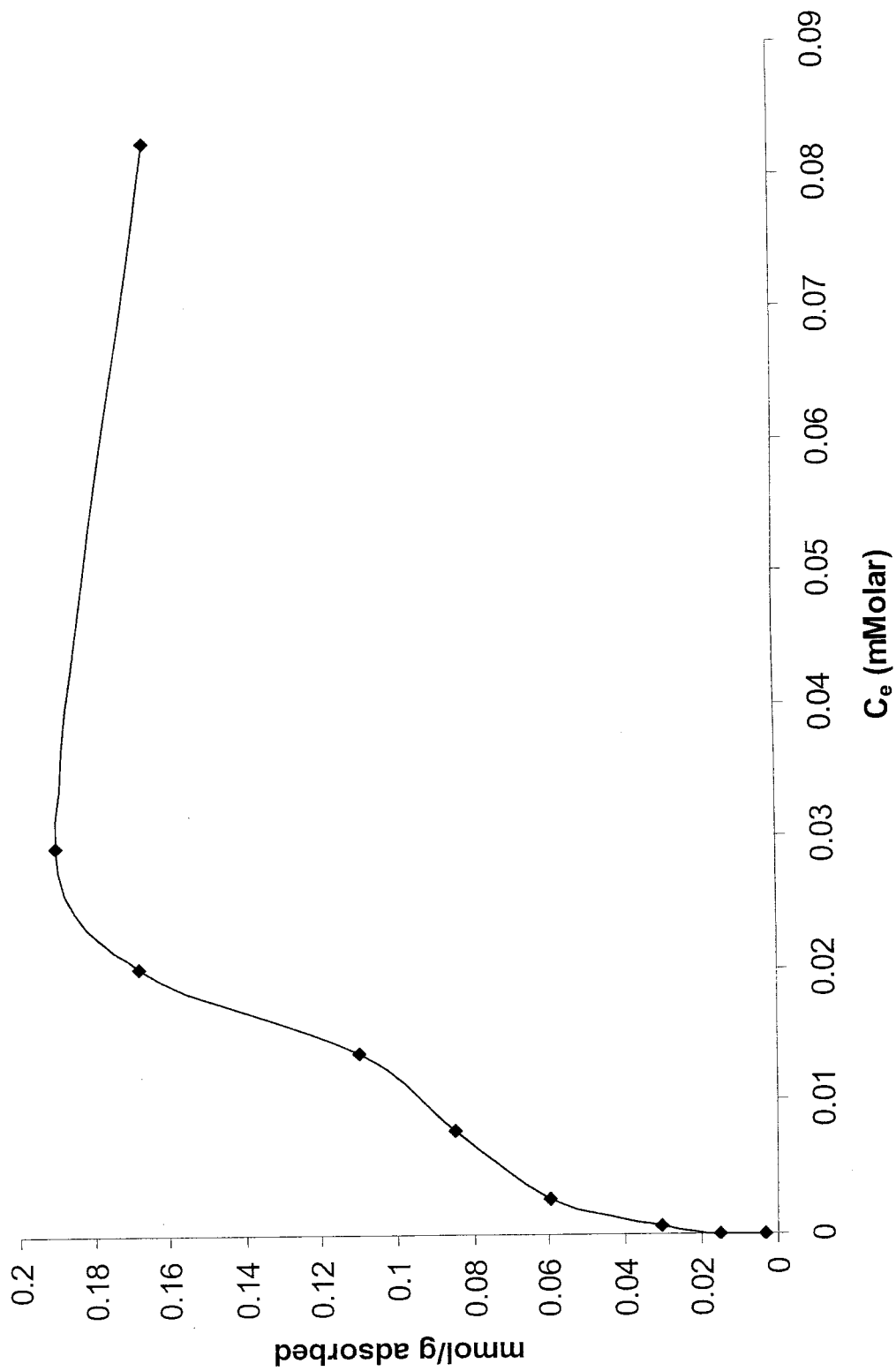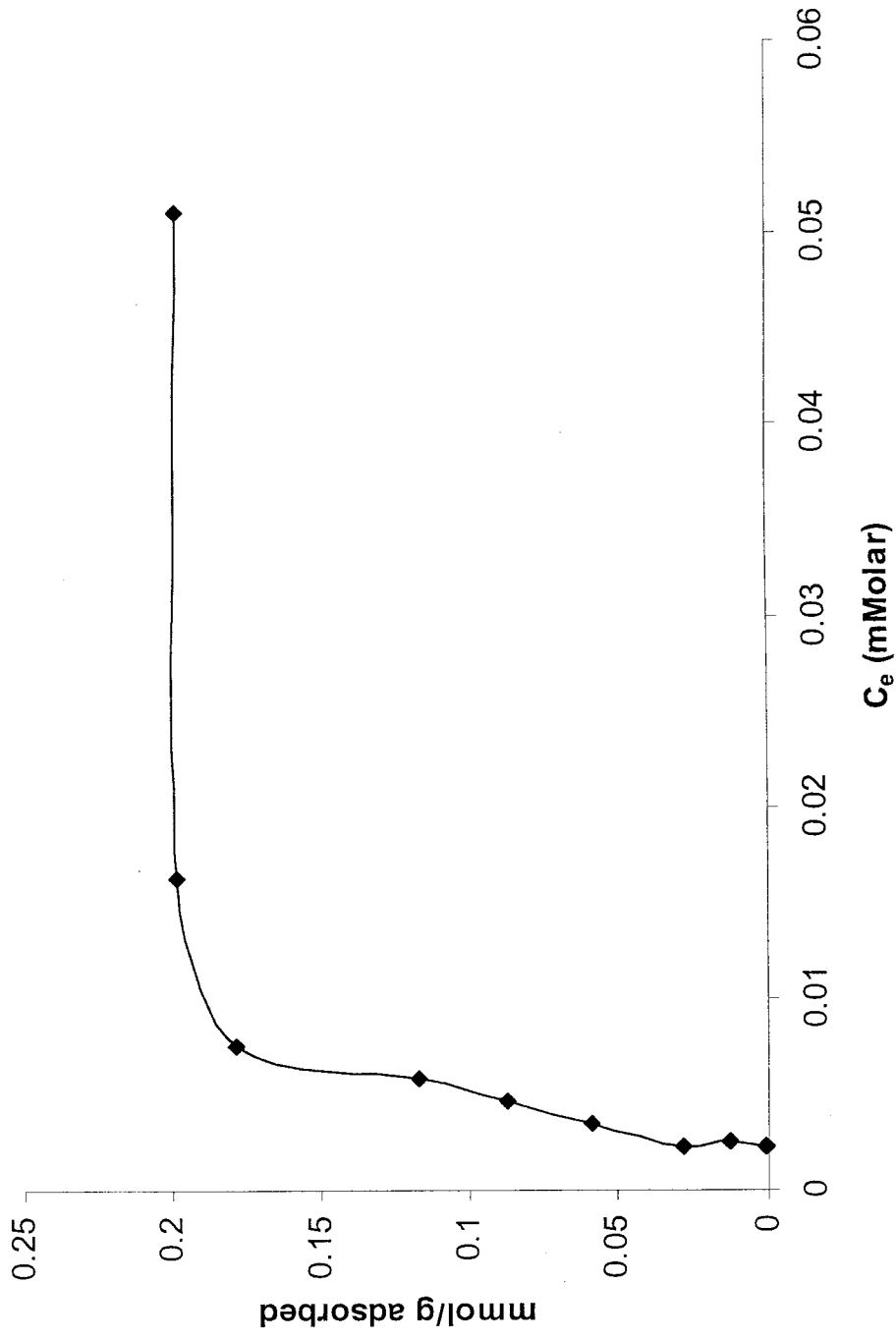Figure 49: Adsorption isotherm of methylene blue adsorption onto amine treated Cab-O-Sil® at pH 7

S.No	Original conc of MB (ppm)	Mass of HMDS modified Cab-O-Sil® (g)	Equilibrium conc of MB (mMolar)	MB adsorbed on adsorbent mmol/g
1	80	0.0256	0.13128862	0.116043577
2	70	0.0251	0.100329731	0.118050653
3	60	0.0252	0.092303353	0.094528352
4	40	0.0254	0.041851831	0.081896447
5	30	0.0253	0.00916536	0.083625105
6	20	0.0255	0.002637239	0.058717718
7	10	0.0255	0.001077828	0.029594929
8	5	0.0253	0.000114663	0.015333661
9	1	0.0249	-0.000359276	0.00349974

Table 7: Adsorption data for methylene blue adsorption onto HMDS modified Cab-O-Sil® at pH 7
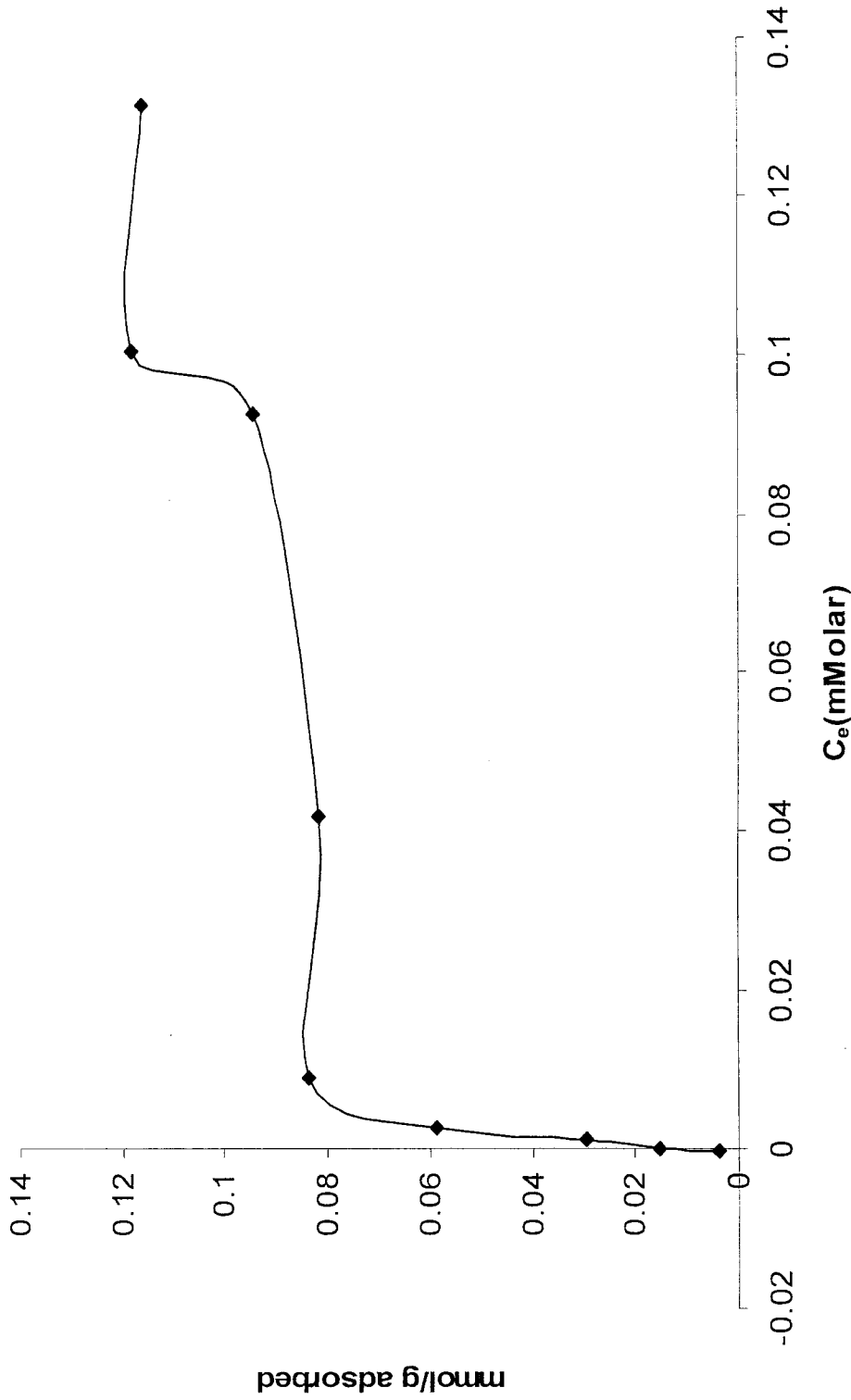
Figure 50: Adsorption isotherm of methylene blue adsorption onto HMDS treated Cab-O-Sil® at pH 7
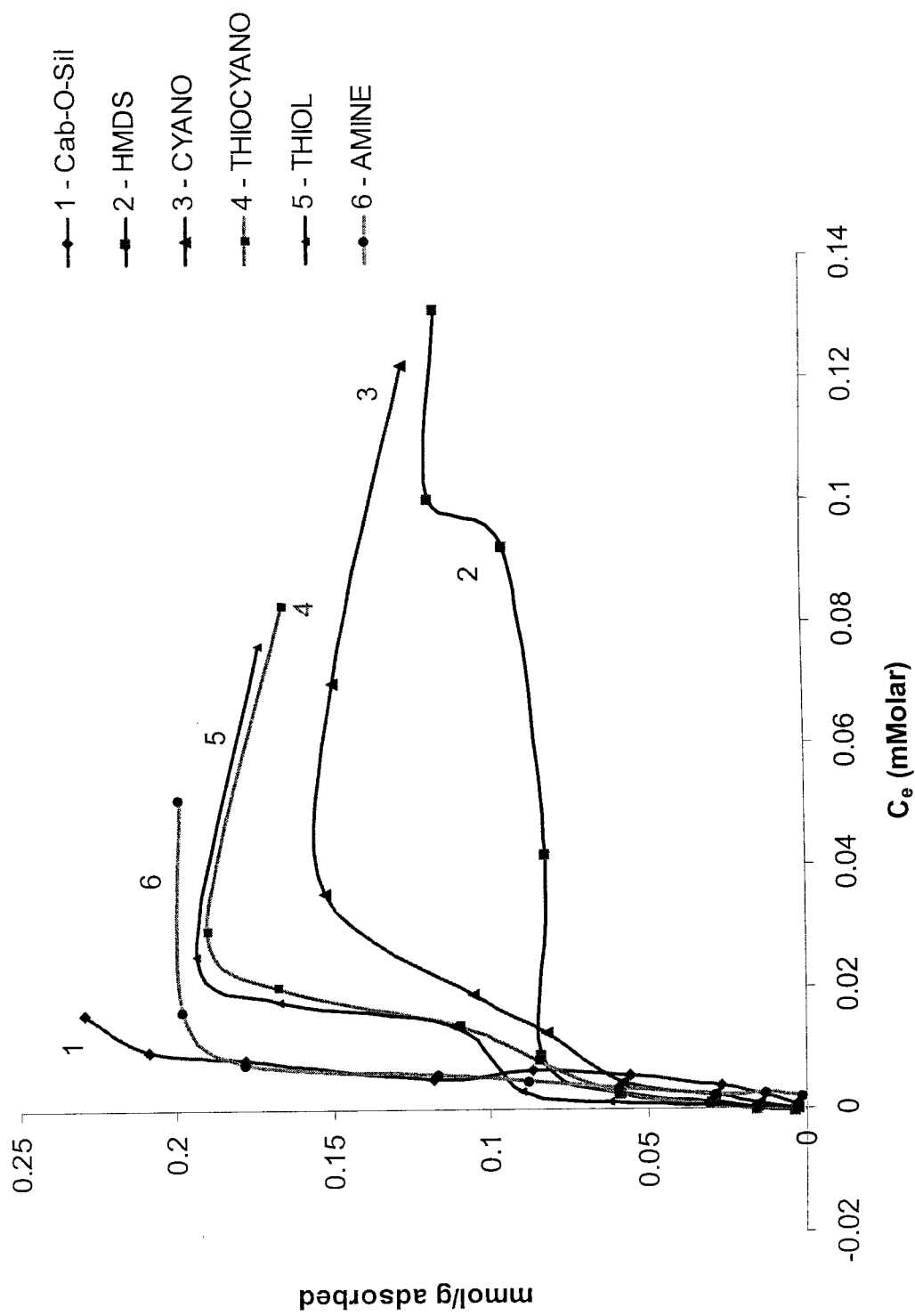
Figure 51: Adsorption isotherms of methylene blue adsorption onto various modified silicas
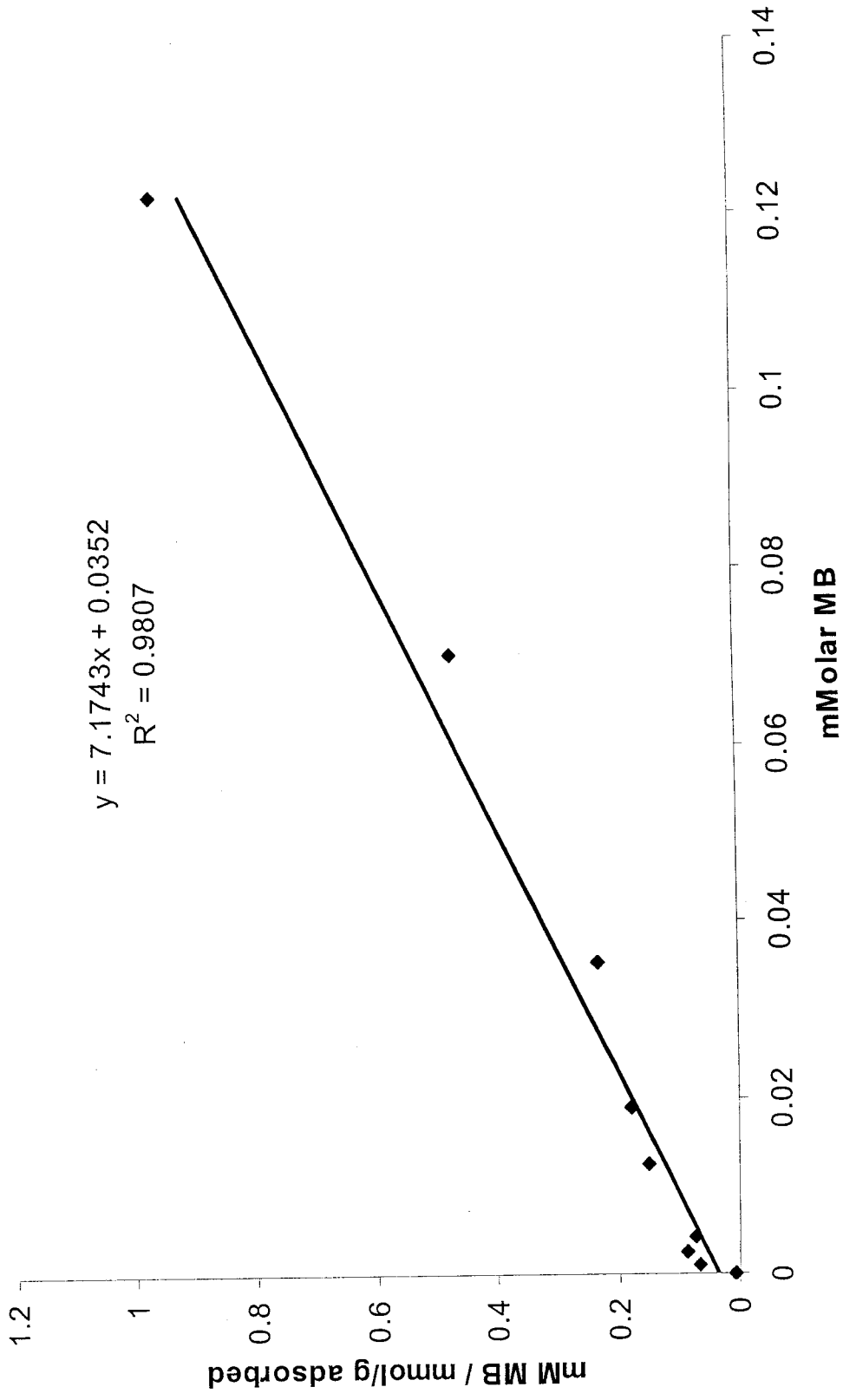
Figure 52: Langmuir plot for CN groups modified Cab-O-Sil® at pH 7

$$y = 5.7518x + 0.0181$$
$$R^2 = 0.9819$$
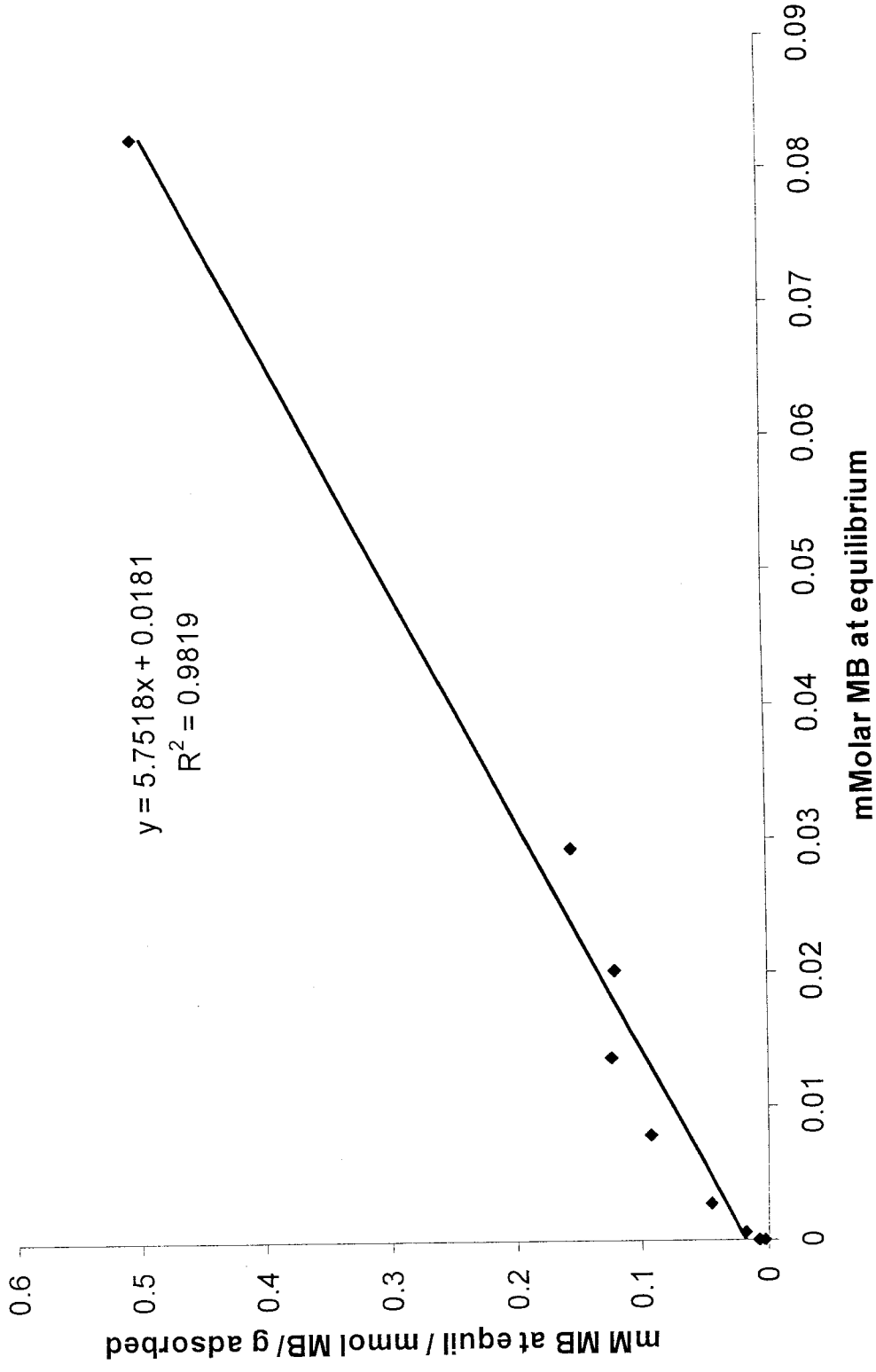
Figure 53: Langmuir plot for SCN groups modified onto Cab-O-Sil® at pH 7

The chart shows a Langmuir plot with:
- Y-axis: mM MB / mmol/g adsorbed (0 to 0.5)
- X-axis: mMolar MB at equilibrium (0 to 0.09)
- Equation: y = 5.5075x + 0.0169
- $R^2 = 0.9882$
- X-axis label: mMolar MB at equilibrium
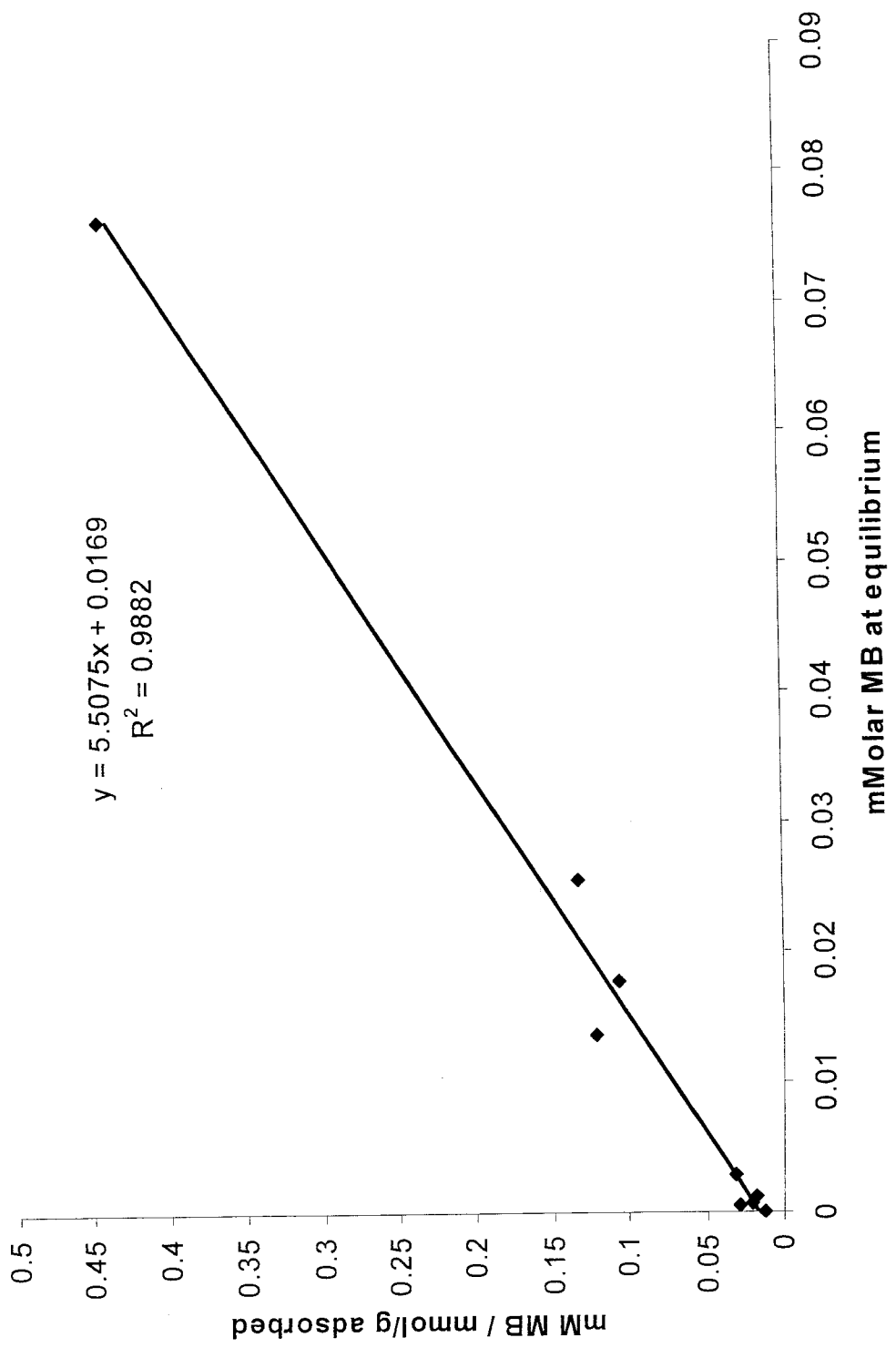
Figure 54: Langmuir plot for SH modified onto Cab-O-Sil® at pH 7

$y = 8.7599x + 0.0436$

$R^2 = 0.9761$

mMolar MB at equilibrium

mM MB at equil / mmol/g adsorbed

0   0.2   0.4   0.6   0.8   1   1.2   1.4

0   0.02   0.04   0.06   0.08   0.1   0.12   0.14
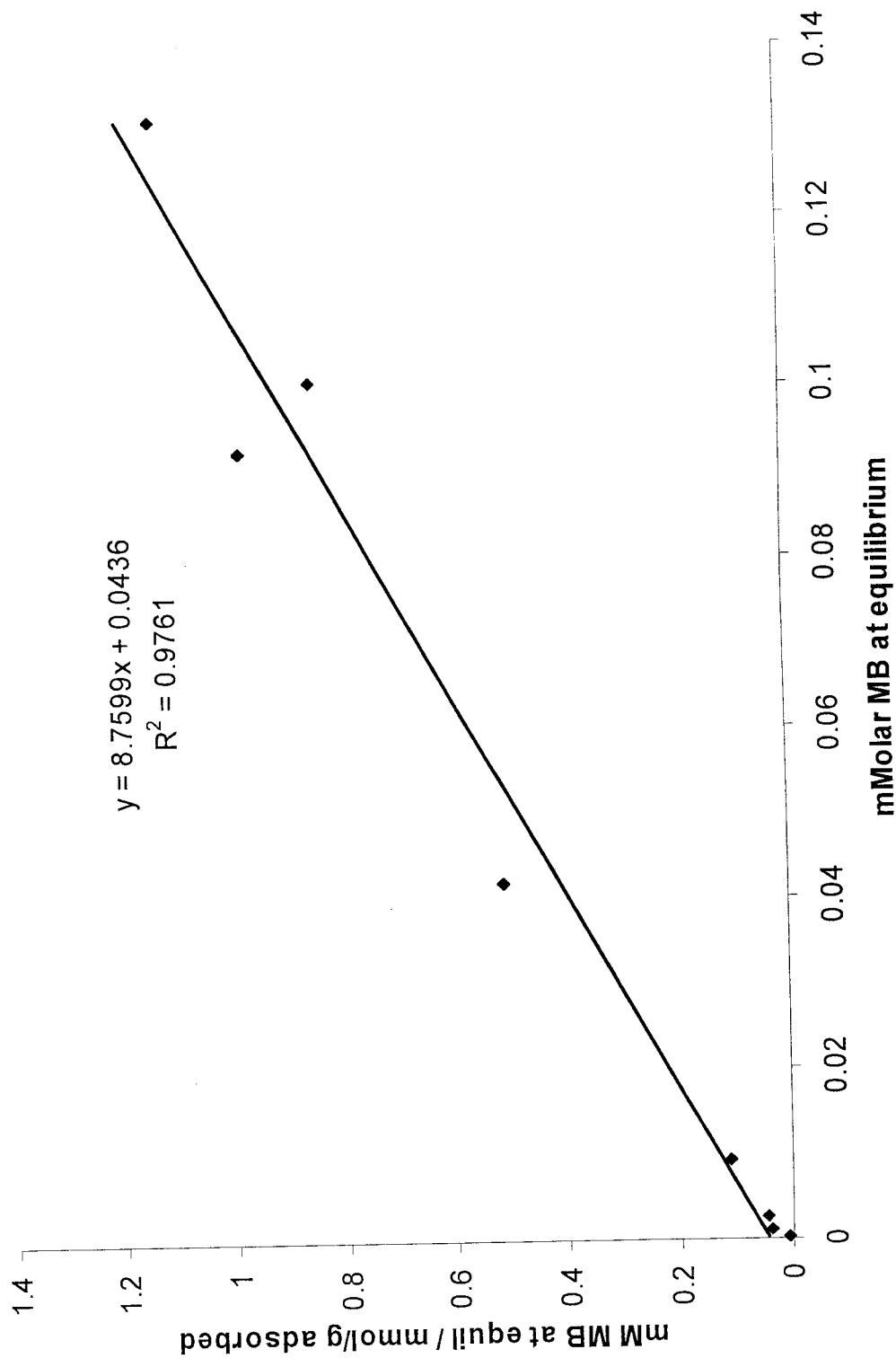
Figure 55: Langmuir plot for HMDS modified Cab-O-Sil® at pH 7

Modified groups	No of adsorption sites (mmol/g)	K	No of groups on silica (mmol/g)	% of groups involved in adsorption	R^2, Correlation coefficient
Cyano	0.139	11312	0.946	14.6	0.9807
Thiocyano	0.173	17637	0.5	34.6	0.9819
Thiol	0.181	18086	0.823	22.06	0.9882
HMDS	0.114	11150	????	???	0.9761

Table 8: Adsorption data for methylene blue adsorption onto different adsorbents. Langmuir parameters and regression coefficient values.
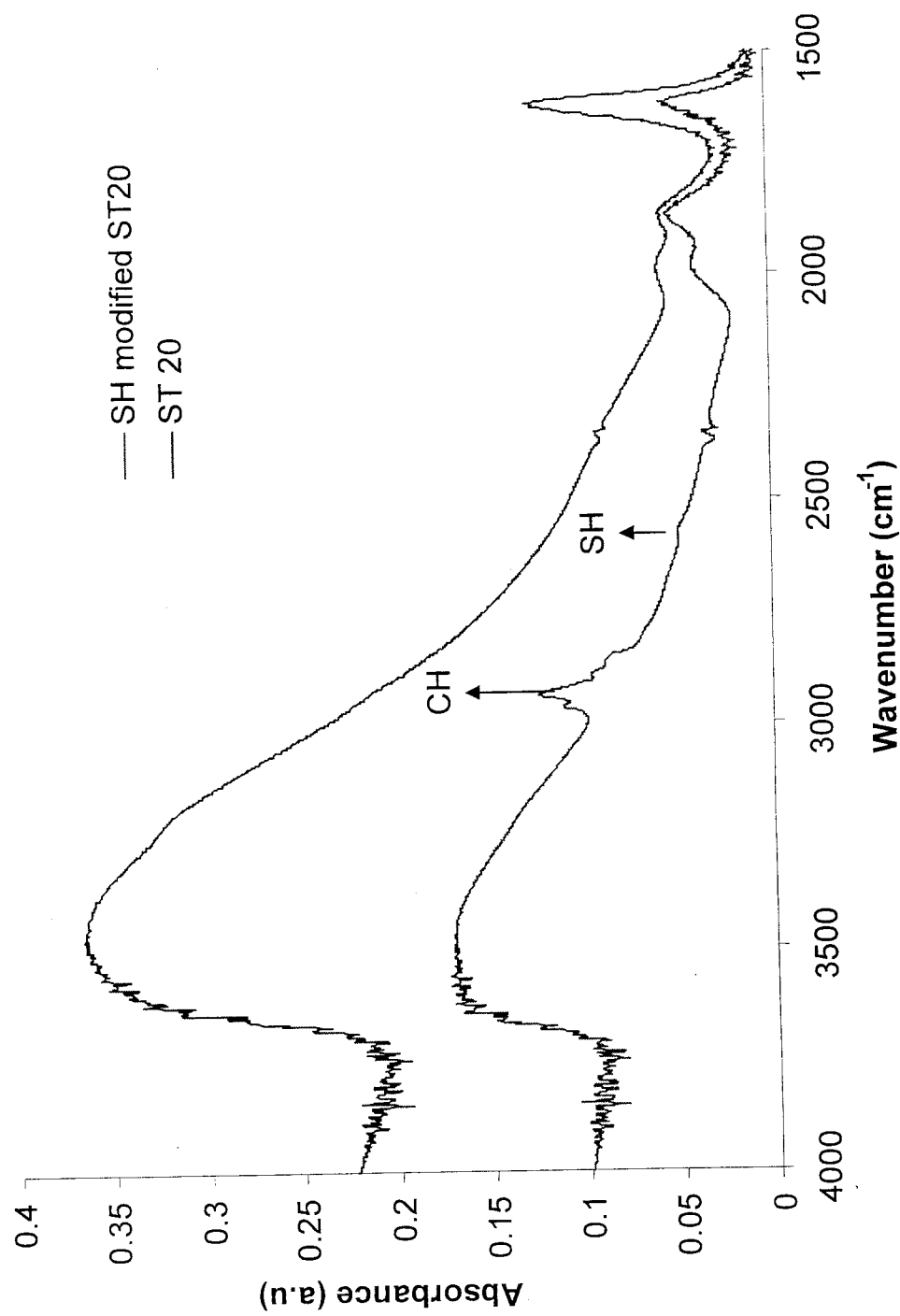
Figure 56: FTIR spectra of ST 20 and SH groups modified over ST 20
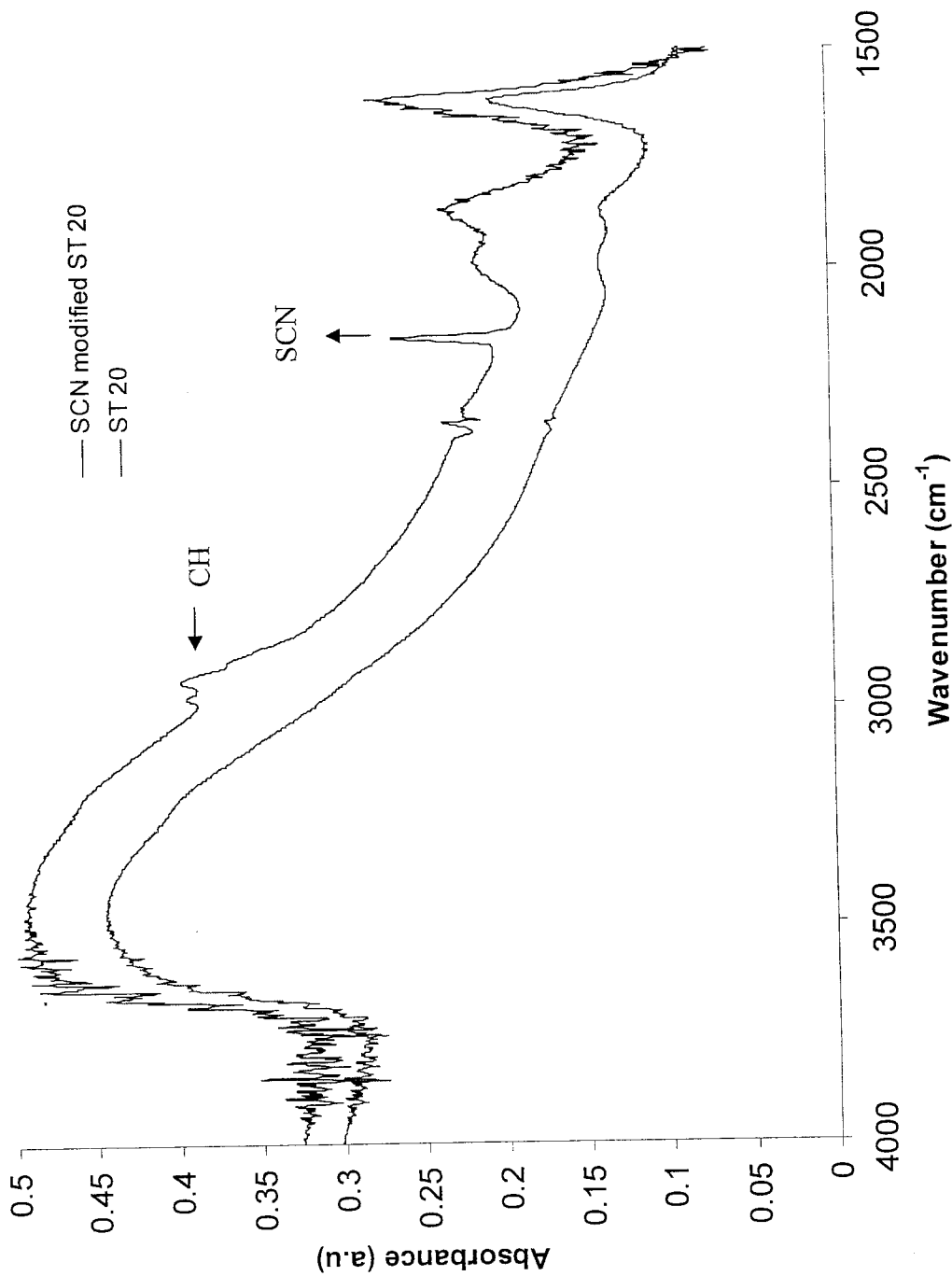
Figure 57: FTIR spectra of ST 20 and SCN groups modified on ST 20

Band area ratio of SCN modified ST 20 before treatment with water	Band area ratio of SCN modified ST 20 after treatment with water
0.378337	0.349046
0.360761	0.32147
0.363437	0.33244
0.386984	0.36794

Table 9: Band area ratios of thiocyano modified ST 20 before and after treatment with water.

t-calculated	2.49
t-test	2.45
P(T<=t) two-tail	0.046

Table 10: *t*-test and *t*-calculated values obtained assuming two samples with equal variances at 95% confidence level.

S.No	Original conc of MB (ppm)	Mass of ST 20 (g)	Equilibrium conc of MB (mMolar)	MB adsorbed on adsorbent mmol/g
1	80	0.0259	0.172909529	0.07452482
2	70	0.0248	0.150995051	0.068404775
3	60	0.0259	0.112752138	0.072235322
4	40	0.0261	0.067204399	0.055415921
5	30	0.0254	0.044000834	0.049008988
6	20	0.0259	0.011247713	0.049499611
7	10	0.0259	0.007105447	0.023319699
8	5	0.0258	0.002945993	0.01229296
9	1	0.0249	0.001227211	0.001906882

Table 11: Adsorption data for methylene blue adsorption onto ST 20 at pH 7

S.No	Original conc of MB (ppm)	Mass of SH modified ST 20 (g)	Equilibrium conc of MB (mMolar)	MB adsorbed on adsorbent nmol/g
1	80	0.0259	0.203143818	0.045341143
2	70	0.0257	0.187855478	0.03015283
3	60	0.0259	0.138168373	0.047702277
4	40	0.0261	0.087334642	0.036134079
5	30	0.0254	0.065930966	0.027424212
6	20	0.0259	0.03191441	0.029551063
7	10	0.0259	0.015464156	0.015251447
8	5	0.0258	0.006535765	0.008814498
9	1	0.0259	0.00106254	0.001984544

Table 12: Adsorption data for methylene blue adsorption onto thiol modified ST 20 at pH 7
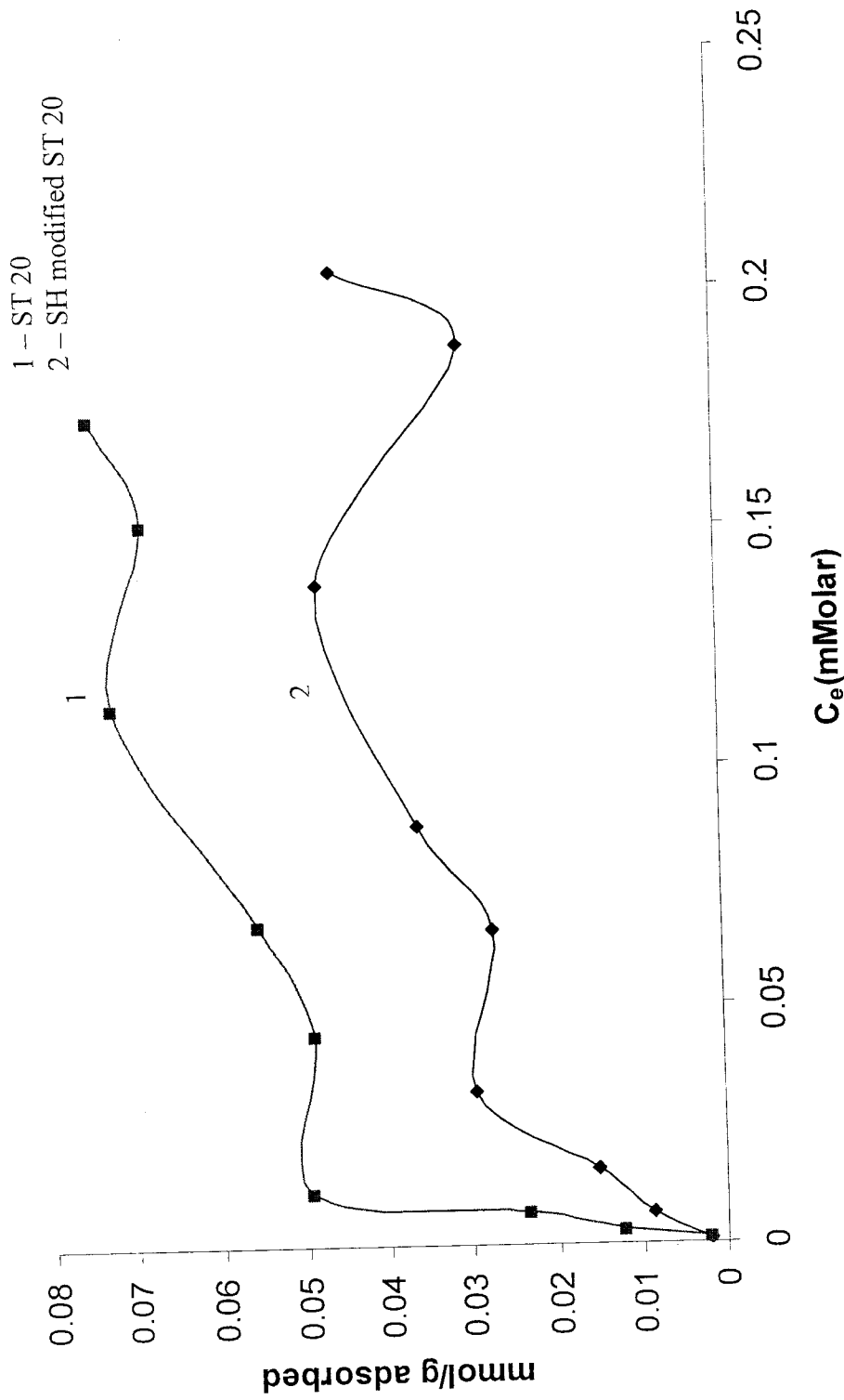
Figure 58: Adsorption isotherms for methylene blue adsorption onto ST 20 and SH modified ST 20

S.No	Original conc of MB (ppm)	Mass of SCN modified ST 20 (g)	Equilibrium conc of MB (mMolar)	MB adsorbed on adsorbent mmol/g
1	80	0.0254	0.229199658	0.020588173
2	70	0.0251	0.205996093	0.012805273
3	60	0.025	0.155721703	0.031866229
4	40	0.0247	0.097283095	0.028112881
5	30	0.0251	0.075368617	0.018351942
6	20	0.0249	0.047438399	0.015151517
7	10	0.0248	0.01080083	0.020628856
8	5	0.0254	0.0026538	0.012774141
9	1	0.0252	0.000780327	0.002327518

Table 13: Adsorption data for methylene blue adsorption onto thiocyano modified ST 20 at pH 7
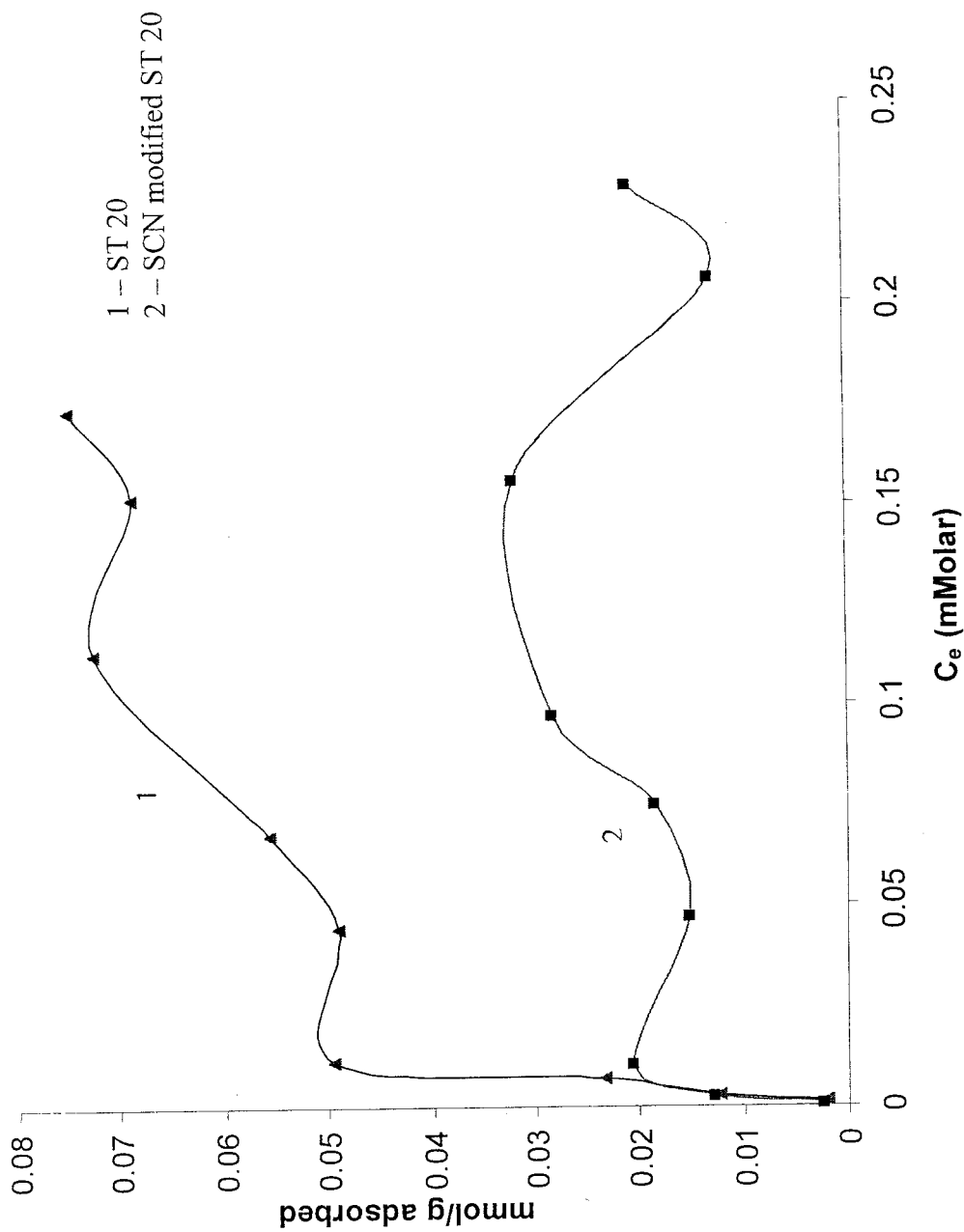
Figure 59: Adsorption isotherm for methylene blue adsorption onto ST 20 and SCN modified ST 20 at pH 7

Figure 60: Langmuir plot for ST 20 at pH 7

The chart shows the following: x-axis labelled "mMolar MB at equilibrium" with values 0, 0.02, 0.04, 0.06, 0.08, 0.1, 0.12, 0.14, 0.16, 0.18, 0.2; y-axis labelled "mMolar MB at equil / mmol MB /g adsorbed" with values 0, 0.5, 1, 1.5, 2, 2.5.

$y = 11.933x + 0.312$
$R^2 = 0.9618$
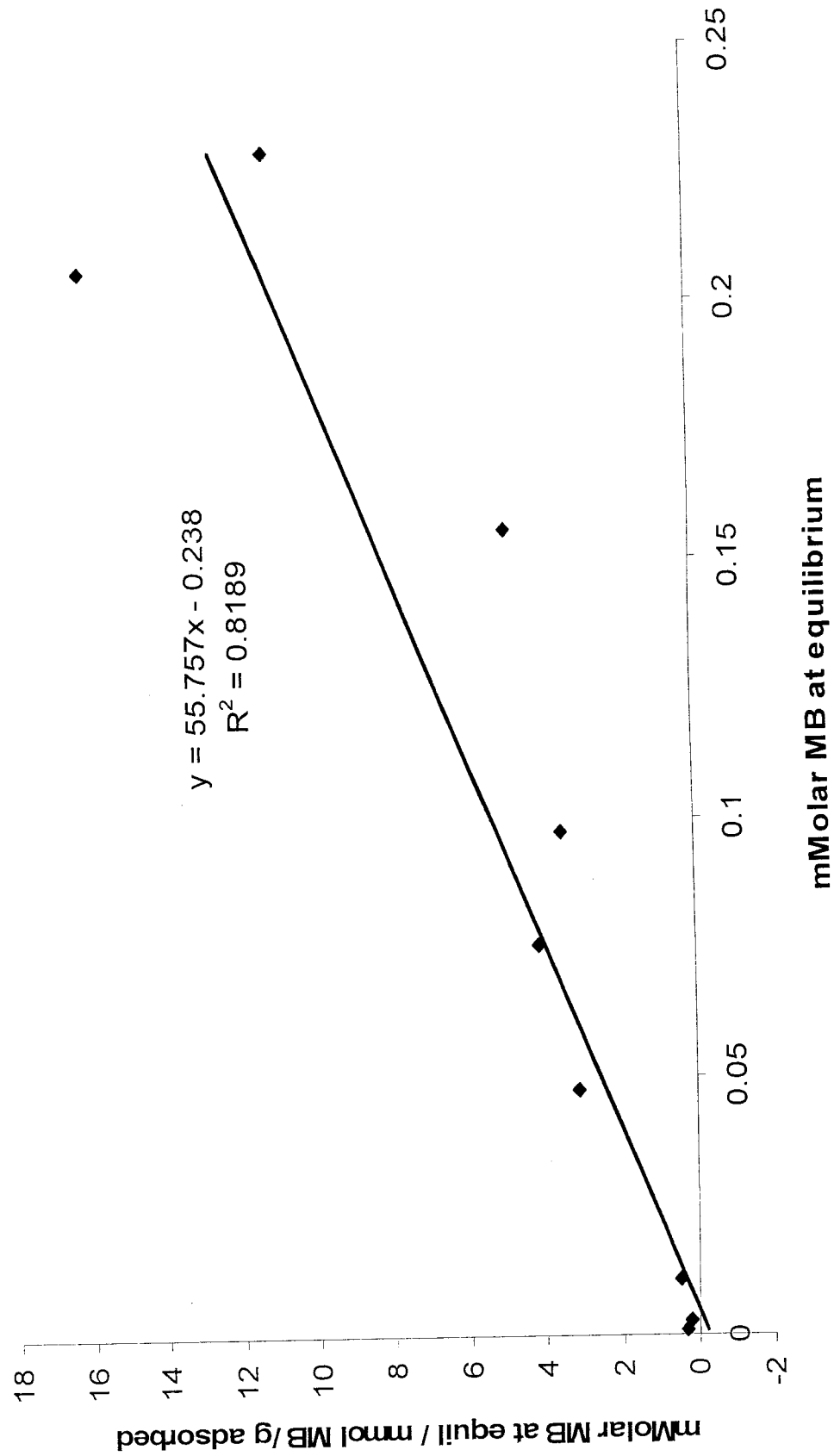
Figure 61: Langmuir plot for SCN modified ST 20 at pH 7

$y = 55.757x - 0.238$
$R^2 = 0.8189$

mMolar MB at equilibrium

mMolar MB at equil / mmol MB /g adsorbed

Modified groups	No of adsorption sites (mmol/g)	K	No of groups on silica (mmol/g)	% of groups involved in adsorption	R^2, Correlation coefficient
ST 20	0.083	21227	????	???	0.9618
SCN ST 20	0.0179	130021	????	???	0.8189

Table 14: Adsorption data of methylene blue adsorption on ST 20 and SCN modified ST 20. Langmuir parameters and regression coefficient values

S.No	Original conc of MB (ppm)	Mass of ST 20 (g)	Equilibrium conc of MB (mMolar)	MB adsorbed on adsorbent mmol/g
1	5	0.0259	0.002945993	0.01229296
2	4	0.0248	0.001794409	0.010711453
3	3	0.0259	0.001536592	0.007874302
4	2	0.0261	0.001416277	0.004875659
5	1	0.0254	0.001227211	0.001906882
6	0.5	0.0259	0.000849079	0.000722828

Table 15: Adsorption data for methylene blue adsorption onto ST 20 at pH 7

S.No	Original conc of MB (ppm)	Mass of SCN modified ST 20 (g)	Equilibrium conc of MB (mMolar)	MB adsorbed on adsorbent mmol/g
1	5	0.0259	0.0026538	0.012774141
2	4	0.0248	0.001433465	0.01120688
3	3	0.0259	0.001089708	0.008159142
4	2	0.0261	0.000952206	0.00521725
5	1	0.0254	0.000780327	0.002327518
6	0.5	0.0259	0.000660013	0.000914191

Table 16: Adsorption data for methylene blue adsorption onto thiocyano modified ST 20 at pH 7

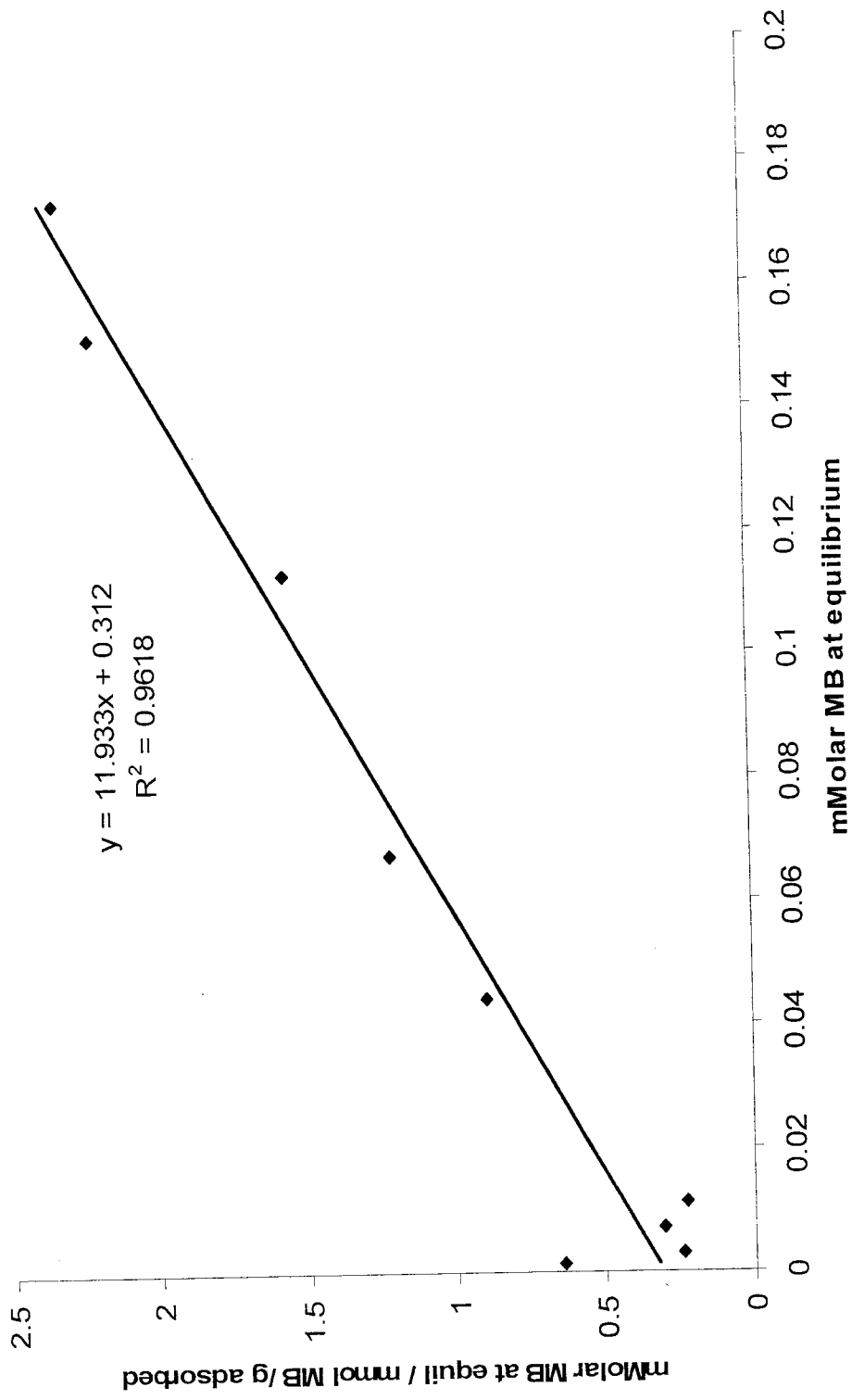Figure 62: Adsorption isotherms of methylene blue adsorption onto ST 20 and thiocyano groups modified over ST 20 at lowest concentrations (0.5-5ppm)
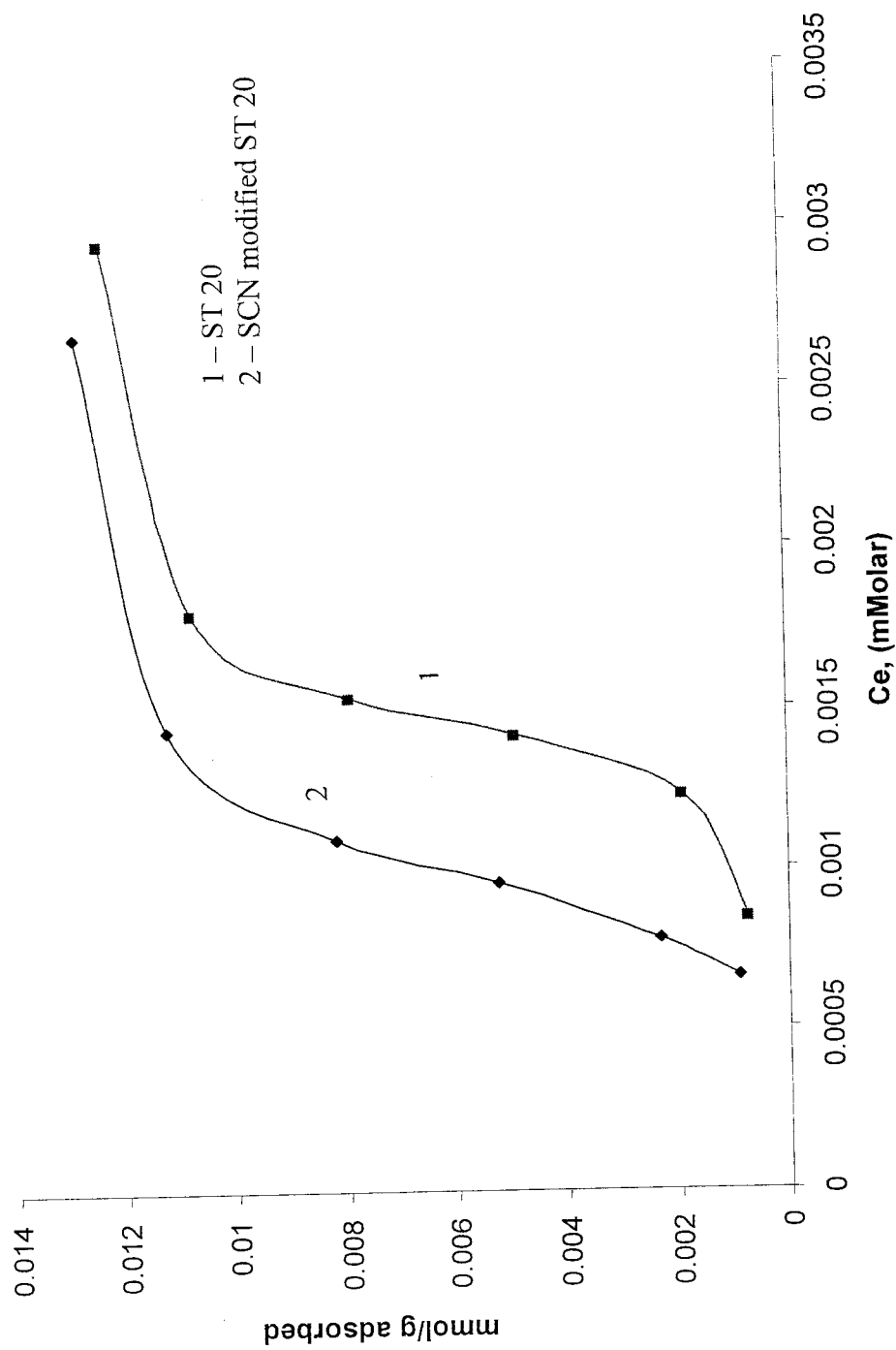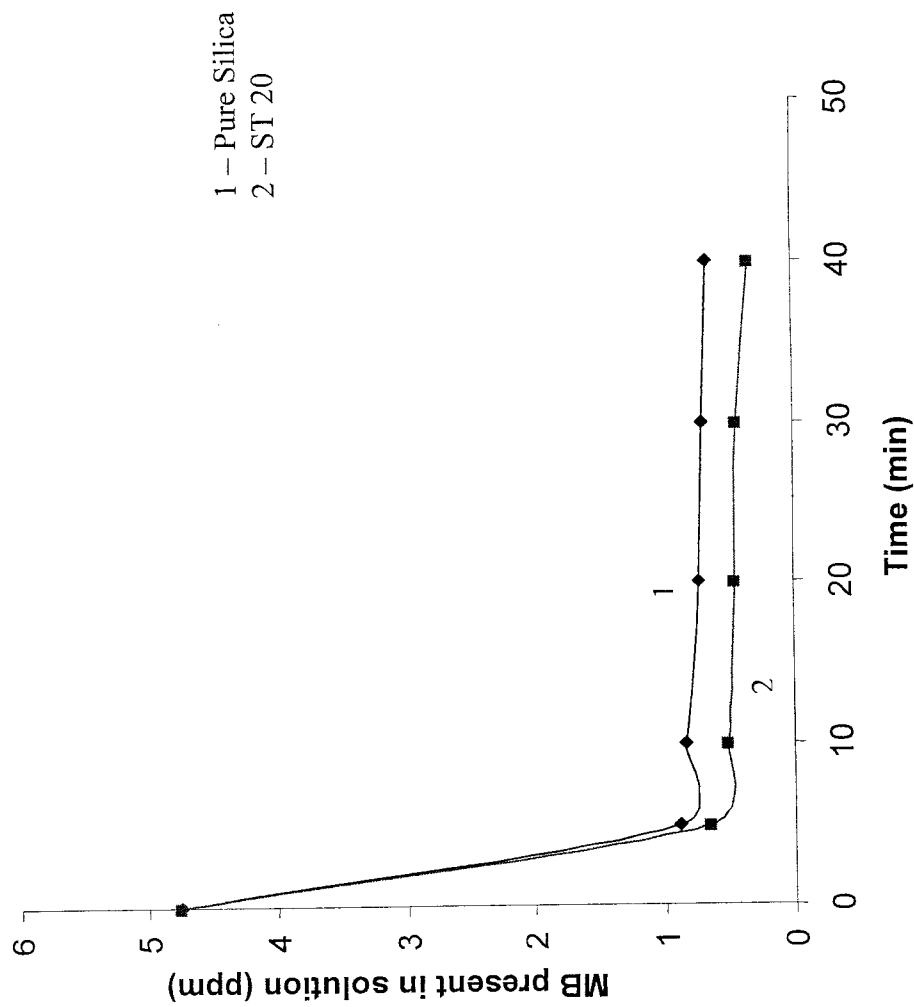
Figure 63: Photocatalytic decomposition of pure silica and ST 20 in the presence of methylene blue at pH 7.

Time (min)	Conc of MB present in solution before PD using ST 20 (ppm)	Conc of MB present in solution before PD using SCN modified ST 20 (ppm)	Conc of MB in solution after PD using ST 20 (ppm)	Conc of MB in solution after PD using SCN modified ST 20 (ppm)
0	5.230346344	5.230346344	5.230346	5.230346
5	0.623419461	4.268279274	0.458494	3.075316
10	0.513468939	3.031335899	0.354041	1.376581
15	0.463991204	1.909840572	0.315558	0.606927
20	0.458493678	1.145684442	0.31006	0.409016
25	0.414513469	0.760857614	0.31006	0.332051
30	0.354040682	0.727872457	0.299065	0.332051
35	0.354040682	0.650907092	0.299065	0.326553
40	0.354040682	0.573941726	0.299065	0.299065

Table 17: Photocatalytic data showing the conc of MB present in solution before and after irradiating with UV light using ST 20 and

SCN modified ST 20 as adsorbents at pH 7.
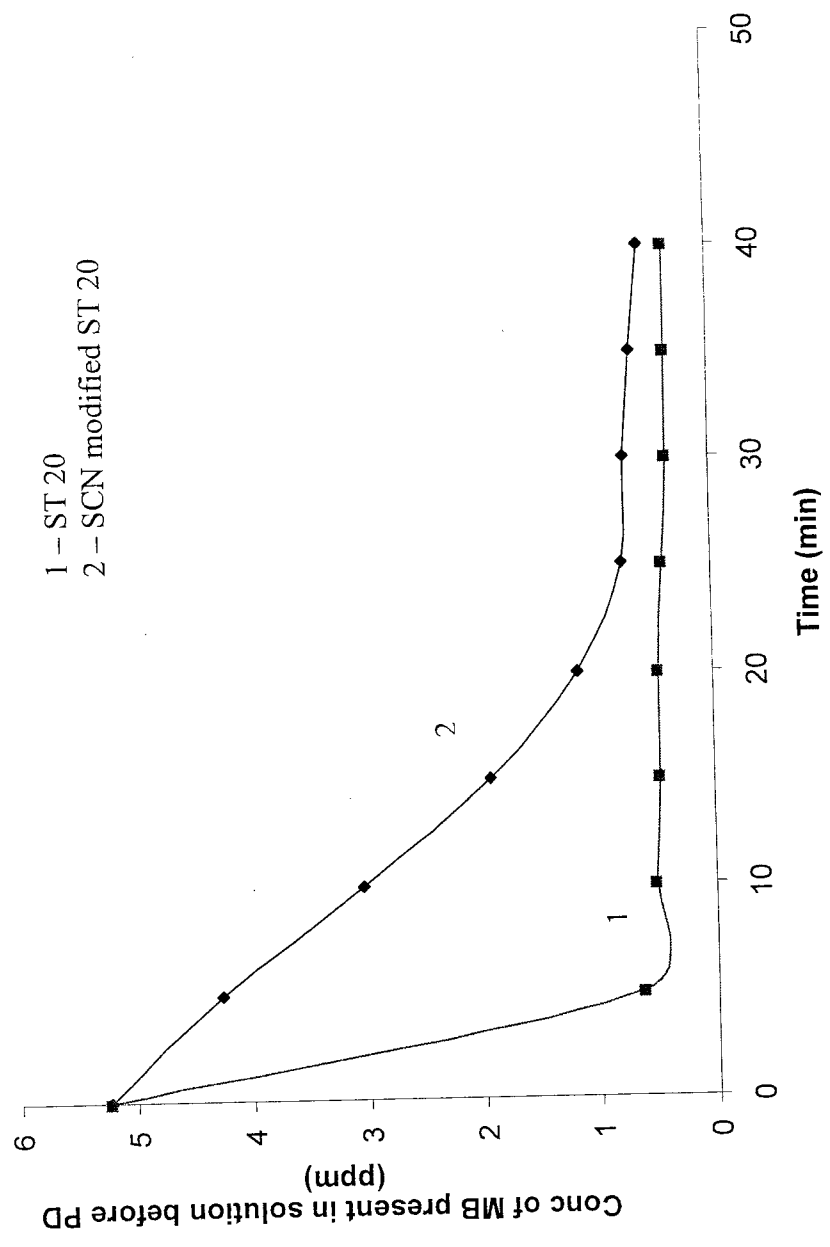
Figure 64: Concentration of methylene blue present in solution before PD. (Blank photocatalytic experiments, i.e., in the absence of UV light)
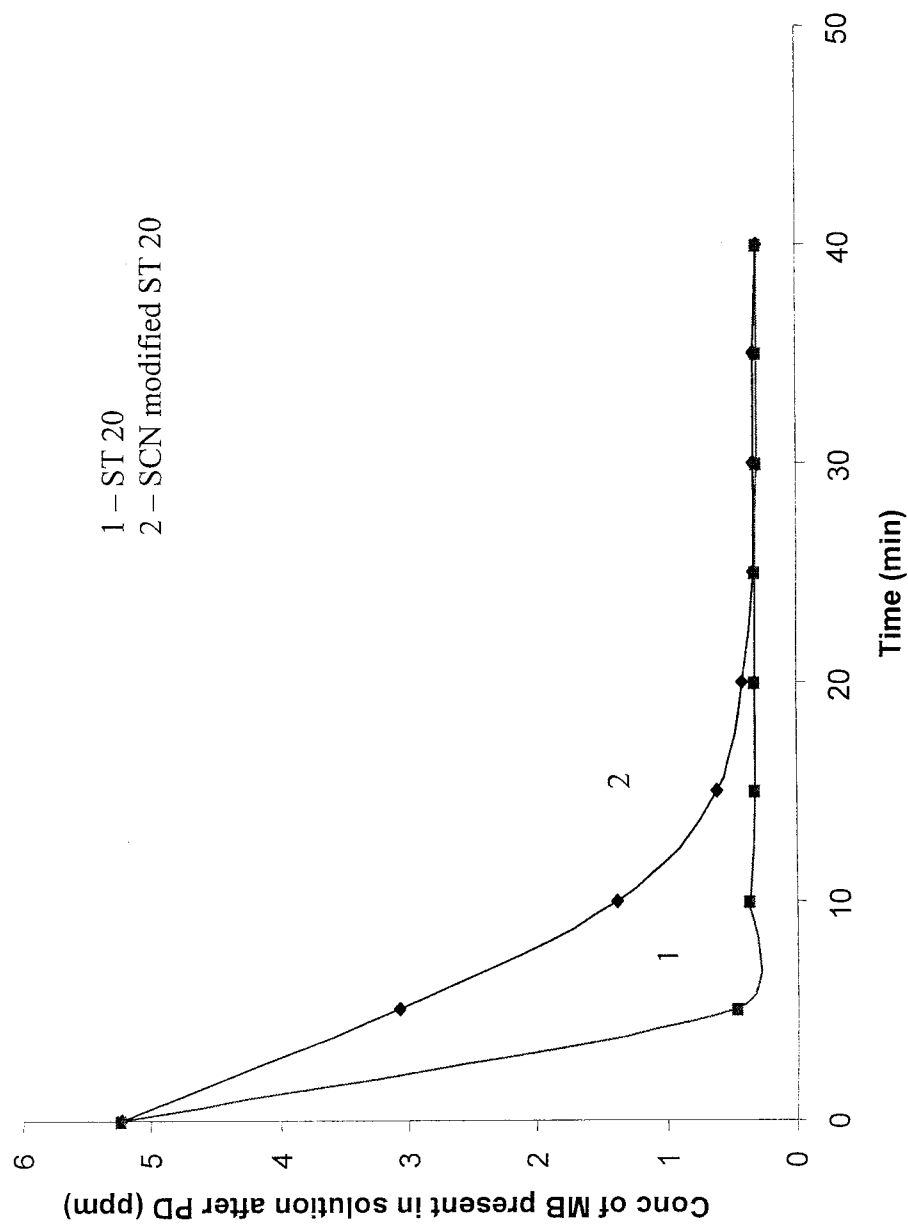
Figure 65: Concentration of methylene blue present in solution after irradiating with UV light at pH 7.

Time	Original conc of methylene blue (ppm)	Adsorbed conc of methylene blue (ppm)	Reacted conc of methylene blue (ppm)	Photocatalytic equilibrium conc (ppm)
0	5.23	0	0.12	5.11
5	5.23	4.60	0.28	0.340
10	5.23	4.72	0.28	0.24
15	5.23	4.76	0.27	0.2
20	5.23	4.77	0.27	0.19
25	5.23	4.82	0.22	0.19
30	5.23	4.88	0.17	0.18
35	5.23	4.88	0.17	0.18
40	5.23	4.88	0.17	0.18

Table 18: Photocatalytic data of ST 20 in degradation of methylene blue at pH 7.

Time	Original conc of methylene blue (ppm)	Adsorbed conc of methylene blue (ppm)	Reacted conc of methylene blue (ppm)	Photocatalytic equilibrium concentration (ppm)
0	5.23	0	0.12	5.11
5	5.23	0.96	1.31	2.96
10	5.23	2.12	1.77	1.26
15	5.23	3.32	1.42	0.49
20	5.23	4.08	0.85	0.29
25	5.23	4.47	0.55	0.21
30	5.23	4.50	0.51	0.21
35	5.23	4.58	0.44	0.21
40	5.23	4.66	0.39	0.18

Table 19: Photocatalytic data of SCN modified ST 20 in degradation of methylene blue at pH 7.
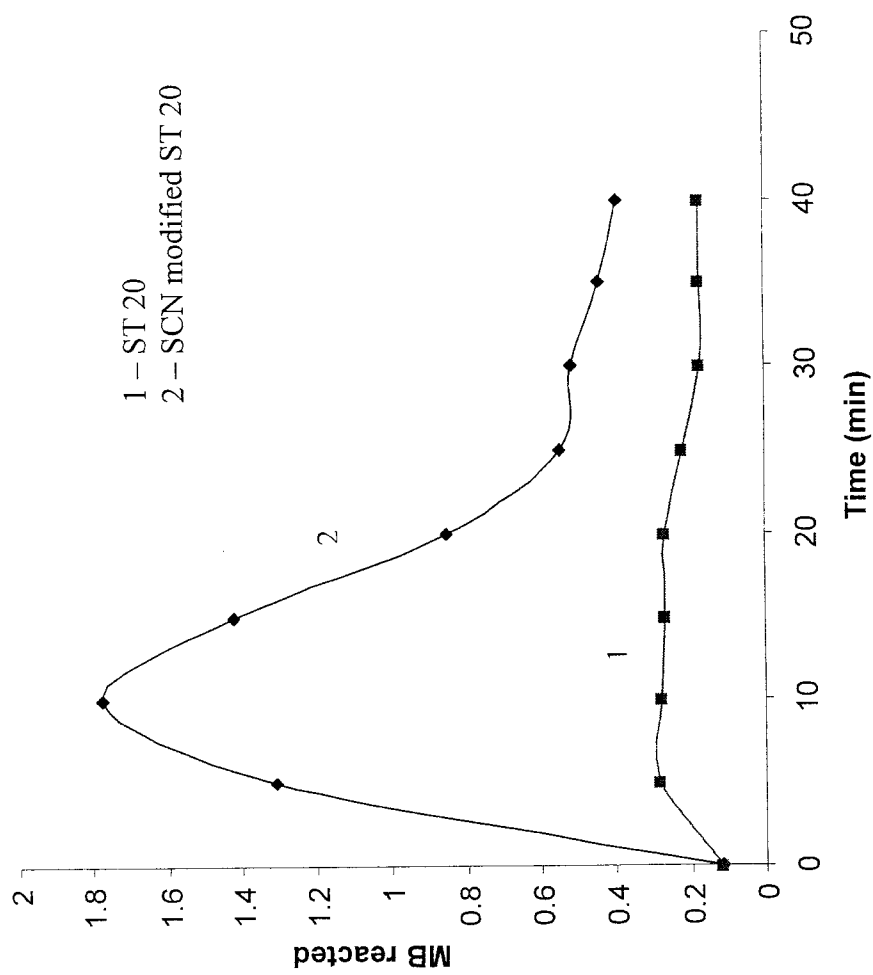
Figure 66: Photocatalytic performance of ST 20 and SCN modified ST 20 in degradation of methylene blue at pH 7
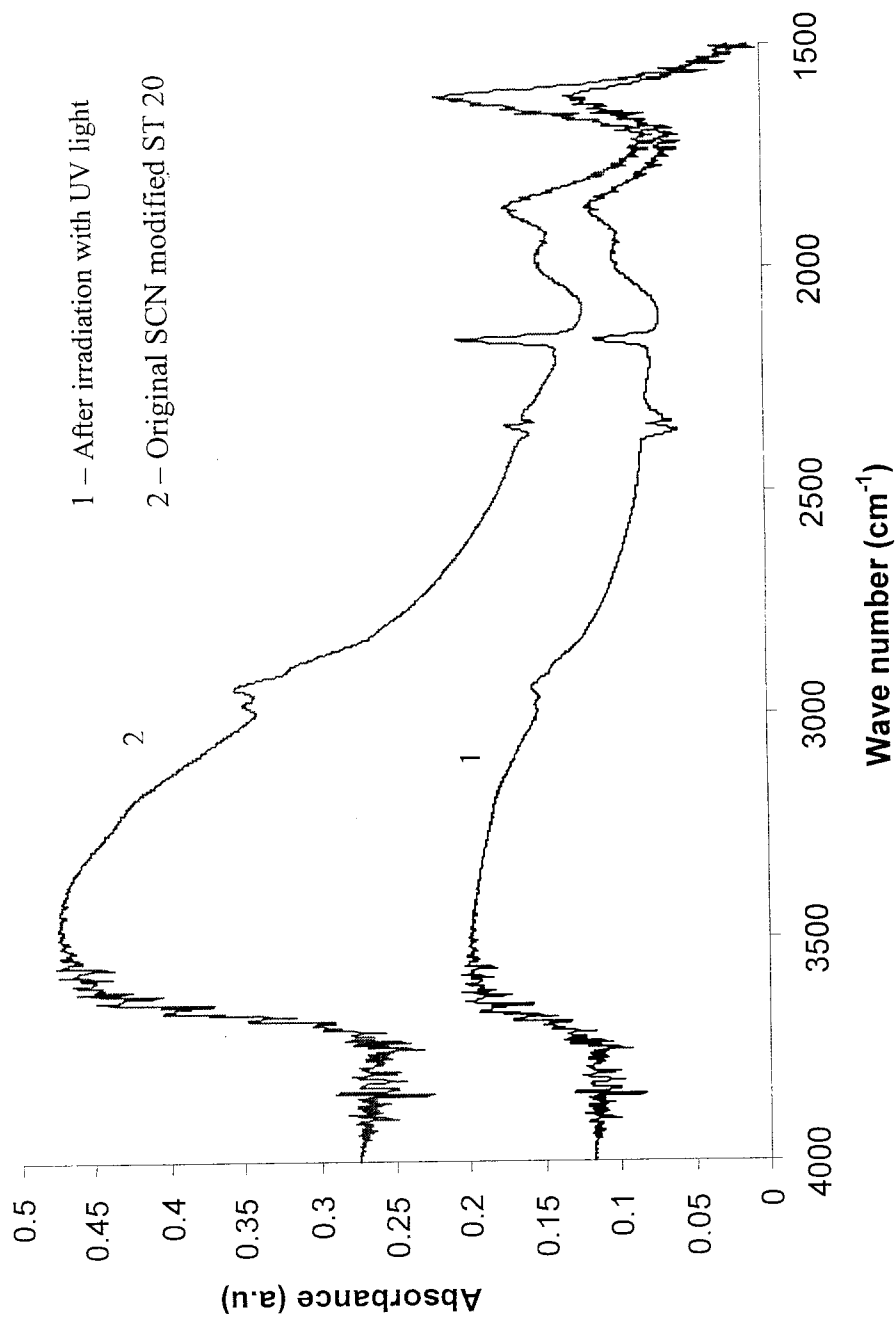
Figure 67: FTIR spectra of SCN modified ST 20 (Original sample) and SCN modified ST 20 with irradiation of UV light in the presence of water at pH 7

CHAPTER V

CONCLUSION

The characterization of surface silanols for pure silica, alumina, titania, SA, ST, AST samples revealed a non-linear dependence of silica phase as the contents of alumina or titania changes. Thermogravimetric analysis performed on all the samples revealed that the OH stretching vibrations detected in the FTIR are only from surface hydroxyls but not water. ST 20 which does not show much loss in silanol content and yet has sufficient TiO_2 for photocatalysis is chosen for surface modification with thiol or thiocyano groups. Adsorption isotherms show greater strength of adsorption for SCN modified ST 20 than ST 20 in the presence of methylene blue at lower concentrations. Photocatalytic decomposition studies on ST 20 and SCN modified ST 20 show that the SCN modified ST 20 exhibits more photocatalytic degradation of methylene blue than ST 20. The photocatalytic degradation of methylene blue for ST 20 and SCN modified ST 20 increased up to 10 minutes, but showed a decrease in degradation after 10 minutes. This result is not believable since MB is not expected to be regenerated during the experiment. Clearly the role of adsorption has not been adequately taken into account. Nevertheless if these results are to be believed even qualitatively, they show that surface modification has increased the rate of MB photocatalysis on these modified silica-titania samples.

REFERENCES

1. Suzdal'tsev, I. E.; Lesnikov, K. A. *Refractories and Industrial Ceramics,* **2005,** *46,* 189-192.

2. Dugas, V.; Chevalier, Y, *Journal of Colloid and Interface Science,* **2003,** *264,*354-361.

3. Gun' ko, M. V.; Turov, V. V.; Zarko. I. V.; Voronin, Tischenko, A. V.; Dudnik, V. V.; Pakhlov, M. E.; Chuiko, A. A, *Langmuir,* **1997,** *13,* 1529-1544.

4. Bandopadhyay, K. A.; Roy, K. S.; Murthy, S. G, *Indian Journal of Chemistry,* **1989,** *28A,* 222-225.

5. Litter, I. M, *Applied Catalysis,* **1999,** *23,* 89-114.

6. Gun' ko, M. V.; Zarko. I. V.; Chibowski, E.; Dudnik, V. V.; Leboda, R.; Zaets. A. V.; *Journal of Colloid and Interface Science,* **1997,** *188,* 39-57.

7. Hashimoto, K.; Irie, H.; Fujishima, A, *Japanese Journal of Applied Physics,* **2005,** *44,* 8269-8285.

8. Gao, X.; Wachs, E. I.; *Catalysis Today,* **1999,** *51,* 233-254.

9. Hoffmann, R. M.; Martin, T. S.; Wonyong, C.; Bahnemann, W. *Chemical Reviews,* **1995,** *95,* 69-96.

10. Pichat, P.; Herrmann, J. M.; Adsorption-Desorption, *Photocatalysis: Fundamentals and Applications,* John Wiley, **1989,** 217-250.

11. Van Der Voort, P.; Vansant.; *Journal of Liquid Chromatography and Related Technologies,* **1996,** *19,* 2723-2752.

12. Blitz, P. J.; Gun' ko, M. V, *Encyclopedia of Surface and Colloid Science,* Marcel Decker, **2002,** 2939-2950.

13. Blitz, P. J.; Shreedhara Murthy, S. R.; Leyden, E. D. *Journal of Colloid and Interface Science,* **1988,** *121*, 63-69.

14. Blitz, P. J.; Gun' ko, M. V. *Surface Chemistry in Biomedical and Environmental Science,* Springer, The Netherlands, **2006**. vol.228.

15. El Qada, N. E.; Allen, J. S.; Walker, M. G. *Chemical Engineering Journal*, **2006,** *124,* 103-110.

16. Chun Hu, Yizhong, W.; Hongxiao, T.; *Applied Catalysis B: Environmental,* **2001,** *30,* 277-285.

17. Aguado, J.; Grieken, V. R.; Lopez-Munoz, J. M.; Marugan, J.; *Applied Catalysis A: General,* **2006,** *312,* 202-212.

18. Wong, C. Y.; Szeto, S. Y.; Cheung, H. W.; McKay, G.; *Process Biochemistry,* **2004,** *39,* 693-702.

19. Adamson, W. Arthur.; Gast, P. Alilce, *Physical Chemistry of Surfaces,* John Wiley & Sons, Inc, NY, **1997.**

20. Zhang, X.; Zhang, F.; Chan, Y. K.; *Applied Catalysis A: General,* **2005,** *284,* 193-198.

21. Saeed, R.; Uddin, F.; Summer, S.; *Asian Journal of Chemistry,* **2005,** *17,* 737-742.

22. Hamdaoui, O.; Naffrechoux, E.; *Journal of Hazardous Materials,* **2007,** 1-14.

23. Blitz, P. J.; *Colloid and Surfaces,* **1992,** *63,* 11-19.

24. Proctor, A.; Toro-Vazquez, F. J. *JAOCS,* **1996,** *12,* 1627-1629.

25. Xie, Chao.; Xu, Zili., Yang, Qiujing.; Xue, Baoyong.; Du, Yaoguo.; Zhang, Jiahua.; *Material Science and Engineering B*, **2004,** *112,* 34-41.

26. Vedamuthu, S.M.; Painter, S.; Ancheta, J.; Blitz, P.J.; *Journal of Undergraduate Chemistry Research,* **2002,** *1,* 5-8.

27. Giles, H.C.; Macewan, H.T.; Nakhwa, N.S.; Smith, D.; *Journal of Chemical Society,* **1960,** *10,* 3973-3993.

28. Luechinger, Marco.; Prins, Roel.; Pirngruber, D.Gerhard.; *Microporous and Mesoporous Materials,* **2005,** *85,* 111-118.

29. Nakamura, R.; Ueda, K.; Sato, S.; *Langmuir,* **2001,** *17,* 2298-2300.

30. Uosaki, K.; Yano, T.; Nihonyanagi, S.; *Journal of Physical Chemistry,* **2004,** *108,* 19086.

31. Blitz, P. J.; *Diffuse Reflectance Spectroscopy;* Mirabella, M. F.; John Wiley, Newyork, **1998.**

32. Gun' ko, M. V.; Nychiporuk, M. Y.; Zarko, I.V.; Goncharuk,V.E.; Mishchuk, A.O.; Leboda, R.; Skubiszewska-Zieba, J.; Skwarek, E.; Janusz, W.; Yurchenko, R.G.; Osovskii, D.V.; Ptushinskii, G.Y.; T.urov, V.V.; Gorbik, P.P.; Blitz, P.J.; Gude, K. *Applied Surface Science,* **2007,** *253,* 3215-3230.

33. Gun'ko, M.V.; Blitz, P.J.; Gude, K.; Zarko, I. V.; Goncharuk,V.E.; Nychiporuk, M.Y.; Leboda, R.; Skubiszewska-Zieba, J.; Osovskii, D.V.; Ptushinskii, G.Y.; Mishchuk, A.O.; Gorbik, P.P. *Journal of Colloid and Interface Science,* **2007,** 314, 119-130.